International Doctorate Program in Molecular Oncology and Endocrinology
Doctorate School in Molecular Medicine

XXII cycle - 2006–2009
Coordinator: Prof. Giancarlo Vecchio

The Receptor Tyrosine Kinase RET is a Hsp90 client protein and is degraded upon exposure to 17-AAG

Luigi Alfano

University of Naples Federico II
Dipartimento di Biologia e Patologia Cellulare e Molecolare
"L. Califano"

Administrative Location

Dipartimento di Biologia e Patologia Cellulare e Molecolare “L. Califano”
Università degli Studi di Napoli Federico II

Partner Institutions

Italian Institutions
Università degli Studi di Napoli “Federico II”, Naples, Italy
Istituto di Endocrinologia ed Oncologia Sperimentale “G. Salvatore”, CNR, Naples, Italy
Seconda Università di Napoli, Naples, Italy
Università degli Studi di Napoli “Parthenope”, Naples, Italy
Università del Sannio, Benevento, Italy
Università di Genova, Genoa, Italy
Università di Padova, Padua, Italy
Università degli Studi “Magna Graecia”, Catanzaro, Italy
Università degli Studi di Firenze, Florence, Italy
Università degli Studi di Bologna, Bologna, Italy
Università degli Studi del Molise, Campobasso, Italy
Università degli Studi di Torino, Turin, Italy
Università di Udine, Udine, Italy

Foreign Institutions
Université Libre de Bruxelles, Brussels, Belgium
Universidade Federal de Sao Paulo, Brazil
University of Turku, Turku, Finland
Université Paris Sud XI, Paris, France
University of Madras, Chennai, India
University Pavol Jozef Šafàrik, Kosice, Slovakia
Universidad Autonoma de Madrid, Centro de Investigaciones Oncologicas (CNIO), Spain
Johns Hopkins School of Medicine, Baltimore, MD, USA
Johns Hopkins Krieger School of Arts and Sciences, Baltimore, MD, USA
National Institutes of Health, Bethesda, MD, USA
Ohio State University, Columbus, OH, USA
Albert Einstein College of Medicine of Yeshiwa University, N.Y., USA

Supporting Institutions
Ministero dell’Università e della Ricerca
Associazione Leonardo di Capua, Naples, Italy
Dipartimento di Biologia e Patologia Cellulare e Molecolare “L. Califano”, Università degli Studi di Napoli “Federico II”, Naples, Italy
Istituto Superiore di Oncologia (ISO), Genoa, Italy
Università Italo-Francese, Torino, Naples, Italy
Università degli Studi di Udine, Udine, Italy
Agenzia Spaziale Italiana
Istituto di Endocrinologia ed Oncologia Sperimentale “G. Salvatore”, CNR, Naples, Italy

Italian Faculty

Giancarlo Vecchio, MD, Co-ordinator
Salvatore Maria Aloj, MD
Francesco Saverio Ambesi Impiombato, MD
Francesco Beguinot, MD
Maria Teresa Berlingieri, MD
Angelo Raffaele Bianco, MD
Bernadette Biondi, MD
Francesca Carlomagno, MD
Gabriella Castoria, MD
Angela Celetti, MD
Mario Chiariello, MD
Lorenzo Chiariotti, MD
Vincenzo Ciminale, MD
Annamaria Cirafici, PhD
Annamaria Colao, MD
Alma Contegiacomo, MD
Sabino De Placido, MD
Gabriella De Vita, MD
Monica Fedele, PhD
Pietro Formisano, MD
Alfredo Fusco, MD
Michele Grieco, MD
Massimo Imbriaco, MD
Paolo Laccetti, PhD
Antonio Leonardi, MD
Paolo Emidio Macchia, MD
Barbara Majello, PhD
Rosa Marina Melillo, MD
Claudia Miele, PhD
Francesco Oriente, MD
Roberto Pacelli, MD
Giuseppe Palumbo, PhD
Silvio Parodi, MD
Nicola Perrotti, MD
Giuseppe Portella, MD
Giorgio Punzo, MD
Antonio Rosato, MD
Guido Rossi, MD
Giuliana SalvatoreMD,
Massimo Santoro, MD
Giampaolo Tortora, MD
Donatella Tramontano, PhD
Giancarlo Troncone, MD
Giuseppe Viglietto, MD
Roberta Visconti, MD
Mario Vitale, M

Foreign Faculty

Université Libre de Bruxelles, Belgium
Gilbert Vassart, MD
Jacques E. Dumont, MD

Universidade Federal de Sao Paulo, Brazil
Janete Maria Cerutti, PhD
Rui Monteiro de Barros Maciel, MD PhD

University of Turku, Turku, Finland
Mikko Laukkanen, PhD

Université Paris Sud XI, Paris, France
Martin Schlumberger, MD
Jean Michel Bidart, MD

University of Madras, Chennai, India
Arasambattu K. Munirajan, PhD

University Pavol Jozef Šafàrik, Kosice, Slovakia
Eva Cellárová, PhD
Peter Fedoročko, PhD

Universidad Autonoma de Madrid - Instituto de Investigaciones Biomedicas, Spain
Juan Bernal, MD, PhD
Pilar Santisteban, PhD

Centro de Investigaciones Oncologicas, Spain
Mariano Barbacid, MD

Johns Hopkins School of Medicine, USA
Vincenzo Casolaro, MD
Pierre A. Coulombe, PhD
James G. Herman MD
Robert P. Schleimer, PhD

Johns Hopkins Krieger School of Arts and Sciences, USA
Eaton E. Lattman, MD

National Institutes of Health, Bethesda, MD, USA
Michael M. Gottesman, MD
J. Silvio Gutkind, PhD
Genoveffa Franchini, MD
Stephen J. Marx, MD
Ira Pastan, MD
Phillip Gorden, MD

Ohio State University, Columbus, OH, USA
Carlo M. Croce, MD
Ginny L. Bumgardner, MD PhD

Albert Einstein College of Medicine of Yeshiwa University, N.Y., USA
Luciano D'Adamio, MD
Nancy Carrasco, MD

“The Receptor Tyrosine Kinase RET is a Hsp90 client protein and is degraded upon exposure to 17-AAG”

TABLE OF CONTENTS

LIST OF PUBLICATIONS

During the PhD program I have contributed to two projects that resulted in the following manuscripts. The first one represents the core of the thesis while the second one is appended to the thesis:

1) RET is a Hsp90 client protein and is knocked-down upon Hsp90 pharmacological block
Luigi Alfano*, Teresa Guida*, Livia Provitera, Giancarlo Vecchio, Marc Billaud, Massimo Santoro, Francesca Carlomagno. **Submitted**
(*these two authors equally contributed to the study)

2) Protein NCOA4 inhibits initiation of eukaryotic DNA replication
Francesca Carlomagno, Teresa Guida, Livia Provitera, Luigi Alfano, Donata Vitagliano, Nina A. Dathan, Domenico Grieco, Vincenzo Costanzo, Alfredo Fusco, Massimo Santoro. **In preparation**

ABSTRACT

Molecular alterations of the receptor tyrosin kinase RET are involved in the pathogenesis of thyroid cancer. Germline point mutations in the extracellular and intracellular domains of the receptor are responsible of a group of inherited cancer diseases defined as Multiple Endocrine Neplasia type 2 syndromes (MEN2), whose major feature is represented by Medullary Thyroid Carcinoma (MTC). Somatic point mutations of RET are also found in around 40% of sporadic MTC.

Hsp90 is part of the molecular chaperone machinery involved in mediating correct folding and stabilization of client proteins. Hsp90 chaperone fuctions in concert with the action of a multitude of other chaperone and co-chaperone proteins like Hsp70, Aha1 and CDC37; its activity depends on ATP and can be hindred by Geldanamycin-like compounds. Several kinases implicated in the process of neoplastic transformation are clients of Hsp90.

In this thesis, we demonstrated that RET is a Hsp90 client protein. In RAT1 murine fibroblasts, stably transfected with RET wt or RET C634R oncogenic mutant, the Geldanamycin-derived drug 17-AAG was able to induce a proteasome dependent degradation of the receptor. Treatment with 17-AAG caused dissociation of Hsp90-RET complex and stabilized the interaction between RET and Hsp70 leading to recruitment of the Hsp70 interacting E3-ligase CHIP. Polyubiquitination by E3-ligases is commonly a destruction signal that mediates recognition of the targetted proteins by proteasome. Overexpression of CHIP wt, but not of two different CHIP defective mutants, CHIP-TPR and CHIP-ΔU, induced RET polyubiquitination and degradation. Interestingly, 17-AAG obstructed RET oncogenic signalling, decreasing RET C634R mediated activation of Ras-MAPK pathway and blocking transactivation of AP1-responsive and Myc-gene promoters. We could not observe any changes in sensitivity to 17-AAG-induced degradation among several RET MTC-associated mutants carrying mutations in the intracellular domain of the receptor, the region where Hsp90 chaperone has been shown to bind to receptor tyrosine kinases.

In human MTC cells carrying oncogenic RET mutants, Hsp90 inhibition by 17-AAG induced receptor degradation and signalling hindrance as shown by reduced phosphorylation of Shc and MAPK proteins. In such cells, 17-AAG caused a robust growth arrest, measured by decreased incorporation of BrdU, but failed to induce apoptosis.

In conclusion we demonstrated that RET is a Hsp90 client protein and the chaperone is required for folding and stabilization of the receptor.

1.BACKGROUND

1.1 Thyroid cancer

Thyroid cancer is the most common endocrine neoplasia, accounting for the majority of the deaths due to endocrine cancers.

Malignant thyroid carcinoma is classificated after the state of differentiation of tumour cells: well-differentiated, poorly differentiated, not differentiated and medullary thyroid carcinoma. The group of well-differentiated carcinoma include various histological subtypes: papillary thyroid carcinoma (PTC), follicular-papillary thyroid carcinoma and follicular carcinoma (FTC). The category of poorly differentiated carcinoma (PDC) has been recently identified and represents a histological derivation between the undifferentiated and the differentiated tumour. The category of not-differentiated carcinoma includes the anaplastic thyroid carcinoma (ATC). All these groups derive from follicular cells. Medullary thyroid carcinoma (MTC) derives from the calcitonin-secerning parafollicular C cells.

1.2 Histotypes of thyroid cancer

1.2.1 Papillary Thyroid carcinoma

Papillary thyroid carcinoma (PTC) is the most frequent neoplasia of the thyroid gland (50-90% of the total malignant thyroid differentiated tumours). PTC typically is detected as an irregular, solid or cystic mass. PTC can show papillae within a single- or multi-layer cubic ephitelium. Cytologically it displays eosinophilic inclusions in the nuclei and cytoplasmatic invaginations. These structures are not present in medullary and follicular thyroid carcinoma. Papillary thyroid cancer is highly curable with ten years survival rates estimated at 80-90%. Cervical metastasis (spread to lymph nodes in the neck) are present in 50% of small tumors and in over 75% of the larger thyroid cancers.

Typically, well-differentiated papillary thyroid carcinoma has indolent behavior and can be effectively treated by surgery followed by radioiodine therapy.

Some risk factors for PTC have been identified. Ionizing radiation exposure of the thyroid gland is the first risk factor known to definitively increase the incidence of papillary thyroid cancer. The exposure to ionizing radiation causes the tendency to chromosomal breaks and rearrangements with activation of oncogenes or loss-of-tumour suppressor genes. A frequent molecular alteration of papillary thyroid

tumour is characterized by fusion of the kinase domain of the tyrosine kinase receptor RET with the N-terminal region of constitutively expressed, heterologous genes, such as H4 (RET/PTC1) or NCOA4 (RET/PTC3). The fusion protein RET/PTC displays a constitutive activation of RET kinase function that becomes ligand indipendent (Santoro et al. 1994). Other molecular alterations of PTC include point mutations in BRaf (45%) and Ras (10%) proteins.

1.2.2 Follicular Thyroid carcinoma

Follicular thyroid carcinoma (FTC) is a well-differentiated cancer developing from thyroid follicular cells. FTC is generally a lonely nodule, either capsulated or infiltrating the adjacent compartments. As for PTC, therapy for FTC consists in surgery followed by metabolic treatment with ^{131}I. Prognosis is very good with a survival rate at 10 years ranging from 90 to 98%. Most common molecular lesions responsible of FTC are mutation on K-, H- and N-Ras (Challeton et al. 1995). More recently it has been shown that a portion of FTC carries the PAX8/PPARγ rerrangement (Nikiforova et al. 2003). PAX8 encodes a thyroid-specific transcription factor, while PPARγ is a nuclear receptor involved in lipid metabolism and tumorigenesis. The resulting fusion protein has a dominant negative activity on wild type PPARγ protein (Kroll et al. 2000).

1.2.3 Anaplastic Thyroid carcinoma

Anaplastic Thyroid carcinoma (ATC) represents the 1-5% of the total thyroid carcinoma and it occurs around the 6^{th}-7^{th} decade of life. The neoplasia is characterized by elevated level of malignancy and it causes a rapid invasion of the adjacent structure with frequent metastasis. Histologically the tissue of ATC appears wholly or partially composed of undifferentiated cells.

Point mutations in Ras and PI3KCA (catalytic subunit of PI3K) oncogenes and in the tumour suppressor p53 have been described in anaplastic carcinoma (Garcia-Rostan et al. 2003; Donghi et al. 1993; Fagin et al. 1993). BRaf mutations are highly variable in ATC, ranging from 0 to 50%. The variability in BRaf mutation detection in ATC is probably due, in part, to small sample sizes and different laboratory methodologies. When ATCs with a papillary component were examined, this mutation was observed in both the differentiated and undifferentiated regions (Begum et al. 2004; Soares et al. 2004; Takano et al. 2007).

No effective therapy is known for ATC and prognosis is quite negative with a mean survival of less than one year. These tumours, given their undifferentiated nature, do not significatively incorporate

radioiodine; however, it can be utilized in the treatment protocols if a residual ability to incorporate can be ascertained. Only very few responses have been reported with combined antracyclines-palliate regimens. If the tumour is sensible, radiation therapy of the neck can be exploited for a palliative cure.

1.2.4 Medullary Thyroid carcinoma

Medullary thyroid carcinoma was recognized in the 1950s by Hazard et al. as a distinct clinicophatologic entity (Hazard et al. 1959). Since the description, sequential pathologic, biochemical and molecular genetic studies have progressed to render this one of the best characterized solid malignancies of the thyroid (Hazard et al. 1959). In 1959, Hazard described MTC as a solid thyroid neoplasm without follicular histology but with a high degree of lymph node metastases that accounted for 3-5% of thyroid cancers. In the 1966, Williams suggested that MTC arose from the parafollicular cells (Williams, 1966). Parafollicular, or C cells, arise embryologically from the neural crest and are located primarily in the upper and middle thirds of the thyroid lobes, with a particular posterior concentration; these cells produced the Calcitonin hormone, a 32-amino acid peptide involved in calcium homeostasis representing an important marker for the diagnosis of MTC. The majority of patients with MTC have sporadic diseas. Nevertheless, 25% to 30 % of cases are due to hereditary forms of MTC (Kouvaraki et al. 2005). Hereditary MTC is classified according to three distinct clinical subtypes: MEN2A, MEN2B and FMTC. The most common of these subtypes MEN2A, accounts for 70% to 80% of individuals with hereditary medullary thyroid carcinoma (MTC). MEN2A is characterized by MTC, pheochromocytoma and primary hyperparathyroidism, although the penetrance is highly incomplete (Brandi et al. 2001). Two rare variants of MEN2A have been identified, one with congenital megacolon (Hirshsprung's disease) and the other with cutaneous lichen amyloidosis (Kouvaraki et al. 2005). MEN2B, accounts for only 5% of hereditary MTC cases. MEN2B is characterized by clinically aggressive MTC, pheochromocytoma, Marfanoid body habitus, mucosal neuroma and intestinal tumours (Brandi et al. 2001). The onset of MTC is generally before 5 years of age. The third inherited subtype of MEN2 is familiar MTC (FMTC). This subtype accounts for 10% to 20 % of hereditary MTC cases and only the thyroid gland is affected.

In the early 1990's, mutations in the RET proto-oncogenes were found to cause MEN2A, MEN2B and FMTC (Donis-Keller et al. 1993; Carlson et al. 1994). Activating RET germline mutations have been identified as the primary cause of all the hereditary MTC syndromes;

somatic RET mutations account for another quarter to half of all sporadic MTC (Eng et al. 1996).

The specific site of the particular mutated residue within the RET protein has been correlated to phenotypic differences among patients with inherited MTC. Patients with MEN2A characteristically have missense mutations in exon 10 (codons 609, 610, 611, 618, 620) and exon 11 (codon 634 that is the most common mutation in patients with MEN2A) (Brandi et al. 2001). These are mutations present in the RET extracellular domain and affect cysteine residues that can change to different aminoacids (Asai et al. 1996). Mutations in these cysteine residues lead to receptor homodimerization via the formation of disulfide bonds, rendering the receptor activated regardless of the presence of ligand. In the case of MEN2B, more than 95% of patients have mutation in exon 16 (M918T), in the tyrosine kinase domain of the protein. This mutation renders the receptor activated in its monomeric state, and leads to increased phosphorylation of intracellular tyrosine residues as well as a change in substrate specificity (Santoro et al. 1995; Salvatore et al. 2001). Patients with FMTC harbor mutations in exons 10, 11, 13 (codon 768), and 14 (codon 804, 806) (Brandi et al. 2001) (Table 1).

Domain	MEN2A	MEN2B	FMTC
Cystein rich	Cys 609, 611.618.,620, 630,634		Cys 609, 611.618.620, 630,634
TK1			Glu768Asp Tyr791Phe Leu790Phe Val804Met/Leu
TK2		Ala883Phe Met918Thr	Ser891Ala

Table 1: Principal RET point mutations in MEN2 syndromes

MTC is quite resistant to conventional chemotherapy and radiotherapy and the only effective cure is still represented by early surgery. Therefore this tumour is a suitable candidate for alternative therapeutic approaches such as molecular targeted therapy. Clinical trials using inibitors of RET tyrosine kinase activity are being used in patients with MTC. Various classes of small molecule TKI (Tyrosine Kinase Inhibitors) have shown anti-RET activity in preclinical studies, including pyrazolopyrimidine inhibitors PP1 and PP2, idolocarbazole derivatives CEP-701 and anilinoquinazoline ZD6474 (Cuccuru et al. 2004; Carlomagno et al. 2002; Carlomagno et al. 2002; Carlomagno et

al. 2003). Among this group of compounds, the clinical development of ZD6474 (Vandetanib) is the most advanced. Vandetanib is an orally available TKI that targets VEGF-dependent tumour angiogenesis through inhibition of its receptor KDR as well as EGFR and RET-dependent tumour cell proliferation. ZD6474 competes with ATP and blocks autophosphorylation and signal transduction. Pre-clinical studies showed that ZD6474 inhibits RET with a 50% inhibitory concentration (IC50) of 100nM (Carlomagno et al. 2002). In addition, ZD6474 was shown to inhibit growth of RET-transformed cell xenografts (Carlomagno et al. 2002). There are other multikinase ihibitors such as: Sorafenib, Sunitinib, Motesanib that share the ability of inhibiting RET, VEGFRs, KIT and the receptors for platelet-derived growth factor (PDGFR) (Schlumberger et al. 2008). All these compounds are being tested in clinical trials for MTC, as well.

1.2 The RET receptor

RET was first identified by Takahashi et al. in 1985 as a proto-oncogene able to undergo activation after genetic rearrangements during transfection of NIH3T3 cells with human lymphoma-derived DNA (Takahashi et al. 1985). The RET proto-oncogene is located on chromosome 10q11.2 and includes 21 exons; it encodes several protein isoforms that are expressed as a result of alternative splicing of mRNA (Ishizaka et al. 1989). The principal isoforms of this receptor are RET9 of 1072 aa and RET51 of 1114 aa. RET is highly conserved over a broad range of species.

1.2.1 RET structure and function

RET is a single-pass transmembrane protein. The basic structure of RET is similar to other RTKs with extracellular, transmembrane and intracellular domains (Fig.1). The extracellular domain of RET has no homology with other receptor tyrosine kinases (Takahashi et al. 1988). It contains a cleavable signal sequence of 28 aa, as well as a conserved cysteine-rich region close to the cell membrane. Molecular modeling studies have determined the presence of four cadherin–like domains in the NH2-ter sequence of the extracellular region. The extracellular domains binds to the four RET ligands (GFLs) which are neurotrophins belonging to the superfamily of TGFβ growth factor and are secreted in a dimeric structure. In particular, GFLs are Glial-derived Neurotrophic Factor (GDNF), Neurturin (NRTN), Artemin (ARTN) and Persephin (PSPN). GFLs signal through a multisubunit complex comprising RET and one of the four glycosyl phosphatidylinositol (GPI)-linked proteins known as GDNF family receptors α (GFRα-1 to 4). GFRα is localized in a zone rich of

sphingolipids and cholesterol (lipid rafts) where the receptor RET is recruited after being activated by GDNF.

The intracellular domain (IC) contains the Juxta-membrane region (JMR) and the tyrosin kinase domain divided into two domains spaced out by 27 amino acids. This domain is responsible of the RET signalling activation and consequent signal transduction.

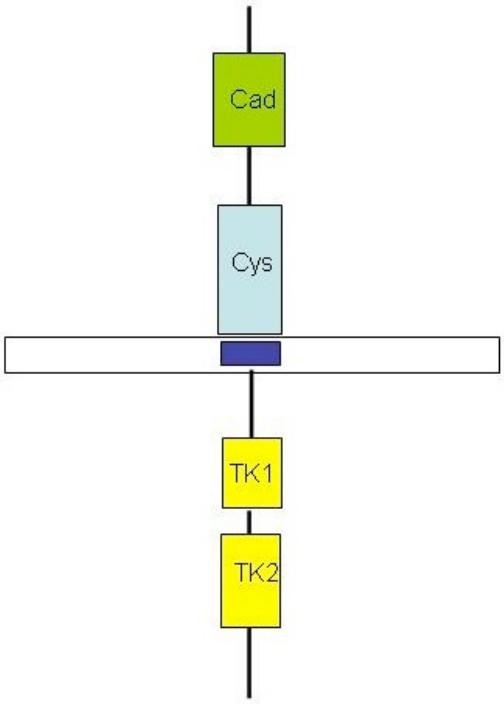

Figure 1. RET structure: the extracellular domain is composed by a Cadherin-like domain (Cad), indicated in green, and a Cystein-rich domain (Cys), indicated in light blue; transmembrane domain is indicated in blu; the intracellular compartment (yellow) displays the Tyrosine Kinase domain divided in two subdomains (TK1 and TK2) by 27 aa.

1.2.2 RET signalling

Upon activation by ligands, RET dimerizes and autophosphorylates on specific tyrosine residues in the IC domain. As for all Receptor Tyrosine Kinases, phosphorylated tyrosines serve as docking sites for adaptor signalling molecules containg SH2 (Src homology 2) or PTB (Phospho Tyrosine Binding) domains. The recruitment of these adaptors to the receptor switches on signalling pathways controlling cell proliferation, survival, motility, differentiation and neoplastic transformation. Interactions of RET with a variety of downstream targets have been identified (Simons et al. 1997; Ikonen et al. 1998). Thus, the intracellular domain of RET contains at least 12

autophosphorylation sites (Liu et al. 1996; Salvatore et al. 2000; Coulpier et al. 2002; Kawamoto et al. 2004). Sites Tyr1090 and Tyr1096 are present only in the RET51 isoform. Phosphorylated tyrosine residues Tyr905, Tyr981, Tyr1015, and Tyr1096 have been identified as docking sites for Grb7/Grb10, Src, Phospholipase C-γ (PLC-γ), and Grb2, respectively (Pandey et al. 1995; Pandev et al. 1996; Encinas et al. 2004; Borrello et al. 1996; Alberti et al. 1998). Phosphorylation of Tyr905, located in the activation loop, stabilizes the active conformation of the kinase and facilitates the autophosphorylation of other tyrosine residues (Iwashita et al. 1996). Tyr1062 acts as a docking site for many adaptor or effector proteins: Shc, ShcC, FRS2, IRS1/2, Dok1, Dok4/5, Dok6, Enigma, and indirectly for PKCα (Asai et al. 1996; Durick et al. 1996; Arighi et al. 1997; Lorenzo et al. 1997; Ohiwa et al. 1997; Hennige et al. 2000, Kurokawa et al. 2001, Melillo et al. 2001a; Melillo et al. 2001b, Grimm et al. 2001, Murakami et al. 2002; Pelicci et al. 2002; Andreozzi et al. 2003; Crowder et al. 2004). Upon ligand stimulation, at least two distinct protein complexes assemble on phosphorylated Tyr1062 via Shc, one leading to activation of the Ras/ERK pathway through recruitment of Grb2/Sos and another to the PI3K/Akt pathway through recruitment of Grb2/GAB1/2. This latter complex can also assemble directly onto phosphorylated Tyr1096, offering an alternative route to PI3K activation by GDNF (Besset et al. 2000; Hayashi et al., 2000) (Fig.2).

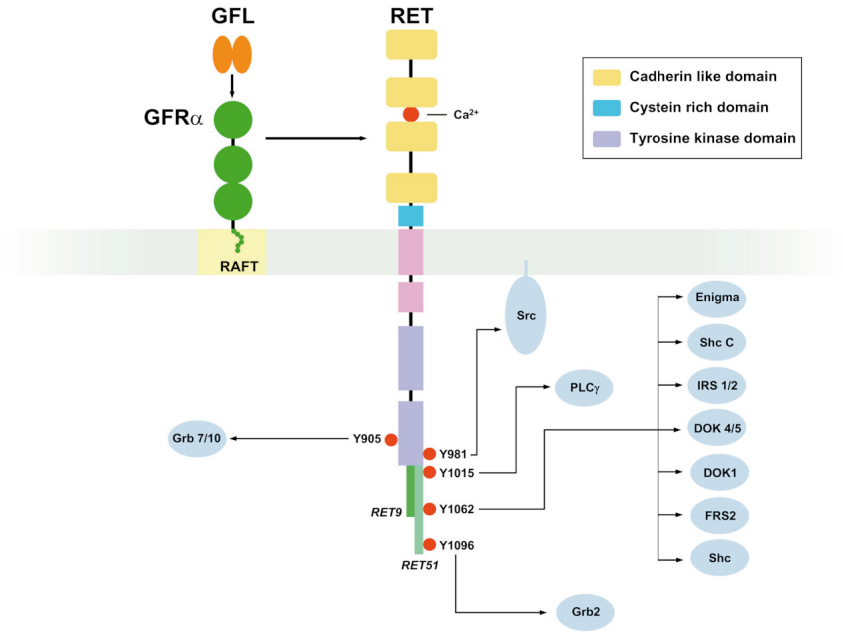

Figure 2: Signaling pathways activated by RET

Beyond Ras/ERK and PI3K/AKT, RET activates several pathways typical of Receptor Tyrosine Kinase signalling such as: 1) Jun NH2-terminal protein kinase (JNK) (Chiariello et al. 1998), 2) p38MAPK (Kurokawa et al. 2003), 3) ERK5 (Hayashi et al. 2001) and 4) PLC-γ (Borrello et al. 1996).

1.3 The Chaperonins

The primary amino acid sequence of a polypeptide chain already contains sufficient information to direct its folding to the native state. Under cellular conditions, which feature both higher temperature and higher macromolecular solute concentration than those typically employed in vitro, misfolding is a common occurrence. Misfolding usually results in the exposure of hydrophobic surfaces that should have been buried in the interior of a protein in its native state. These hydrophobic surfaces can associate with those from other proteins to produce multimolecular aggregation. Molecular chaperones are a group of specialized proteins that bind such exposed surfaces through their own exposed hydrophobic binding sites carrying out the remarkable activity of mediating ATP-dependent protein folding to the native state. Their role is to provide kinetic assistance, utilizing the energy of ATP for the folding process and thus to prevent or reverse misfolding that can lead to irreversible protein aggregation. There are many types of molecular chaperones in various organisms such as in chloroplast, bacterial cytosol, archea and eukaryotic. The major chaperone systems in the eukaryotic cytosol, including Hsp70, CCT (chaperonin containing TCP1) and Hsp90 are essential for viability.

1.3.1 Hsp90

The 90-KDa heat shock proteins (Hsp90) are a widespread family of molecular chaperones found in bacteria and all eukaryotes. Many eukaryotes possess multiple Hsp90 homologues, including endoplasmic reticulum, mitochondrial and chloroplast-specific isoforms.

1.3.1.1 Structure and conformation

Crystallization of full-length Hsp90 was first reported nearly 10 years ago (Prodromou et al. 1996).

The protein Hsp90 is divided into tree domains: N-terminal, middle segment and C-terminal domain (Fig.3).

The N-terminal portion forms a 25 KDa domain and

crystallography revealed a two layers α/β sandwich structure in which the helixes delimit a pocket extending from the surface to the buried face of highly twisted antiparallel β–sheet. In the human structure, this pocket was found to be the binding site for ATP and for the macrocyclic antitumour agent geldanamycin, whose binding to Hsp90 had been shown to disrupt productive complexes of Hsp90 with client protein such as kinases and steroid hormone receptors (Whitesell et al. 1994; Chavany et al. 1996).

The middle domain consists of a large αβα (α helix-β sheet-α helix) domain at the N-terminus connecting to a small αβα (α helix-β sheet-α helix) domain at the C-terminus via series of short α–helixes in a tight coil. The middle segment is the major site for client protein interactions, with a conserved hydrophobic patch centred on Trp 300 and an unusual amphipatic protrusion formed by residues 327-340. The middle segment also contributed a key catalytic lysine residue that would interact with the γ–phosphate of an ATP molecule bound in the N-terminal domain (Meyer et al. 2003).

The C-terminal domain is essential for Hsp90 dimerization. The dimer interface is formed by a pair of helixes at the C-terminal end of the domain packing together to create a four-helix bundle. The C-terminal domain presents the MEEVD motif implicated in binding to cochaperones with tetratricopeptide repeat (TRP) domains (Young et al. 1998).

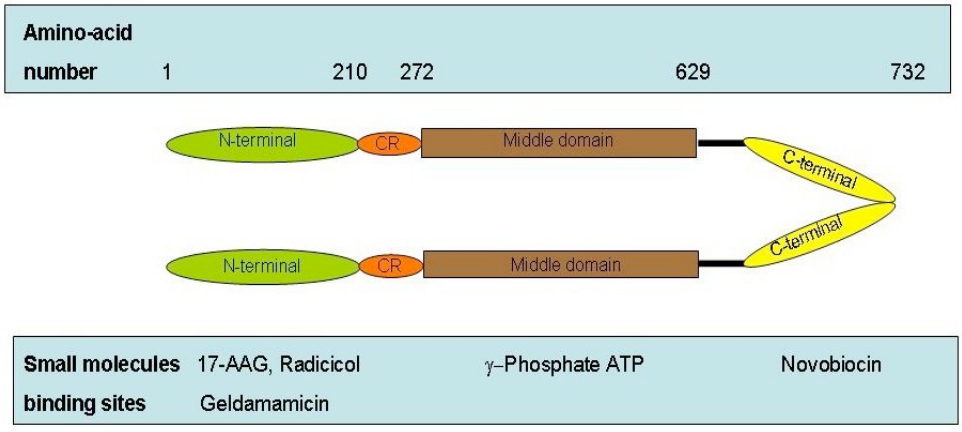

Figure 3: Structure of the Hsp90 dimer. The numbering 1–732 indicates the approximate positions in the amino acid sequence of the human protein that define its functional domains. 'CR' refers to a charged region which serves as a flexible linker between the N-terminal and middle domains. The locations where ATP and inhibitors (small molecules) bind Hsp90 (heat-shock protein of 90 kDa) and modulate its function are indicated. 17AAG, 17-allylaminogeldanamycin; GA, geldanamycin.

1.3.1.2 Hsp90 function

Hsp90 is a chaperone protein. As already explained, chaperones constitute a functionally related collection of highly conserved and ubiquitous proteins that specifically recognize non-native proteins. Thus, chaperones prevent unwanted inter- and intra-molecular interactions and influence the partitioning between productive and unproductive folding steps but do not form part of the final structure of the folded protein. Several *in vitro* assays demonstrate that Hsp90 acts as a molecular chaperone: it suppresses the aggregation of non-native proteins and promotes their refolding, sometimes in cooperation with the Hsp70 system.

1.3.1.3 ATP cycle

The ATP molecule is essential for the function of Hsp90; conformational changes of Hsp90 in presence of ATP had been previously observed, and they have been interpreted in terms of a structural transition from an open hydrophobic state to a more closed conformation due dimerization of the N-terminal domain (Csermely et al. 1993; Grenert et al. 1997; Sullivan et al. 1997).

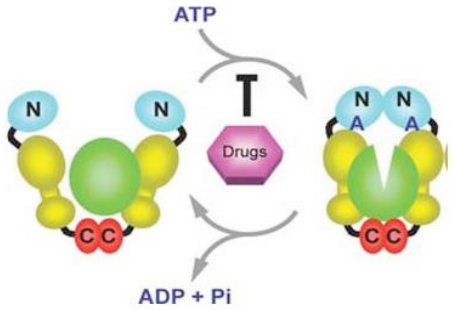

Figure 4. Current model for the gross conformational changes that accompany binding and hydrolysis of ATP by Hsp90. The N-,middle, and C-terminal regions in the Hsp90 dimer (colored *cyan*, *yellow*, and *red*, respectively) are shown; a client protein (*green*) is able to bind in the absence of ATP and undergoes changes of folding state when bound to the "tense" ATP-bound chaperone. Inhibition of ATP binding by drugs, such as geldanamycin, blocks client protein correct folding

In this conformation the chaperone is able to interact more stably with the client protein and mediates its correct folding. On the other hand interaction with the substrate activates Hsp90 ATPase activity inducing the transition to the open conformation and release of the client protein.

1.3.1.4 Hsp90 client proteins

Hsp90 is an important chaperone for a vast array of client proteins. Hsp90-associated proteins can be categorized into two general groups: protein kinases and transcription factor. To the aim of this thesis we will focus on the former class of proteins.

Many RTKs are Hsp90 client proteins such as Ron, Kit, Her-2, and TrkA (Germano et al. 2006, Fumo et al. 2004, Citri et al. 2002, Farina et al. 2009, Grovic et al. 2006).

Her-2 (p185erbB2) is a receptor tyrosine kinase overexpressed in a significant proportion of malignancies, including breast, ovarian prostate and gastric cancers, and is associated with a poor prognosis (Slamon et al. 1987; Miller et al. 1994). Her-2 binds to Hsp90 and its endoplasmic reticulum homolog, Grp94 (heat shock protein 90kDa beta) (Xu et al. 2002). Treatment with benzoquinone ansamycins (BA) like Geldanamycin leads to disruption of these complexes, resulting in rapid polyubiquitination of the transmembrane protein followed by its proteasome-dependent degradation (Hartmann et al. 1997).

The proto-oncogene c-Kit encodes the receptor for stem cell factor (SCF) and it is required for normal hematopoiesis. Mutations in Kit result in ligand-independent tyrosine kinase activity, autophosphorylation and uncontrolled cell proliferation (Moriyama et al. 1996). Recent studies report that the Hsp90 inhibitor 17-allylamide-17-demethoxygeldanamycin induces apoptosis and differentiation of Kasumi-1 cells harboring the Asn822Lys Kit mutation and down-regulates KIT protein level (Yu et al. 2006).

The IKK complex, containing two catalytic subunits IKKalpha and IKKbeta and a regulatory subunit NEMO, plays central roles in signal dependent activation of NF-kappaB. Cdc37 and Hsp90 are two additional components of the IKK complex. IKKalpha/IKKbeta/NEMO and Cdc37/Hsp90 form an approximately 900 kDa heterocomplex, which is assembled via direct interactions of Cdc37 with Hsp90 and with the kinase domain of IKKalpha/IKKbeta (Chen et al. 2002).

Cdk4/cyclin D complexes play an essential role during progression through the G1 phase of the cell cycle by phosphorylation of the retinoblastoma protein (Magnuson et al. 1994). The mammalian homolog of the yeast cell cycle control protein Cdc37, p50Cdc37, assembles with Cdk4 in high molecular weight complexes that also contain Hsp90 (Stepanova et al. 1996). Pharmacological disruption of Hsp90 with Geldanamycin results in loss of association of Cdc37 with Cdk4 and half-life of newly synthesized Cdk4 (Stepanova et al. 1996).

Raf-1 is part of a conserved signal transduction pathway that transmits signals from cytosolic and transmembrane tyrosine kinases to mitogen activated protein kinases (Magnuson et al. 1994). Raf-1 kinase associates with the Hsp90 chaperone complex containing

p50Cdc37, leading to Raf-1 stabilization and inhibiting its proteasome-dependent degradation. Disruption of Hsp90 function also inhibits Raf-1 signaling, in part by preventing newly synthesized Raf protein from reaching the plasma membrane (Schulte et al. 1996).

1.3.2 Hsp70 and cochaperones

Hsp70 is a conserved molecular chaperone that can prevent protein aggregation. In particular Hsp70 molecular chaperones play diverse roles in cells, including chaperoning nascent protein chains, assisting in importing of proteins into organelles, enabling survival under stress conditions such as heat shock, and dissociation of macromolecular complexes and aggregates (Bukau et al. 2006; Whitesel et al. 2005). All such functions are mediated by interaction of extended, hydrophobic regions of substrate proteins with the Hsp70 C-terminal substrate-binding domain (SBD). The Hsp70 molecule is composed of an N-terminal 40-kDa ATP-binding domain and a C-terminal 30-kDa substrate-binding domain composed of a α-helical lid topped by a β–sheet base. The dynamic closing and reopening of the base onto the lid is regulated by ATP hydrolysis in the nucleotide-binding domain (Mayer et al. 2005; Popp et al. 2005). In the mammalian system, the molecular chaperones Hsp70 and Hsp90 are involved in the folding and maturation of key regulatory proteins, like steroid hormone receptors, transcription factors, and kinases, some of which are involved in cancer progression. Hsp70 and Hsp90 form a multichaperone complex, in which both proteins are connected by a third one called Hop.

Many proteins function as cochaperones of Hsp90. Aha1 is involved in client protein activation of the Hsp90 sytstem, interacting directly with Hsp90 and activating the basal ATPase activity of Hsp90 (Lotz et al. 2003). Another cochaperone Cdc37 is found associated with a wide range of Hsp90-dependent protein kinases and acts as a specific adaptor or scaffold protein, binding the client protein kinases via its N-terminal region and Hsp90 via its central and C-terminal domains (Silverstein et al. 1998; Shao et al. 2003). The largest definable class of cochaperones and the first to be identified are those that possess one or more TPR domains, a helical coil structure (Das et al. 1998), which binds to an MEEVD motif at the extreme C terminus of Hsp90 (Chen et al. 1998; Young et al. 1998; Radanyi et al. 1994; Owens-Grillo et al. 1996; Carrello et al. 1999; Ratajczak et al. 1996). A closely related IEEVD motif occurs at the C terminus of some Hsp70 chaperone family members and several TPR-domain cochaperones are able to bind to either Hsp90 or Hsp70. Some TPR-domain cochaperones incorporate additional enzymatic functionality: the immunophilin Cyp40 (Smith et al. 1993), the Ser/Thr protein

phosphatase PP5 (Silverstein et al. 1997) and the E3 ubiquitin ligase CHIP (Jiang et al. 2001). CHIP has a single TRP domain that facilitates exclusive binding of either Hsp90 or Hsp70 (Ballinger et al. 1999; Connell et al. 2001). Structural studies of CHIP bound to a C-terminal Hsp70 peptide (Zhang et al. 2005) show an interaction between the TPR domain and the common EEDV motif.

1.3.4 CHIP E3-ligase

Most cellular proteins in eukaryotic cells are targeted for degradation by the 26S proteasome, a eukaryotic ATP-dependent protease, usually after they have been covalently attached to a ubiquitin molecules in the form of a polyubiquitin chain with linkages involving lysine 48 (K48-linked polyubiquitin chain). Polyubiquitination, functions as a degradation signal (Glickman and Ciechanover 2002). Ubiquitynation reaction is catalyzed by a cascade system, consisting of activating (E1), conjugating (E2), and ligating (E3) enzymes. Of these ubiquitilating enzymes, E3s are believed to exist as molecules with a large diversity, presumably in hundreds of species, and play a critical role in the selection of substrate for degradation. The ubiquitin–proteasome system is considered to play a key role in protein homeostasis by catalyzing the immediate destruction of misfolded or impaired (i.e. abnormal) cellular proteins (Bercovich et al. 1997; Jungmann et al. 1993; Lee, 1996). Such protein tend to have exposed hydrophobic regions, which are then recognized by molecular chaperones such as Hsp70 and Hsp90. Molecular chaperones try to prevent these abnormal proteins from irreversible aggregation, and assist in their conversion to a properly folded and functional state. However, when these chaperones fail to refold the abnormal proteins, the ubiquitin–protease system disposes of unfolded, non-functional proteins. CHIP (carboxyl-terminus of Hsp70 interacting protein) was identified as a 35-kDa protein interacting with Hsp70 protein and as a candidate ubiquitin ligase. Thus CHIP is associated with the carboxyl-terminus of Hsp70, Hsc70, and Hsp90 through its TRP and adjacent charged domain (Ballinger et al. 1999; Connell et al. 2001; Meacham et al. 2001).

The other important and unique domain that is not found in other TPR containing proteins is the U-box domain at the carboxyl-terminal region, which resembles the tertiary structure RING-finger domain responsible for E3 activities of many ubiquitin ligases such as c-Cbl, mdm2, Parkin (Aravind and Koonin 2000).

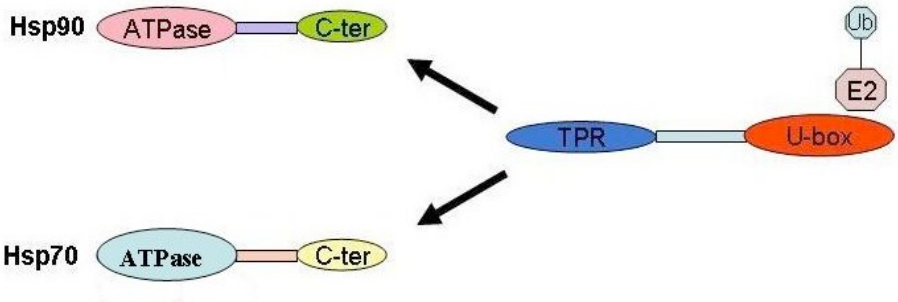

Figure 5. Association of CHIP with molecular chaperones. CHIP associates with the carboxyl terminus of Hsp90 and Hsc70 through its TPR motif at the N-terminus. The U-box domain mediates CHIP interaction with the E2 enzyme bound to Ubiquitin.

As a matter of fact, CHIP is the major E3 ligase associated with the Hsp90-Hsp70 chaperon complexes and responsible for polyubiquitination of misfolded proteins (Fig.5).

1.4 Hsp90 inibitors

Because many of its client proteins are involved in cell signalling, proliferation and survival, Hsp90 is a potential target of anticancer therapy.

HSP90-binding drugs

Binding site	Chemical class	Selected examples
N-terminal ATP-binding pocket	Benzoquinone ansamycin	GA, 17AAG, 17DMAG
N-terminal ATP-binding pocket	Macrolide	Radicicol and related oxime derivatives, zearalenol
N-terminal ATP-binding pocket	Purine scaffold	PU24FC1
N-terminal ATP-binding pocket	Pyrazole	CCT018159
N-terminal ATP-binding pocket	Hybrid	Radamycin, GA dimer, GAtestosterone,GA-oestrogen
C-terminus crosslinker	Noviosylcoumarin	Novobiocin, coumermycin, cisplatin
Unknown Histone	deacetylase inhibitor	Depsipeptide, SAHA

Figure 6. Hsp90-binding drugs

Many classes of natural inhibitors of Hsp 90 have been discovered and some of them have been exploited in clinical trials for different types of tumours (Fig.6).

1.4.1 Geldanamycin and derivatives

Geldanamycin (GA) is a benzoquinone ansamycin that was first isolated as an antibiotic in 1970 from *Streptomyces hygroscopicus* (DeBoer et al. 1970). It was identified along with the ansamycin herbimycin as an agent that was able to revert the phenotype of v-src oncogenes transformed cells and had potent broad based and selective anti-cancer activity against a panel of human tumor cell lines as well as in tumor xengrafts (Whitesell et al. 1992). The co-crystal structure of GA with yeast Hsp90 shows that it binds tightly to the ATP pocket of the N-terminal domain (Roe et al. 1999). The benzoquinone ring is found near the entrance of the binding pocket and the ansa ring is directed towards the bottom of the pocket. When bound to Hsp90, GA adopts a C-shaped conformation similar to that of ADP. GA is a potent cytotoxic agent, but its clinical translation has thus far been precluded by a number of factors (Supko et al. 1995; Neckers et al. 1999). First, it exhibits severe hepatotoxicity, which has been associated with the benzoquinone ring and imposes strict dosing limitations. Secondly, it is metabolically and chemically unstable. Also, it has very low solubility in aqueous media resulting in formulations requiring DMSO. As a result, a substantial effort has been made in modifying its structure to improve safety, stability, potency and water solubility. Much effort has been made at modifying the quinone ring, especially at the 17-position but also at the 19-position (Schnur et al. 1995; Tian et al. 2004). The derivative 17-allylamino-17-desmethoxy-geldanamycin (17-AAG) has potent in vivo activity and is less toxic than GA (Solit et al. 2002; de Candia et al. 2003) (Fig.7). 17-AAG entered clinical trials in cancer patients in the US and UK (Sausville et al. 2003; Goetz et al. 2005). Although initial trials were disappointing, development of an improved formulation of 17-AAG by Kosan Pharmaceuticals resulted in KOS-953 (Tanespimycin), a clinical agent with promising activities. Under the new formulation, encouraging clinical results were noted in trastuzumab-refractory HER2-positive breast cancer and in multiple myeloma, especially in bortezomib-refractory patients (Solit et al. 2008).

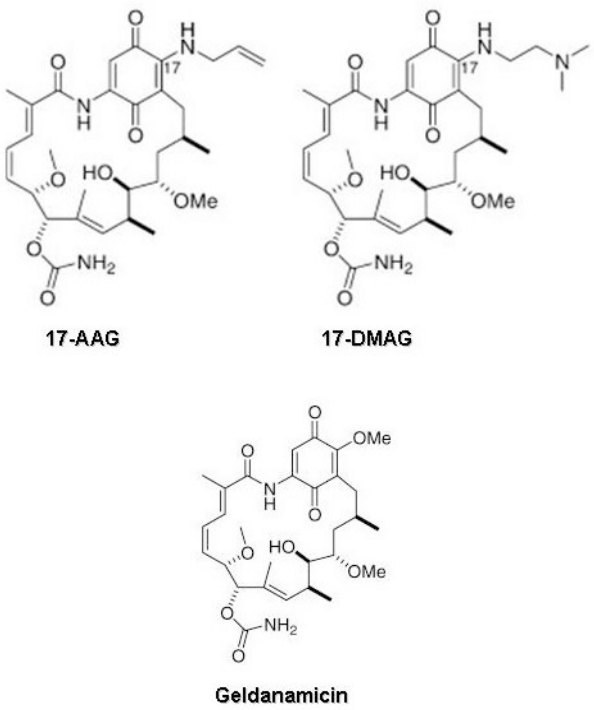

Figure 7. Chemical structures of Geldanamicin and its derivates

Despite its promising activity in clinical studies, 17-AAG has several limitations that restrict its optimal clinical development. A lack or reduced activity of this agent in certain cells has been observed due to drug efflux by multidrug resistance elements or metabolic inactivation of these agents by nucleophiles, such as glutathione. In addition, 17-AAG has a liability with respect to metabolism by the polymorphic cytochrome P450. Finally, the compound is also reductively metabolized by the polymorphic oxidoreductase NQO1 or DT-diaphorase to a more potent hydroquinone inhibitor, which introduces another source of pharmacological variability and potential for drug resistance (Solit et al. 2008).

1.4.2 Radicicol

Radicicol (RD) is a macrocyclic lactone antibiotic first isolated from the fungus Monosporium bonorden (Delmotte et al. 1953). It can reverse the transformed phenotype of v-src transformed fibroblasts (Kwon et al. 1992) and suppress transformation by the Ras oncogenes (Zhao et al. 1995). It specifically binds to the N-terminal domain of Hsp90 and depletes SKBr3 cells of the receptor tyrosine kinase Her2, Raf-1 and mutant p53 (Schulte et al. 1998; Sharma et al. 1998). It also inhibits Ras-dependent phosphorylation of MAPK in K-Ras transformed rat epithelial cell lines by destabilization of Raf-1 protein

(Soga et al. 1998).

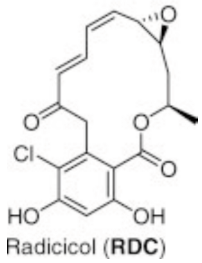

Figure 8. Chemical structure of Radicicol

The co-crystal structure of RD with yeast Hsp90 shows that it binds tightly to the N-terminal ATP-pocket in a C-shaped conformation similar to ADP (Roe et al. 1999). Occupancy of this pocket by RD disrupts chaperone function resulting in an inactive Hsp90-protein complex. It has cellular effects similar to ansamycins but lacks hepatotoxicity (Soga et al. 2003). RD is not stable in serum and thus has no activity in vivo (Soga et al. 1999)(Fig.8).

1.4.3 Novobiocin

Novobiocin, a cumarin-type antibiotic, antagonizes Hsp90 function in vitro and in vivo in a manner similar to GA and radicicol that have a binding site in the N-terminal domain of Hsp90. On the contrary, the binding site of novobiocin is the C-terminal domain of Hsp90 and the cells expose to novobiocin demonstrate rapid destabilization of various Hsp90 client proteins, including Raf-1, mutated p53, p60 (v-Src), and p185 (Her2).

The structural requirements for novobiocin binding to Hsp90 are unique. Analysis of progressively smaller C-terminal Hsp90 peptides revealed the novobiocin-binding site to be contained within amino acids 538-728 (Marcu et al. 2000).

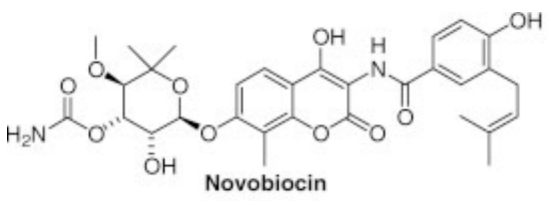

Figure 9. Chemical structure of Novobiocin

Within this region, the removal of amino acids 657-677 severely compromised novobiocin binding and synthetic peptide composed of amino acids 663-676 efficiently competed the binding of Hsp90 to immobilized novobiocin (Marcu et al. 2000). These data localize the novobiocin-binding site to a region in Hsp90 known to be important both for its dimerization and association of other co-chaperones (Marcu et al. 2000)(Fig.9).

2. AIMS OF STUDY

The RET receptor tyrosine kinase might represent a key target in the treatment of RET-dependent Medullary Thyroid Carcinoma (MTC). Several small molecular weight kinase inhibitors were shown to inhibit constitutively active RET tyrosine kinase. Recently a Phase II clinical study to evaluate the efficacy and tolerability of ZD6474 in patients with advanced or metastatic hereditary MTC has been launched by AstraZeneca.

Alternatively to enzymatic inhibiton, oncogenic kinases can be targeted by altering protein stability through blockade of the Hsp90 chaperone function with Geldanamycin-derived compounds.

A previous report showed that RET/PTC1 (the H4-RET fusion product) was degraded upon treatment with the Geldanamycin (GA) derivative 17-Allylammino-17-Demethoxygeldanamycin (17-AAG) (Marsee et al. 2004). In addiction, Cohen and coworkers reported that 17-AAG was able to block RET C634W phosphorylation in MTC-derived cells without affecting total RET protein levels.

Here we investigated the molecular pathway responsible for degradation of the receptor tyrosine kinase RET upon inhibition of Heat Shock Protein 90 (Hsp90) by 17-Allyl-Ammino-17-demethoxygeldanamycin (17-AAG) and the biological effects of such compound in MTC-derived cell lines.

In particular:

- We verified 17-AAG-mediated dose and time dependent degradation of wt RET protein and MEN2-associated RET mutants exogenously expressed in RAT1 murine fibroblasts.

- We identified the molecular pathway responsible for 17-AAG-induced proteasome-dependent degradation of RET

- We analyzed the molecular and cellular effects of 17-AAG on human MTC cell lines endogenously expressing MEN2-associated RET oncogenic mutants

3.MATERIALS AND METHODS

3.1 Compounds

17-allylamino-17-demethoxygeladamycin and radicicol were purchased at Calbiochem. Stock solutions (1.7 mM) were made in 100% DMSO and diluted with culture media before use. Culture media containing an equivalent DMSO concentration served as vehicle controls.

3.2 Cell culture and plasmids

Mutations C634R, M918T, A883F, E768D, L790F, Y791F, V804L, V804M and S891A were introduced in RET-9 cDNA, encoding the short isoform of RET protein, cloned in the pBABE expression vector and stably transfected in RAT1 cells (Pasini et al. 1997). Parental RAT1 cells and RAT1 transfected with RET wt and RET mutants were cultured in DMEM supplemented with 10% fetal calf serum, 2 mM L-glutamine and 100 units/ml penicillin-streptomycin (GIBCO). HEK293 and HeLa cells were from American Type Culture Collection (ATCC, Manassas, VA) and were grown in Dulbecco's Modified Eagle Medium (DMEM) supplemented with 10% fetal calf serum (GIBCO, Paisley, PA). PCDNA 3.1 CHIP-myc, CHIP-ΔU-myc (H260Q) and CHIP-TPR-myc (K30A) vectors were a kind gift by Len Neckers (Xu et al. 2002). PCDNA-HA-Ubiquitin vector was a kind gift by S. Giordano. Transient transfections were carried out with the lipofectamine reagent according to manufacturer's instructions (GIBCO). Cells were seeded at a density of $1.5x10^6$/dish the day before transfection, transfected with 5 μg of DNA and harvested 48 hours later. The TT and the MZCRC1cell lines, derived from a MTC harboring the RET/C634W and RET/M918T mutations, respectively (Carlomagno et al. 1995), were cultured in RPMI with 20% fetal calf serum, 2 mM L-glutamine and 100 units/mL penicillin-streptomycin (GIBCO).

3.3 Immunoblotting

Protein lysates were prepared according to standard procedures. Cells were lysed in a buffer containing 50 mM N-2-hydroxyethylpiperazine-N'-2-ethanesulfonic acid (HEPES; pH 7.5), 1% (vol/vol) Triton X-100, 150 mM NaCl, 5 mM EGTA, 50 mM NaF, 20 mM sodium pyrophosphate, 1 mM sodium vanadate, 2 mM phenylmethylsulphonyl fluoride (PMSF), and 1 μg/ml aprotinin. Lysates were clarified by centrifugation at 10,000 x g for 15 min.

Lysates containing comparable amounts of proteins, estimated by a modified Bradford assay (Bio-Rad, Munchen, Germany), were subjected to western blot. Immunocomplexes were detected with the enhanced chemiluminescence kit (Amersham Pharmacia Biotech, Little Chalfort, UK). Anti- Hsp90 (#SPA-835) and anti-Hsp70 (#SPA-810) were purchased from Stressgen biotechnologies, Victoria, BC, Canada. Anti-phospho-SHC (Y317) (#07-206) was from Upstate Biotechnology, Lake Placid, NY, USA. Anti -MAPK (#9101) and anti-phospho-MAPK (#9102) were from New England Biolabs (Beverley, MA). Anti-MYC (sc-40) and anti-HA (sc-7392) antibodies were from Santa Cruz Biotechnology (Palo Alto, CA). Anti-poly(ADP-ribose) polymerase (anti-PARP) monoclonal antibody, which detects full-length PARP and the large fragment (89 kDa) produced by caspase cleavage, was from BD Biosciences (#556494). Anti-RET is a polyclonal antibody raised against the tyrosine kinase protein fragment of human RET (Santoro et al. 1994). Anti-phosphoRET are affinity-purified polyclonal antibodies raised against RET peptides containing phosphorylated Y905 (Iwashita et al. 1996; Carlomagno et al. 2003). Secondary antibodies coupled to horseradish peroxidase were from Biorad, Munchen, Germany.

3.4 Luciferase activity

Transient transfections were carried out with the lipofectamine reagent according to manufacturer's instructions (GIBCO). $1x10^6$ HeLa cells were transiently transfected with vector expressing RET/C634R or with the empty vector. We used two reporter vectors: the AP1-Luc vector (Stratagene, Garden Grove, CA) containing six AP1 binding sites upstream from the *Firefly* luciferase cDNA or the MYC-Luc vector containing the MYC gene promoter sequence. MYC-Luc vector was kindly provided by S. J. Gutkind. Twenty-four hours after transfection, cells were serum-starved. Ten ng of pRL-null (a plasmid expressing the enzyme Renilla luciferase from *Renilla reniformis*) was used as an internal control of transfection efficiency. *Firefly* and *Renilla* luciferase activities were assayed using the Dual-Luciferase Reporter System (Promega Corporation, Madison, WI). Light emission was quantitated using a Berthold Technologies luminometer (Centro LB 960) and expressed as ratio of *Firefly* and *Renilla* luciferase activities . The ANOVA Post-Hoc Tukey-Kramer multiple comparison test was used to assess statistical significance of luciferase assay. InStat3 GraphPad Software was used.

3.5 BrdU incorporation and TUNEL assay

For BrDU incorporation analysis, cells were seeded on glass

coverslips. The day after cells were treated with 100 or 500 nM 17-AAG or vehicle for 24 or 48 hours. Bromodeoxyuridine (BrdU; Sigma Chemical Co.) was added to the cell culture media at a final concentration of 100μg/ml for two hours before harvest. Cells were fixed with paraformaldehyde (4%) and permeabilized with Triton X-100 (0.2%) prior to staining. Coverslips were incubated with anti-BrdU mouse monoclonal antibody and then with a Texas red-conjugated anti-mouse antibody (Boehringer Mannheim, Germany). All coverslips were counterstained in PBS containing Hoechst 33258 (final concentration, 1μg/ml; Sigma Chemical Co.), rinsed in PBS and mounted in Moviol on glass slides. The fluorescent signal was visualized with an epifluorescent microscope (Axiovert 2, Zeiss) interfaced with the image analyzer software KS300 (Zeiss).

For terminal desoxynucleotidyl transferase-mediated desoxyuridine triphosphate nick end-labeling (TUNEL), cells were seeded on glass coverslips. The day after cells were treated with 100 or 500 nM 17-AAG or vehicle for 24 or 48 hours. Then, cells were fixed in 4% (w/v) paraformaldehyde and permeabilized by the addition of 0.1% Triton X-100/0.1% sodium citrate. Slides were rinsed twice with PBS, air-dried and subjected to the TUNEL reaction (Roche). All coverslips were counterstained in PBS containing Hoechst 33258, rinsed in water and mounted in Moviol on glass slides. The fluorescent signal was visualized with an epifluorescent microscope (Axiovert 2, Zeiss) (equipped with a 100X objective) interfaced with the image analyzer software KS300 (Zeiss).

4. RESULTS

4.1 17-AAG induced degradation of wt RET and C634R oncogenic mutant.

We first explored whether inhibition of Hsp90 by 17-AAG could induce degradation of RET wt and RET C634R proteins, stably transfected in RAT1 murine fibroblasts. RET protein abundance was measured by Western blotting. Anti-RET antibody recognized two molecular species of 150 and 170 kDa, that corresponded to the high mannose immature form of the receptor (150kDa) and the plasma membrane-associated mature form of RET (170 kDa), respectively (Carlomagno, 1996). As shown in Fig. 10A and B, upon treatment with 17-AAG, both wt RET and C634R mutant were degraded with a similar kinetics in a time and dose dependent fashion. After 8 hours of treatment, 20 nM dose was able to induce partial degradation of both proteins; 50 nM 17-AAG reduced protein levels to less than 50%. Both 150 and 170 kDa isoforms decreased upon 17-AAG treatment, althought the 170 kDa one, being less abundant, almost disappeared.

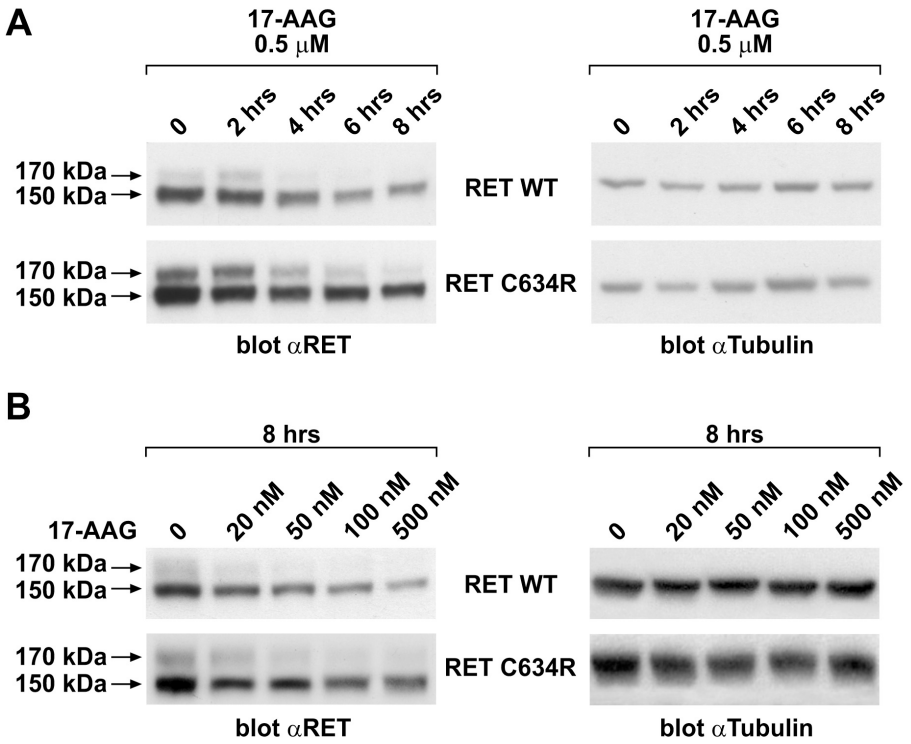

Figure 10. RET wt and RET C634R mutant degradation by 17-AAG treatment– RAT1 cells stably transfected with RET wt or RET/C634R expressing vectors were treated for the indicated time points with the indicated concentration of Hsp90 inhibitor 17-AAG. Equivalent amounts of protein lysates were subjected to Western blotting with αRET or with αTubulin for normalization. The 150 and 170 kDa RET forms are indicated.

We also tested if Radicicol, a different Hsp90 inhibitor (Workmann et al. 2007), was able to induce degradation of RET wt and C634R mutant. As shown in Fig 11 both RET wt and C634R were sensitive to Radicicol-induced degradation in a dose dependent manner. Once again both RET 150 and 170 KDa isoforms were sensitive to the compound induced degradation with an IC50 dose between 20 and 50 nM.

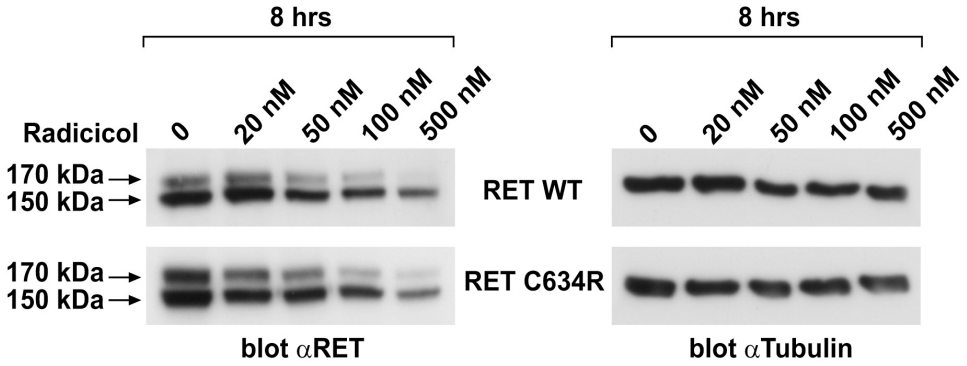

Figure 11. RET wt and RET C634R mutant degradation by Radicicol treatment – RAT1 cells stably transfected with RET wt or RET/C634R expressing vectors were treated for 8 hrs with the indicated concentration of Radicicol. Equivalent amounts of protein lysates were subjected to Western blotting with αRET or with αTubulin for normalization. The 150 and 170 kDa RET forms are indicated.

4.2 17-AAG induced degradation of MEN2-associated RET tyrosine kinase domain mutants

In order to verify if 17-AAG was able to induce degradation of RET intracellular mutants associated to MEN2 syndromes, we performed a time course experiment using the RAT1 cells stably transfected with RET E768D, L790F, Y791F, V804M, A883F, F891A and M918T mutants. As shown in figure 12A, all RET isoforms displayed a degradation kinetic similar to RET wt and C634R mutant. Besides, we tested the degradation of RET V804M and RET M918T proteins in a dose response experiment. RET V804M mutation has been reported to be associated to sporadic and familial cases of MTC and corresponds to RET gatekeeper site mediating resistance to small molecular weight kinase inhibitors, such as PP1, PP2 and ZD6474 (Carlomagno et al. 2004). M918T is RET most frequent mutation in sporadic MTC and, in familial cases, is associated to the very aggressive MEN2B phenotype (Ponder 1999). RET V804M and RET M918T proteins showed a degradation profile identical to wild type and C634R (Fig. 12B).

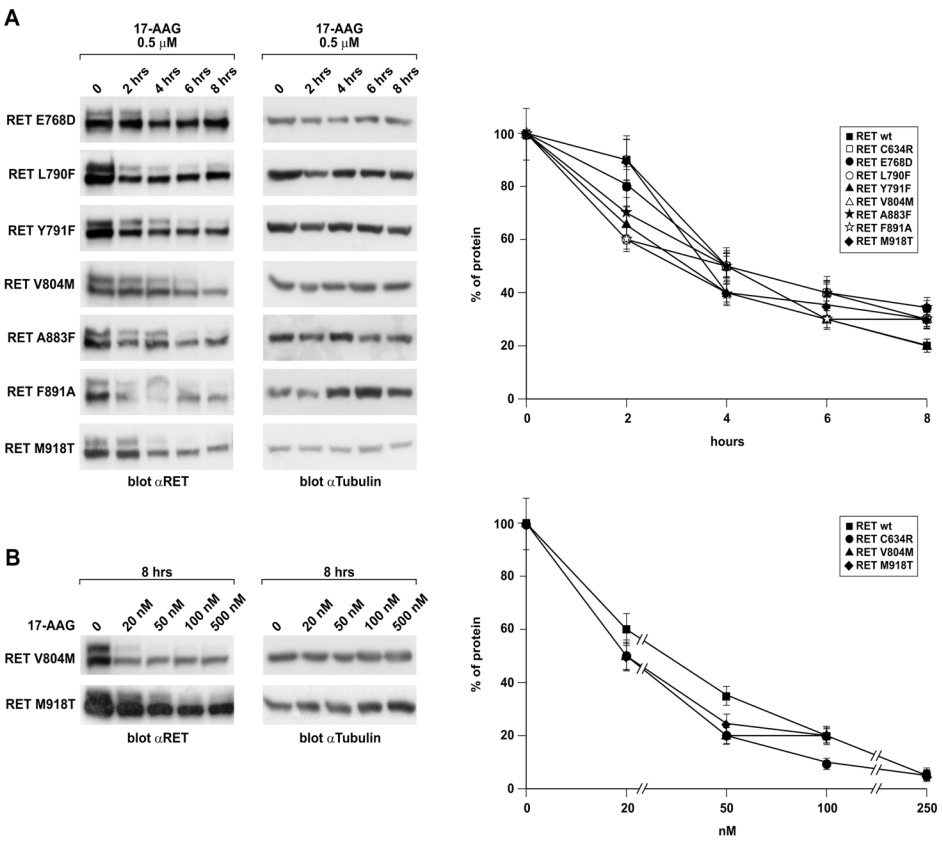

Figure 12. Sensitivity of RET kinase domain mutants to 17-AAG –RAT1 cells stably transfected with RET E768D, L790F, Y791F, V804M, A883F, F891A and M918T expressing vectors were treated for the indicated time with the indicated concentration of 17-AAG. Protein lysates were subjected to Western blotting. Average densitometric analysis of three independent experiments were reported (also from Fig 12A and B). SD are indicated. Values represent the % of signal compared to non-treated cells.

4.3 Analysis of molecular pathway mediating RET degradation upon 17-AAG treatment

We decided to characterize the molecular pathway responsible for RET degradation after treatment with 17-AAG. 17-AAG induced degradation of RET C634R in RAT1 cells was mediated by 26S protaesome since it could be hindered by the proteasome inhibitor MG132 (Fig.13A). Overexposure of the Western Blot filter of RAT1 C634R cells treated with MG132 displayed an accumulation of high molecular weigh bands recognized by the anti-RET antibody. Most likely those bands corresponded to polyubiquitinated forms of the receptor saved from degradation by the proteasome inhibition. These species increased in the presence of 17-AAG indicating that 17-AAG induced proteosomal degradation through polyubiquitination of the receptor (Fig.13B) and therefore Hsp90 was required for the correct

folding and stabilization of the RET protein.

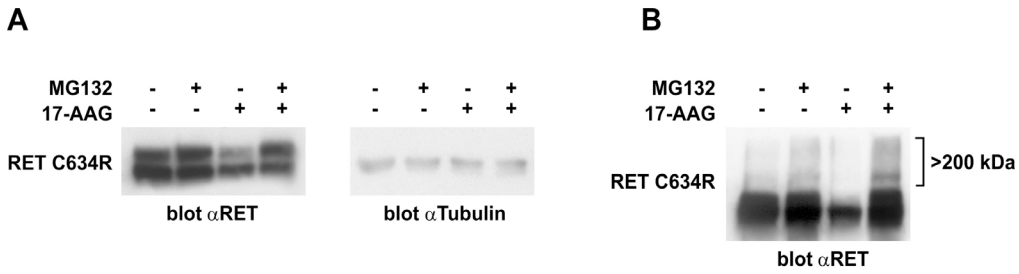

Figure 13. 17-AAG-mediated degradation of RET/C634R depends on proteasome –RAT1 cells transfected with RET/C634R were treated for 4 hours with vehicle or 40 μM MG132 and/or 0.5 μM 17-AAG. Equivalent amounts of proteins were subjected to Western blotting with the indicated antibodies. In *B,* the position of protein species that migrate above the 200 kDa marker is indicated (> 200 kDa).

We performed co-immunoprecipitation experiment to verify interaction between stably transfected RET C634R mutant and endogenous Hsp90 and Hsp70 proteins in RAT1 cells. As shown in figure 14, RET interacted with Hsp90 at the steady state and this interaction was decreased by treatment with 17-AAG. Oppositely, RET interaction with Hsp70 was stabilized in the presence of 17-AAG. In summary, these data clearly indicated that RET was a Hsp90 client protein whose inhibition by 17-AAG mediated polyubiquitination of RET and degradation by proteasome.

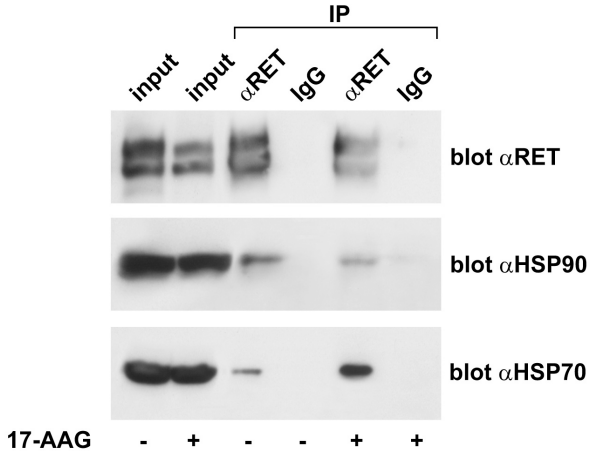

Figure 14. RET/C634R interaction with the Hsp90/Hsp70 chaperone complex –RAT1 cells stably transfected with RET/C634R were treated for 4 hours with vehicle or with 0.5 μM 17-AAG. Equivalent amounts of RET proteins were subjected to immunoprecipitation with preimmune (IgG) or αRET sera followed by Western blotting with the indicated antibodies.

We ought to test whether RET, as many Hsp90 client proteins, represented a CHIP E3 ligase substrate. Therefore, we transfected RET C634R and myc-tagged wt-CHIP-E3 ligase or two defective myc-tagged CHIP mutants (CHIP-TPR and CHIP-ΔU) in HEK293 cells in order to 1) verify RET protein stability upon overexpression of CHIP and 2) its interaction with the E3 ligase by co-immunoprecipitation experiment. As already discussed, CHIP interacts with Hsp70 via the tetratricopeptide repeat (TPR) present in the N-terminal domain of the protein while the enzymatic activity depends on the U-box motif present in C-terminal domain that is necessary to interact with ubiquitin and E2 enzyme. CHIP proteins deprived of TPR (CHIP-TPR) or the U-box motif (ΔU) function as defective mutants, being unable to interact with the Hsp90/70 chaperone complex or with ubiquitin-bound E2 protein, respectively (Xu et al. 2002). As shown in Fig 15A and 15B, overexpression of CHIP wt, but not of its defective mutants, induced a decrease of total amount of RET C634R protein. In addition, CHIP wt protein was co-immunoprecipitated by the anti-RET antibody, indicating interaction between the two proteins (Fig.15B).

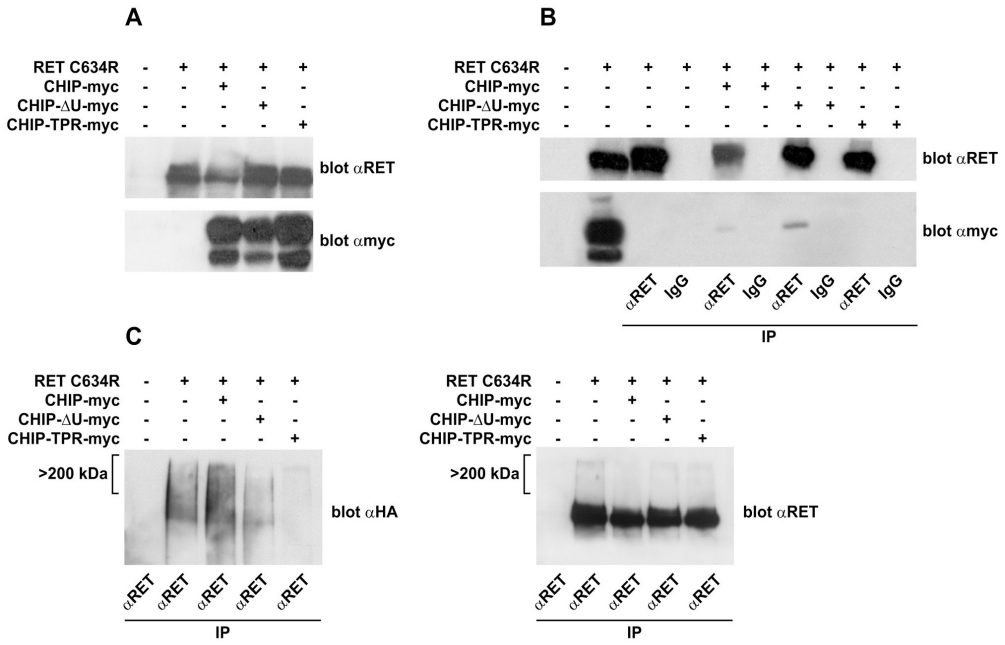

Figure 15. RET C634R interaction with CHIP – *A, B)* HEK293 cells were transiently transfected with RET/C634R in association with CHIP-myc, CHIP-ΔU-myc or CHIP-TPR-myc or with the empty vector. Equivalent amounts of protein lysates were subjected to (*A*) direct Western blotting with the indicated antibodies or (*B*) immunoprecipitation with preimmune (IgG) or αRET sera followed by Western

blotting with the indicated antibodies. *C*) HEK293 cells were transiently transfected with PCDNA-Ubiquitin-HA and the expressing vectors for RET/C634R, together with CHIP-myc, CHIP-ΔU-myc or CHIP-TPR-myc. Equivalent amounts of protein lysates were subjected to immunoprecipitation with anti-RET antibody and then subjected to western blotting with αHA and αRET antibodies, as indicated. The position of protein species that migrate above the 200 kDa marker is indicated (> 200 kDa).

CHIP TRP lost the capacity to interact with RET while CHIP ΔU was still found in association with it, as expected (Fig.15B). Finally, to verify if CHIP wt induced an accumulation of polyubiquitinated species of RET, we transfected HEK293 cells with HA tagged ubiquitin, RET C634R, wt-CHIP-E3 ligase or the two defective myc-tagged CHIP mutants (CHIP-TPR and CHIP-ΔU) and we performed an immunoprecipitation experiment with anti-RET antibody followed by western blotting with anti-HA antibody or anti-RET antibody as a control. As shown in Fig. 15C CHIP wt was able to induce an accrual of polyubiquitinated species of RET protein, differently from the two defective mutants that indeed displayed a dominant negative effect on RET endogenous polyubiquitination.

4.4 Blockade of RET C634R signalling by 17-AAG

MEN 2 mutations cause ligand-independent hyper-activation of RET switching on different oncogenic signaling cascades. As an example, murine fibroblasts transformed by RET C634R oncogenic mutant display constitutive RET-mediated phosphorylation of SHC protein that in turn activates the Ras/MAPK pathway (Ohiwa et al. 1997). We tested if 17-AAG was able to induce a block of RET-dependent activation of this pathway. We performed western blotting experiments using total and phospho-specific antibodies to analyze protein extracts from RAT1 cells treated with increasing concentration of 17-AAG. As expected, decrease of RET protein was accompanied to a proportional decrease of RET phosphorylation in these cells (Fig.16) (Fujita et al. 2002). Phosphorylation levels of SHC and of the MAPK ERK1/2 were decreased as well, without any effect on total protein stability (Fig.16). Thus SHC and ERK1/2 have never been described as Hsp90 client proteins and their phosphorylation reduction is a direct effect of RET signaling drop.

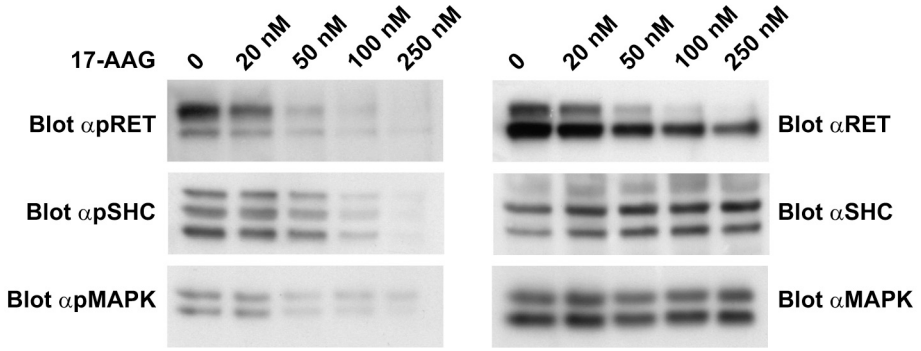

Figure 16. 17-AAG-mediated block of RET/C634R signalling – RAT1 cells stably transfected with RET C634R were treated for 4 hours with the indicated concentration of 17-AAG. Protein lysates were subjected to Western blotting with the indicated antibodies.

To confirm the inhibitory action of the 17-AAG on RET signaling pathway we performed luciferase assay in which we detected the activation of promoters known to be responsive to Receptor Tyrosine Kinases (RTK). We transfected Hela cells with an AP1-responsive and the Myc gene promoters, fused to the luciferase reporter, along with RET C634R expressing vector or the vector alone as a control. As shown in Fig. 17A and 17B RET C634R was able to activate expression of the reporter gene of 5-10 fold. 17-AAG reduced RET C634R activity to less than 50% at 50 nM and completely abolished promoter

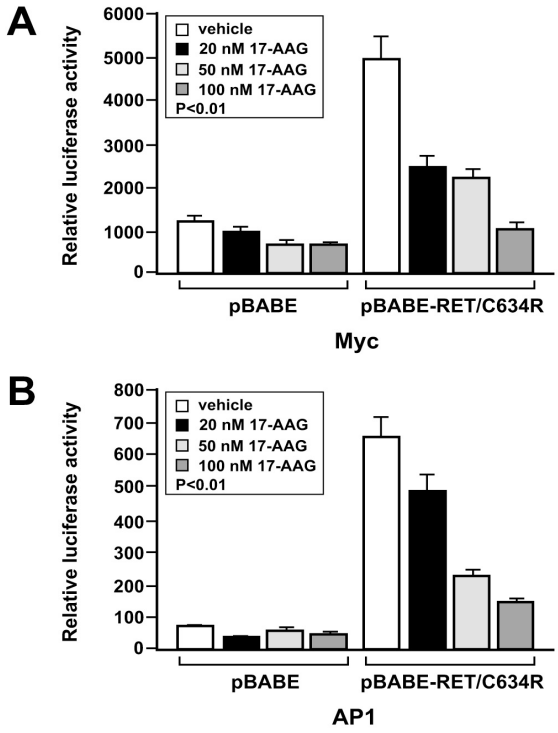

Figure 17. 17-AAG-mediated block of RET/C634R activation of Myc and AP1 promoters –1x10^6 HeLa cells were transiently transfected with RET/C634R together with the AP1-Luc or the Myc-Luc reporters. pRL-null served as an internal control. Average results of three independent assays ± SD are indicated. The ANOVA Post-Hoc Tukey-Kramer multiple comparison test was used to assess statistical significance (P< 0.01).

activation at 100 nM, in agreement with reduction of RET protein levels and downstream signalling. No effect was observed in control cells, transfected with the empty vector.

Finally, we tested the capability of 17-AAG to induce degradation and block of signalling of RET endogenous protein. We used two human medullary thyroid carcinoma-derived cell lines, TT and MZCRC1, which endogenously express RET C634W and RET M918T, respectively (Carlomagno et al. 1994). As shown in Fig. 18A and 18B, in MTC cells 17-AAG induced degradation of RET protein with a sligthly lower efficiency compared to the exogenous protein expressed in RAT1 cells. As expected, also RET phosphorylation and RET-dependent activation of Ras/MAPK pathway, measured as SHC and MAPK phosphorylation, were decreased.

We also analyzed the cellular effects of 17-AAG treatment in MTC cells. After 24 and 48 hours of treatment, the compound caused, in both cell lines, a decrease of DNA synthesis, measured by incorporation of BrdU (Fig.19A). Growth arrest was not mediated by

induction of programmed cell death as shown by TUNEL assay after 72 hours of cell treatment with 17-AAG (0.1 μM and 0.5 μM) (Fig.19A). Absence of apoptosis was also confirmed by Western blotting experiment in which we used anti-poly(ADP-ribose) polymerase (anti-PARP) monoclonal antibody, which detects full-length PARP and the large fragment (89 kDa) produced by caspase cleavage (Fig.19B)

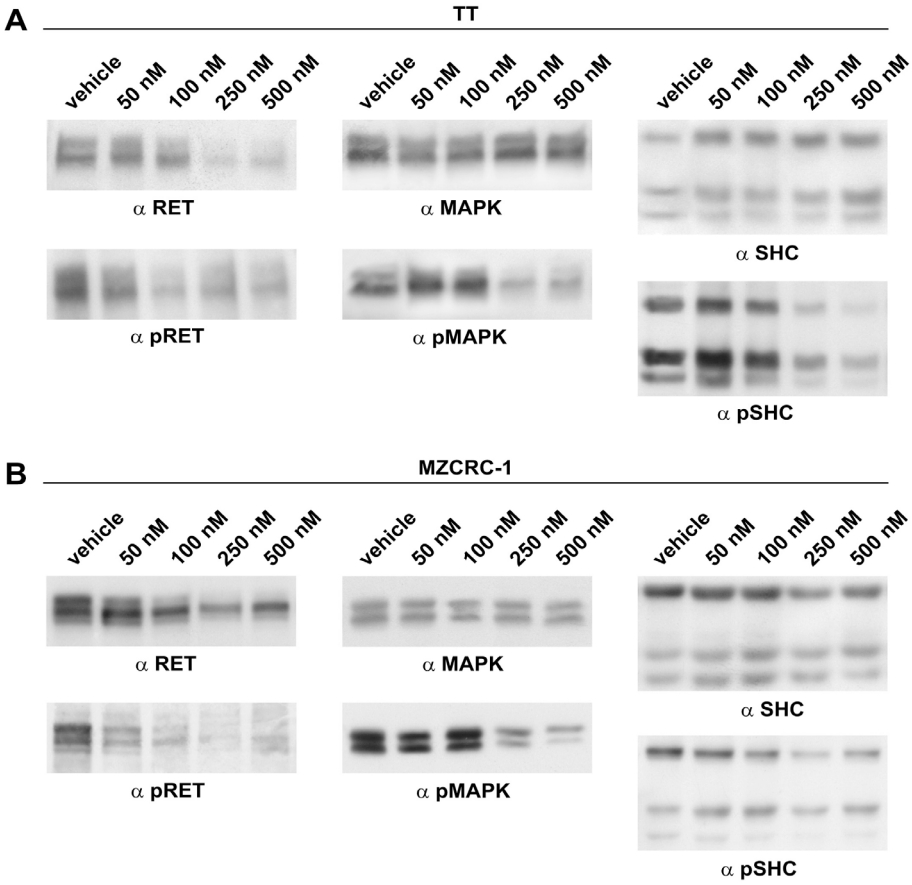

Figure 18. 17-AAG-mediated RET degradation and blockade of signaling in MTC cells –MZCRC-1 and TT cells were treated for 16 hours with 17-AAG. Protein lysates were subjected to Western blotting with the indicated antibodies.

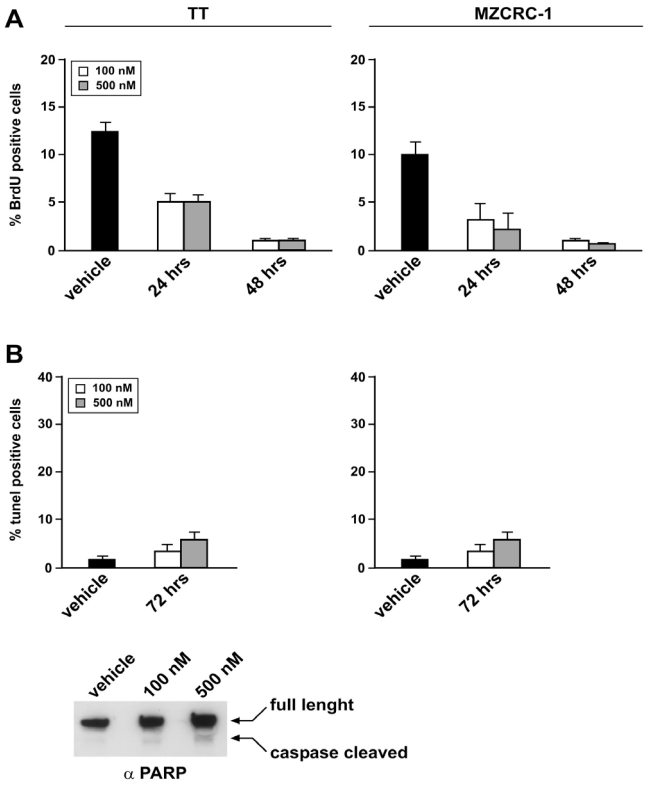

Figure 19. 17-AAG-mediated growth arrest in MTC cells –*A*) Cells were treated with 17-AAG, incubated with BrdU and then subjected to immunofluorenscence with anti-BrdU antibody. *B*) TT and MZCRC1 cells were treated for 72 hours with 17-AAG and then subjected to TUNEL assay or to Western blotting with anti-PARP antibody.

5. Conclusions

In this paper we showed that protein stability of the receptor tyrosine kinase RET and its C634R mutant required Hsp90 chaperone function. Thus, 17-Allyl-Ammino-17-demethoxygeldanamycin (17-AAG), a benzoquinoid ansamycin antibiotic, structurally related to Geldanamycin, and functioning as a specific inhibitor of the Heat Shock Protein 90 (Hsp90), reduced protein stability of both wt RET and C634R mutant in RAT1 cells. 17-AAG induced proteasome dependent degradation of RET C634R oncogenic protein mutant, interfering with Hsp90/RET interaction and stabilizing Hsp70/RET complex. We also demonstrated that RET C634R was polyubiquitinated by the E3 ligase CHIP wt but not by its defective mutants CHIP-ΔU and CHIP-TPR. 17-AAG was able to interfere with RET C634R dependent activation of specific signalling pathways, resulting in hindrance of AP1-responsive and Myc gene promoters activation by oncogenic RET. Interestingly, none of the most common MEN2-associated mutations in the tyrosine kinase domain of RET affected the receptor sensitivity to 17-AAG induced degradation. Finally, we observed that in MTC-derived cells, TT and MZCRC1, 17-AAG treatment induced degradation of endogenously expressed RET C634W and M918T oncogenic mutants. We also observed a complete reduction of BrdU incorporation while induction of apoptotis was almost absent. Being 17-AAG a multi-targeted drug, we believe that block of proliferation was due to a pleiotropic effect of 17-AAG on several Hsp90 client proteins' stability, rather than on RET alone.

Inhibition of Hsp90 by ansanamycin-derived antibiotics affects several receptor tyrosine kinases protein stability such as HER family members, KIT, RON and PDGFRalpha (Citri et al. 2004a; Fumo et al. 2004; Germano et al. 2006; Matei et al. 2007). Moreover, mutational activation of some of them, like EGFR, was shown to be associated to increased dependence on Hsp90 function compared to wt protein, probably due a conformational effect on receptor structure (Shimamura et al. 2005). On the contrary, here we showed that RET oncogenic mutants, carrying mutations in the IC or EC domains, displayed a kinetic of degradation basically identically to the RET wt protein. Therefore, it might be envisaged that such mutations do not influence normal folding and stability of the protein and do not change RET sensitivity to Hsp90 inhibitors. This is also true for the chimeric RET/PTC oncoproteins, which could be suspected to be more prone to alteration in folding, resulting from the fusion of two different proteins. As matter of fact, in murine fibroblasts RET/PTC3 protein stability was equally affected by 17-AAG treatment as wt RET and RET C634R

mutant (data not shown).

Hsp90 protein has been shown to recognize a common surface in the amino-terminal lobe of client kinases from diverse families. In particular, the αC-β4 loops surface electrostatics determines the interaction with Hsp90 chaperone complex, and therefore protein sensitivity to its inhibition (Citri et al. 2006; Xu et al. 2005; Tikhomirov et al. 2003). A neutral/positive surface charge is characteristic of Hsp90 client kinases while non-Hsp90 dependent kinases display a negative surface charge (Citri et al. 2006). Mutations in this region might alter interaction with the chaperone and mediate evasion from the Hsp90/70 control, resulting in hyperactivation (Citri et al. 2004b; Shigematsu et al. 2005). RET L790 and Y791 are localized in the αC-β4 loops which overall display a neutral/positive surface charge in RET. Nevertheless, MEN2 L790F and Y791F changes are not associated to altered sensitivity to 17-AAG, suggesting that these mutations do not activate RET by increasing its stability.

Beside understanding the physiological mechanisms that regulate stability of RET protein, our findings provides a rationale for targeting RET by geldanamycin-like compounds in MTC patients. Efficacy of RET targeting as a therapeutic tool for this tumour has been proven in several preclinical settings (Drosten et al. 2004; Vidal et al. 2005; Carlomagno et al. 2006). In addition, phase II clinical trials with RET kinase inhibitors are active for patients affected by familial or sporadic Medullary Thyroid Carcinoma (Santoro et al. 2006; Schlumberger et al. 2008; Wells et al. 2006). Beside enzymatic inhibition, an additional targeting strategy for RET in MTC patients might be represented by induction of protein degradation by Hsp90 inhibitors.

6 Acknowledgments

This study was carried out at the Dipartimento di Biologia e Patologia Cellulare e Molecolare “L.Califano”, Università di Napoli “Federico II” and Istituto di Endocrinologia ed Oncologia Sperimentale “G. Salvatore” of the Consiglio Nazionale delle Ricerche, Napoli.

I want to express my gratitude to Professor Giancarlo Vecchio, coordinator of International Doctorate Program, Università di Napoli “Federico I”, to Professor Massimo Santoro, for his valuable scientific guidance over all these years and to my supervisor Dr. Francesca Carlomagno, who made this thesis possible helping me in troubleshooting the difficulties I faced during my PhD. I’m greatful to Dr. Teresa Guida for her aid in the laboratory. I thank my collegues Dr. Daniela De Majo, Dr. Elvira Avilla and Dr. Livia Provitera and all other members of the lab for creating the most enjoyable working atmosphere.

Finally I want to thank my family for their support during this three years of PhD.

7 References

Alberti L, Borrello MG, Ghizzoni S, Torriti F, Rizzetti MG, Pierotti MA. Grb2 binding to the different isoforms of Ret tyrosine kinase. Oncogene 1998;17:1079-87.

Andreozzi F, Melillo RM, Carlomagno F, Oriente F, Miele C, Fiory F, Santopietro S, Castellone MD, Beguinot F, Santoro M, Formisano P. Protein kinase Calpha activation by RET: evidence for a negative feedback mechanism controlling RET tyrosine kinase. Oncogene 2003;22:2942-9.

Aravind, L, Koonin, E. V. The U box is a modified RING finger—A common domain in ubiquitination. Current Biology 2000; 10: R132–134.

Arighi E, Alberti L, Torriti F, Ghizzoni S, Rizzetti MG, Pelicci G, Pasini B, Bongarzone I, Piutti C, Pierotti MA, Borrello MG. 1997. Identification of Shc docking site on Ret tyrosine kinase. Oncogene 1997;14:773-82.

Asai N, Murakami H, Iwashita T, Takahashi M. A mutation at tyrosine 1062 in MEN2A-Ret and MEN2B-Ret impairs their transforming activity and association with shc adaptor proteins. J Biol Chem 1996;271:17644-9.

Ballinger CA, Connell P, Wu Y, Hu Z, Thompson LJ, Yin LY, Patterson C. Identification of CHIP, a novel tetratricopeptide repeat-containing protein that interacts with heat shock proteins and negatively regulates chaperone functions. Molecular Cell Biology 1999; 19: 4535–4545.

Begum S, Rosenbaum E, Henrique R, Cohen Y, Sidransky D & Westra WH 2004 BRAF mutations in anaplastic thyroid carcinoma: implications for tumor origin, diagnosis and treatment. Modern Pathology 17 1359–1363.

Bercovich B, Stancovski I, Mayer A, Blumenfeld N, Laszlo A, Schwartz AL, Ciechanover A. Ubiquitin-dependent degradation of certain protein substrates in vitro requires the molecular chaperone Hsc70. Journal of Biological Chemistry 1997; 272: 9002–9010.

Besset V, Scott RP, Ibáñez CF. Signaling complexes and

protein-protein interactions involved in the activation of the Ras and phosphatidylinositol 3 kinase pathways by the c-Ret receptor tyrosine kinase. J Biol Chem 2000;275:39159-66.

Borrello MG, Alberti L, Arighi E, Bongarzone I, Battistini C, Bardelli A, Pasini B, Piutti C, Rizzetti MG, Mondellini P, Radice MT, Pierotti MA. The full oncogenic activity of Ret/ptc2 depends on tyrosine 539, a docking site for phospholipase Cgamma. Mol Cell Biol 1996;16:2151-63.

Brandi ML, Gagel RF, Angeli A, et al. Guidelines for diagnosis and therapy of MEN type 1 and type 2. J Clin Endocrinol Metab 2001;86(12):5658–5671.

Bukau B, Weissman J, Horwich A. Molecular chaperones and protein quality control. Cell. 2006 May 5;125(3):443-51.

Carlomagno F, De Vita G, Berlingieri MT, de Franciscis V, Melillo RM, Colantuoni V, Kraus MH, Di Fiore PP, Fusco A, Santoro M. Molecular heterogeneity of RET loss of function in Hirschsprung's disease. EMBO J. 1996 Jun 3;15(11):2717-25.

Carlomagno F, Salvatore D, Santoro M, de Franciscis V, Quadro L, Panariello L, Colantuoni V, Fusco A . Point mutation of the RET proto-oncogene in the TT human medullary thyroid carcinoma cell line Biochem Biophys Res Commun 1995 207:1022-1028.

Carlomagno F, Vitagliano D, Guida T, et al. ZD6474, an orally available inhibitor of KDR tyrosine kinase activity, efficiently blocks oncogenic RET kinases. Cancer Res 2002;62(24):7284–7290.

Carlomagno F, Vitagliano D, Guida T, Napolitano M, Vecchio G, Fusco A, Gazit A, Levitzki A, Santoro M. The kinase inhibitor PP1 blocks tumorigenesis induced by RET oncogenes. Cancer Res. 2002 Feb 15;62(4):1077-82.

Carlomagno F, Vitagliano D, Guida T, et al. Efficient inhibition of RET/papillary thyroid carcinoma oncogenic kinases by 4-amino-5-(4-chloro-phenyl)-7-(t butyl)pyrazolo[3,4-d]pyrimidine (PP2). J Clin Endocrinol Metab 2003;88:1897-902.

Carlson KM, Dou S, Chi D, et al. Single missense mutation in the tyrosine kinase catalytic domain of the RET protooncogene is associated with multiple endocrine neoplasia type 2B. Proc Natl Acad Sci U S A 1994;91(4):1579–1583.

Carrello A, Ingley E, Minchin RF, Tsai S, Ratajczak T. The common tetratricopeptide repeat acceptor site for steroid receptor-associated immunophilins and hop is located in the dimerization domain of Hsp90. J Biol Chem. 1999 Jan 29;274(5):2682-9.

Challeton C, Bounacer A, Du Villard JA, Caillou B, De Vathaire F, Monier R, Schlumberger M, Suárez HG. Pattern of ras and gsp oncogene mutations in radiation-associated human thyroid tumors. Oncogene. 1995 Aug 3;11(3):601-3.

Chavany C, Mimnaugh E, Miller P, Bitton R, Nguyen P, Trepel J, Whitesell L, Schnur R, Moyer J, Neckers L. p185erbB2 binds to GRP94 in vivo. Dissociation of the p185erbB2/GRP94 heterocomplex by benzoquinone ansamycins precedes depletion of p185erbB2. J Biol Chem. 1996 Mar 1;271(9):4974-7.

Chen G, Cao P, Goeddel DV .TNF-induced recruitment and activation of the IKK complex require Cdc37 and Hsp90.. Mol Cell. 2002 Feb;9(2):401-10.

Chen S, Sullivan WP, Toft DO, Smith DF. Differential interactions of p23 and the TPR-containing proteins Hop, Cyp40, FKBP52 and FKBP51 with Hsp90 mutants. Cell Stress Chaperones. 1998 Jun;3(2):118-29

Chiariello M, Visconti R, Carlomagno F, Melillo RM, Bucci C, de Franciscis V, Fox GM, Jing S, Coso OA, Gutkind JS, Fusco A, Santoro M. Signalling of the Ret receptor tyrosine kinase through the c-Jun NH2- terminal protein kinases (JNKS): evidence for a divergence of the ERKs and JNKs pathways induced by Ret. Oncogene 1998;16:2435-45.

Citri A, Alroy I, Lavi S, Rubin C, Xu W, Grammatikakis N, Patterson C, Neckers L, Fry DW, Yarden Y 2002 Drug-induced ubiquitylation and degradation of ErbB receptor tyrosine kinases: implications for cancer therapy EMBO J 21:2407-2417.

Citri A, Harari D, Shohat G, Ramakrishnan P, Gan J, Lavi S, Eisenstein M, Kimchi A, Wallach D, Pietrokovski S, Yarden Y. Hsp90 recognizes a common surface on client kinases J Biol Chem. 2006 281:14361-14369.

Citri A, Kochupurakkal BS, Yarden Y. The achilles heel of ErbB-2/HER2: regulation by the Hsp90 chaperone machine and potential for

pharmacological intervention. 2004 Cell Cycle 3:51-60.

Citri A, Gan J, Mosesson Y, Vereb G, Szollosi J, Yarden Y. Hsp90 restrains ErbB-2/HER2 signalling by limiting heterodimer formation. 2004 EMBO Rep 5:1165-1170.

Connell P, Ballinger CA, Jiang J, Wu Y, Thompson LJ, Höhfeld J, Patterson C. The co-chaperone CHIP regulates protein triage decisions mediated by heat-shock proteins Nat Cell Biol. 2001 Jan;3(1):93-6

Coulpier M, Anders J, Ibáñez CF. Coordinated activation of autophosphorylation sites in the RET receptor tyrosine kinase: importance of tyrosine 1062 for GDNF mediated neuronal differentiation and survival. J Biol Chem 2002;277:1991-99.

Crowder RJ, Enomoto H, Yang M, Johnson EM Jr, Milbrandt J. Dok-6, a novel p62 Dok family member, promotes Ret-mediated neurite outgrowth. J Biol Chem 2004;279:42072-81

Csermely P, Kajtár J, Hollósi M, Jalsovszky G, Holly S, Kahn CR, Gergely P Jr, Söti C, Mihály K, Somogyi J. ATP induces a conformational change of the 90-kDa heat shock protein (hsp90).J Biol Chem. 1993 Jan 25;268(3):1901-7.

Cuccuru G, Lanzi C, Cassinelli G, et al. Cellular effects and antitumor activity of RET inhibitor RPI-1 on MEN2A-associated medullary thyroid carcinoma. J Natl Cancer Inst 2004;96(13):1006–1014.

Das AK, Cohen PW, Barford D. The structure of the tetratricopeptide repeats of protein phosphatase 5: implications for TPR-mediated protein-protein interactions. EMBO J. 1998 Mar 2;17(5):1192-9

DeBoer C, Meulman PA, Wnuk RJ, Peterson DH. Geldanamycin, a new antibiotic. J Antibiot (Tokyo). 1970 Sep;23(9):442-7.

de Candia P, Solit DB, Giri D, Brogi E, Siegel PM, Olshen AB, Muller WJ, Rosen N, Benezra R. Angiogenesis impairment in Id-deficient mice cooperates with an Hsp90 inhibitor to completely suppress HER2/neu-dependent breast tumors. Proc Natl Acad Sci U S A. 2003 Oct 14;100(21):12337-42. Epub 2003 Oct 2

Delmotte P, Delmotte-Plaque J. A new antifungal substance of

fungal origin. Nature. 1953 Feb 21;171(4347):344

Donis-Keller H, Dou S, Chi D, et al. Mutations in the RET proto-oncogene are associated with MEN2A and FMTC. Hum Mol Genet 1993;2(7):851–856.

Durick K, Wu RY, Gill GN, Taylor SS. Mitogenic signaling by Ret/ptc2 requires association with enigma via a LIM domain. J Biol Chem. 1996 May 31;271(22):12691-4.

Encinas M, Crowder RJ, Milbrandt J, Johnson EM Jr. Tyrosine 981, a novel Ret autophosphorylation site, binds c-Src to mediate neuronal survival. J Biol Chem 2004;279:18262-9.

Eng C, Clayton D, Schuffenecker I, et al. The relationship between specific RET proto-oncogene mutations and disease phenotype in multiple endocrine neoplasia type 2. International RET mutation consortium analysis. JAMA 1996;276(19):1575–1579.

Fagin JA, Matsuo K, Karmakar A, Chen DL, Tang SH, Koeffler HP. High prevalence of mutations of the p53 gene in poorly differentiated human thyroid carcinoma. J Clin Invest. 1993 ;91(1):179-84.

Farina AR, Tacconelli A, Cappabianca L, Cea G, Chioda A, Romanelli A, Pensato S, Pedone C, Gulino A, Mackay AR. The neuroblastoma tumour-suppressor TrkAI and its oncogenic alternative TrkAIII splice variant exhibit geldanamycin-sensitive interactions with Hsp90 in human neuroblastoma cells.Oncogene. 2009 Nov 19;28(46):4075-4094.

Fujita N, Sato S, Ishida A, Tsuruo T. Involvement of Hsp90 in signaling and stability of 3-phosphoinositide-dependent kinase-1 J Biol Chem 2002 277:10346-10353.

Fumo G, Akin C, Metcalfe DD, Neckers L17-Allylamino-17-demethoxygeldanamycin (17-AAG) is effective in down-regulating mutated, constitutively activated KIT protein in human mast cells. Blood 2004 103:1078-1084

Germano S, Barberis D, Santoro MM, Penengo L, Citri A, Yarden Y, Gaudino G Geldanamycins trigger a novel Ron degradative pathway, hampering oncogenic signaling J Biol Chem. 2006 281:21710-21719.

Glickman MH, Ciechanover A. The ubiquitin–proteasome proteolytic pathway: Destruction for the sake of construction. Physiological Reviews 2002; 82: 373–428.

Goetz MP, Toft D, Reid J, Ames M, Stensgard B, Safgren S, Adjei AA, Sloan J, Atherton P, Vasile V, Salazaar S, Adjei A, Croghan G, Erlichman C. Phase I trial of 17-allylamino-17-demethoxygeldanamycin in patients with advanced cancer. J Clin Oncol. 2005 Feb 20;23(6):1078-87.

Grenert JP, Sullivan WP, Fadden P, Haystead TA, Clark J, Mimnaugh E, Krutzsch H, Ochel HJ, Schulte TW, Sausville E, Neckers LM, Toft DO. The amino-terminal domain of heat shock protein 90 (hsp90) that binds geldanamycin is an ATP/ADP switch domain that regulates hsp90 conformation.J Biol Chem. 1997 Sep 19;272(38):23843-50

Grimm J, Sachs M, Britsch S, Di Cesare S, Schwarz-Romond T, Alitalo K, Birchmeier W. Novel p62dok family members, dok-4 and dok-5, are 73 substrates of the c-Ret receptor tyrosine kinase and mediate neuronal differentiation. J Cell Biol. 2001;154:345-54.

Hartmann F, Horak EM, Cho C et al. Effects of the tyrosine-kinase inhibitor geldanamycin on ligand-induced Her-2/neu activation, receptor expression and proliferation of Her-2 positive malignant cell lines. Int J Cancer 1997; 70: 221-229.

Hazard JB, Hawk WA, Crile G Jr. Medullary (solid) carcinoma of the thyroid; a clinicopathologic entity.J Clin Endocrinol Metab. 1959;19(1):152-61.

Hayashi H, Ichihara M, Iwashita T, Murakami H, Shimono Y, Kawai K, Kurokawa K, Murakumo Y, Imai T, Funahashi H, Nakao A, Takahashi M. Characterization of intracellular signals via tyrosine 1062 in RET activated by glial cell line-derived neurotrophic factor.Oncogene. 2000 Sep 14;19(39):4469-75.

Hayashi Y, Iwashita T, Murakamai H, Kato Y, Kawai K, Kurokawa K, Tohnai I, Ueda M, Takahashi M. 2001. Activation of BMK1 via tyrosine 1062 in RET by GDNF and MEN2A mutation. Biochem Biophys Res Commun. 2001;281:682-689.

Hennige AM, Lammers R, Arlt D, Hoppner W, Strack V, Niederfellner G, Seif FJ, Haring HU, Kellerer M. Ret oncogene signal transduction via a IRS- 2/PI 3-kinase/PKB and a SHC/Grb-2

dependent pathway: possible 74 implication for transforming activity in NIH3T3 cells. Mol Cell Endocrinol. 2000;167:69-76.

Ikonen E, Simons K. Protein and lipid sorting from the trans-Golgi network to the plasma membrane in polarized cells. Semin Cell Dev Biol. 1998;9:503-9.

Ishizaka Y, Itoh F, Tahira T, Ikeda I, Sugimura T, Tucker J, Fertitta A, Carrano AV, Nagao M. Human ret proto-oncogene mapped to chromosome10q11.2. Oncogene 1989;4:1519- 21.

Iwashita T, Asai N, Murakami H, Matsuyama M, Takahashi M. Identification of tyrosine residues that are essential for transforming activity of the ret proto-oncogene with MEN2A or MEN2B mutation. Oncogene 1996;12(3):481-7.

Jiang J, Ballinger CA, Wu Y, Dai Q, Cyr DM, Höhfeld J, Patterson C. CHIP is a U-box-dependent E3 ubiquitin ligase: identification of Hsc70 as a target for ubiquitylation.vJ Biol Chem. 2001 Nov 16;276(46):42938-44.

Jungmann J, Reins HA, Schobert C, Jentsch S. Resistance to cadmium mediated by ubiquitin-dependent proteolysis. Nature 1993; 361: 369–371.

Kaplan DR, Miller FD. Neurotrophin signal transduction in the nervous System. Curr Opin Neurobiol 2000;10:3813-91.

Kawamoto Y, Takeda K, Okuno Y, Yamakawa Y, Ito Y, Taguchi R, Kato M, Suzuki H, Takahashi M, Nakashima I. Identification of RET autophosphorylation sites by mass spectrometry. J Biol Chem 2004;279:14213-24

Kouvaraki MA, Shapiro SE, Perrier ND, et al. RET proto-oncogene, a review and update of genotypephenotypecorrelations in hereditary medullary thyroid cancer and associated endocrine tumors.Thyroid 2005;15(6):531–544.

Kroll TG, Sarraf P, Pecciarini L, Chen CJ, Mueller E, Spiegelman BM, Fletcher JA. PAX8-PPARgamma1 fusion oncogene in human thyroid carcinoma. Science 2000;289(5483):1357-60.

Kurokawa K, Iwashita T, Murakami H, Hayashi H, Kawai K, Takahashi M. Identification of SNT/FRS2 docking site on RET receptor tyrosine kinase and its role for signal transduction. Oncogene

2001;20:1929-38.

Kurokawa K, Kawai K, Hashimoto M, Ito Y, Takahashi M. 2003. Cell signalling and gene expression mediated by RET tyrosine kinase. J Intern Med 2003;253:627-633.

Kwon HJ, Yoshida M, Abe K, Horinouchi S, Beppu T. Radicicol, an agent inducing the reversal of transformed phenotypes of src-transformed fibroblasts Biosci Biotechnol Biochem. 1992 Mar;56(3):538-9.

Lee DH, Sherman MY, Goldberg AL. Involvement of the molecular chaperone Ydj1 in the ubiquitin-dependent degradation of short-lived and abnormal proteins in *Saccharomyces cerevisiae*. Molecular Cell Biology 1996; 16: 4773–4781

Lindahl M, Timmusk T, Rossi J, Saarma M, Airaksinen MS. Expression and alternative splicing of mouse Gfra4 suggest roles in endocrine cell development. Mol Cell Neurosci. 2000 Jun;15(6):522-33

Liu X, Vega QC, Decker RA, Pandey A, Worby CA, Dixon JE. Oncogenic RET receptors display different autophosphorylation sites and substrate binding specificities. J Biol Chem 1996; 271:5309-12.

Lorenzo MJ, Gish GD, Houghton C, Stonehouse TJ, Pawson T, Ponder BA, Smith DP. RET alternate splicing influences the interaction of activated RET with the SH2 and PTB domains of Shc, and the SH2 domain of Grb2. Oncogene 1997;14:763-71.

Lotz GP, Lin H, Harst A, Obermann WM. Aha1 binds to the middle domain of Hsp90, contributes to client protein activation, and stimulates the ATPase activity of the molecular chaperone.J Biol Chem. 2003 May 9;278(19):17228-35. Epub 2003 Feb 24.

Magnuson NS, Beck T, Vahidi H et al. The Raf-1 serine/threonine protein kinase. Semin Cancer Biol 1994; 5: 247-253.

Marcu MG, Schulte TW, Neckers L. Novobiocin and related coumarins and depletion of heat shock protein 90-dependent signaling proteins
J Natl Cancer Inst. 2000 Feb 2;92(3):242-8

Marcu MG, Chadli A, Bouhouche I, Catelli M, Neckers LM. The heat shock protein 90 antagonist novobiocin interacts with a previously unrecognized ATP-binding domain in the carboxyl terminus of the

chaperone. J Biol Chem. 2000 Nov 24;275(47):37181-6.

Marsee DK, Venkateswaran A, Tao H, Vadysirisack D, Zhang Z, Vandre DD, Jhiang SM. Inhibition of heat shock protein 90, a novel RET/PTC1-associated protein, increases radioiodide accumulation in thyroid cells. J Biol Chem. 2004 Oct 15;279(42):43990-7.

Matei D, Satpathy M, Cao L, Lai YC, Nakshatri H, Donner DB. The platelet-derived growth factor receptor alpha is destabilized by geldanamycins in cancer cells J Biol Chem. 2007 282:445-453.

Mayer, M.P. and Bukau, B. Hsp70 chaperones: cellular functions and molecular mechanism. 2005 Cell. Mol. Life Sci. 62, 670–68

Meacham GC, Patterson C, Zhang W, Younger JM, Cyr DM. The Hsc70 co-chaperone CHIP targets immature CFTR for proteasomal degradation.Nat Cell Biol. 2001 Jan;3(1):100-5.

Melillo RM, Carlomagno F, De Vita G, Formisano P, Vecchio G, Fusco A, Billaud M, Santoro M. The insulin receptor substrate (IRS)-1 recruits phosphatidylinositol 3-kinase to Ret: evidence for a competition between Shc and IRS-1 for the binding to Ret. Oncogene 2001a;20:209- 18.

Melillo RM, Santoro M, Ong SH, Billaud M, Fusco A, Hadari YR, Schlessinger J, Lax I. Docking protein FRS2 links the protein tyrosine kinase RET and its oncogenic forms with the mitogen-activated protein kinase signaling cascade. Mol Cell Biol 2001b;21(13):4177-87.

Meyer P, Prodromou C, Hu B, Vaughan C, Roe SM, Panaretou B, Piper PW, Pearl LH. Structural and functional analysis of the middle segment of hsp90: implications for ATP hydrolysis and client protein and cochaperone interactions. Mol Cell. 2003 Mar;11(3):647-58.

Miller P, Di Orio C, Moyer M et al. Depletion of the erbB-2 gene product p185 by benzoquinooid ansamycins. Cancer Res 1994; 54: 2724-2730.

Moriyama Y, Tsujimura T, Hashimoto K, Morimoto M, Kitayama H, Matsuzawa, Kitamura Y, Kanakura Y. Role of aspartic acid 814 in the function and expression of c-kit receptor tyrosine kinase. J Biol Chem. 1996 Feb 16;271(7):3347-50.

Murakami H, Yamamura Y, Shimono Y, Kawai K, Kurokawa K, Takahashi M. Role of Dok1 in cell signaling mediated by RET tyrosine

kinase. J Biol Chem 2002;277:32781-90.

Neckers L, Schulte TW, Mimnaugh E. Geldanamycin as a potential anti-cancer agent: its molecular target and biochemical activity. Invest New Drugs. 1999;17(4):361-73.

Ohiwa M, Murakami H, Iwashita T, Asai N, Iwata Y, Imai T, Funahashi H, Takagi H, Takahashi M. Characterization of Ret-Shc-Grb2 complex induced by GDNF, MEN 2A, and MEN 2B mutations. Biochem Biophys Res Commun 1997;237:747-51.

Owens-Grillo JK, Stancato LF, Hoffmann K, Pratt WB, Krishna P. Binding of immunophilins to the 90 kDa heat shock protein (hsp90) via a tetratricopeptide repeat domain is a conserved protein interaction in plants.Biochemistry. 1996 Dec 3;35(48):15249-55.

Pandey A, Liu X, Dixon JE, Di Fiore PP, Dixit VM. Direct association between the Ret receptor tyrosine kinase and the Src homology 2-containing adapter protein Grb7. J Biol Chem 1996;271:10607-10.

Pandey A, Duan H, Di Fiore PP, Dixit VM. The Ret receptor protein tyrosine kinase associates with the SH2-containing adapter protein Grb10. J Biol. Chem 1995;270:21461-63.

Pasini A, Geneste O, Legrand P, et al. Oncogenic activation of RET by two distinct FMTC mutations affecting the tyrosine kinase domain. Oncogene 1997;15:393-402.

Pelicci G, Troglio F, Bodini A, Melillo RM, Pettirossi V, Coda L, De Giuseppe A, Santoro M, Pelicci PG. The neuron-specific Rai (ShcC) adaptor protein inhibits apoptosis by coupling Ret to the phosphatidylinositol 3- kinase/Akt signaling pathway. Mol Cell Biol 2002;22:7351-63.

Ponder BA. The phenotypes associated with ret mutations in the multiple endocrine neoplasia type 2 syndrome Cancer Res 1999 59:1736s-1741s

Popp S, Packschies L, Radzwill N, Vogel KP, Steinhoff HJ, Reinstein J. Structural dynamics of the DnaK-peptide complex. J Mol Biol. 2005 Apr 15;347(5):1039-52

Prodromou C, Piper PW, Pearl LH. Expression and crystallization of the yeast Hsp82 chaperone, and preliminary X-ray

diffraction studies of the amino-terminal domain. Proteins. 1996 Aug;25(4):517-22.

Radanyi C, Chambraud B, Baulieu EE. The ability of the immunophilin FKBP59-HBI to interact with the 90-kDa heat shock protein is encoded by its tetratricopeptide repeat domain.Proc Natl Acad Sci U S A. 1994 Nov 8;91(23):11197-201

Ratajczak T, Carrello A. Cyclophilin 40 (CyP-40), mapping of its hsp90 binding domain and evidence that FKBP52 competes with CyP-40 for hsp90 binding J Biol Chem. 1996 Feb 9;271(6):2961-5.

Roe SM, Prodromou C, O'Brien R, Ladbury JE, Piper PW, Pearl LH. Structural basis for inhibition of the Hsp90 molecular chaperone by the antitumor antibiotics radicicol and geldanamycin.J Med Chem. 1999 Jan 28;42(2):260-6.

Salvatore D, Melillo RM, Monaco C, et al. Increased in vivo phosphorylation of ret tyrosine 1062 is a potential pathogenetic mechanism of multiple endocrine neoplasia type 2B. Cancer Res 2001;61 (4):1426–1431.

Salvatore D, Barone MV, Salvatore G, Melillo RM, Chiappetta G, Mineo A, Fenzi G, Vecchio G, Fusco A, Santoro M. Tyrosines 1015 and 1062 are in vivo autophosphorylation sites in ret and ret-derived oncoproteins. J Clin Endocrinol Metab 2000;85(10):3898-907.

Santoro M, Carlomagno F 2006 Drug insight: Small-molecule inhibitors of protein kinases in the treatment of thyroid cancer. Nature Clinical Practice Endocrinology and Metabolism 2: 42-52.

Santoro M, Carlomagno F, Romano A, Bottaro DP, Dathan NA, Greco M, Fusco A, Vecchio G, Matoskova B, Kraus MH, et al. :Activation of RET as a dominant transforming gene by germline mutations of MEN2A and MEN2B. Science. 1995 ; 267(5196):381-3.

Santoro M, Dathan NA, Berlingieri MT, Bongarzone I, Paulin C, Grieco M, Pierotti MA, Vecchio G, Fusco A. Oncogene. 1994 Feb;9(2):509-16

Sausville EA, Tomaszewski JE, Ivy P. Clinical development of 17-allylamino, 17-demethoxygeldanamycin. Curr Cancer Drug Targets. 2003 Oct;3(5):377-83

Schlessinger J. Cell signaling by receptor tyrosine kinases. Cell.

2000
Oct 13;103(2):211-25. Review

Schlumberger M, Carlomagno F, Baudin E, Bidart JM, Santoro M New therapeutic approaches to treat medullary thyroid carcinoma. Nature Clinical Practice Endocrinology and Metabolism 20084: 22-32.

Schnur RC, Corman ML, Gallaschun RJ, Cooper BA, Dee MF, Doty JL, Muzzi ML, DiOrio CI, Barbacci EG, Miller PE, et al. erbB-2 oncogene inhibition by geldanamycin derivatives: synthesis, mechanism of action, and structure-activity relationships. J Med Chem. 1995 Sep 15;38(19):3813-20

Schulte TW, Akinaga S, Soga S, Sullivan W, Stensgard B, Toft D, Neckers LM. Antibiotic radicicol binds to the N-terminal domain of Hsp90 and shares important biologic activities with geldanamycin.Cell Stress Chaperones. 1998 Jun;3(2):100-8

Shao J, Irwin A, Hartson SD, Matts RL. Functional dissection of cdc37: characterization of domain structure and amino acid residues critical for protein kinase binding.Biochemistry. 2003 Nov 4;42(43):12577-88

Sharma SV, Agatsuma T, Nakano HTargeting of the protein chaperone, HSP90, by the transformation suppressing agent, radicicol. Oncogene. 1998 May;16(20):2639-45.

Silverstein AM, Galigniana MD, Chen MS, Owens-Grillo JK, Chinkers M, Pratt WB. Protein phosphatase 5 is a major component of glucocorticoid receptor.hsp90 complexes with properties of an FK506-binding immunophilin. J Biol Chem. 1997 Jun 27;272(26):16224-30

Silverstein AM, Grammatikakis N, Cochran BH, Chinkers M, Pratt WB. p50(cdc37) binds directly to the catalytic domain of Raf as well as to a site on hsp90 that is topologically adjacent to the tetratricopeptide repeat binding site. J Biol Chem. 1998 Aug 7;273(32):20090-5

Slamon DJ, Clark GM, Wong SG et al. Human breast cancer: correlation of relapse and survival with amplification of the HER-2/neu oncogene. Science 1987; 235: 177-182.

Smith DF, Toft DO. Steroid receptors and their associated proteins. Mol Endocrinol 1993; 7: 4-11

Soares P, Trovisco V, Rocha AS, Feijao T, Rebocho AP, Fonseca E, Vieira de Castro I, Cameselle-Teijeiro J, Cardoso-Oliveira M & Sobrinho-Simoes M 2004 BRAF mutations typical of papillary thyroid carcinoma are more frequently detected in undifferentiated than in insular and insular-like poorly differentiated carcinoma. Virchows Archiv 444 572–576.

Soga S, Kozawa T, Narumi H, Akinaga S, Irie K, Matsumoto K, Sharma SV, Nakano H, Mizukami T, Hara M. Radicicol leads to selective depletion of Raf kinase and disrupts K-Ras-activated aberrant signaling pathway J Biol Chem. 1998 Jan 9;273(2):822-8

Soga S, Neckers LM, Schulte TW, Shiotsu Y, Akasaka K, Narumi H, Agatsuma T, Ikuina Y, Murakata C, Tamaoki T, Akinaga S. KF25706, a novel oxime derivative of radicicol, exhibits in vivo antitumor activity via selective depletion of Hsp90 binding signaling molecules.Cancer Res. 1999 Jun 15;59(12):2931-8

Solit DB, Zheng FF, Drobnjak M, Münster PN, Higgins B, Verbel D, Heller G, Tong W, Cordon-Cardo C, Agus DB, Scher HI, Rosen N. 17-Allylamino-17-demethoxygeldanamycin induces the degradation of androgen receptor and HER-2/neu and inhibits the growth of prostate cancer xenografts. Clin Cancer Res. 2002 May;8(5):986-93.

Stepanova L, Leng X, Parker SB, Harper JW. Mammalian p50(Cdc37) is a protein kinase-targeting subunit of Hsp90 that binds and stabilized Cdk4. Genes Dev 1996; 10: 1491-1502.

Sullivan W, Stensgard B, Caucutt G, Bartha B, McMahon N, Alnemri ES, Litwack G, Toft D. Nucleotides and two functional states of hsp90. J Biol Chem. 1997 Mar 21;272(12):8007-12.

Supko JG, Hickman RL, Grever MR, Malspeis L. Preclinical pharmacologic evaluation of geldanamycin as an antitumor agent. Cancer Chemother Pharmacol. 1995;36(4):305-15.

Takahashi M. Structure and expression of the ret transforming gene. IARC Sci Publ. 1988;(92):189-97.

Takahashi M, Ritz J, Cooper GM. Activation of a novel human transforming gene, ret, by DNA rearrangement. Cell 1985;42(2):581–588.

Takano T, Ito Y, Hirokawa M, Yoshida H & Miyauchi A 2007a BRAFV600E mutation in anaplastic thyroid carcinoma and their

accompanying differentiated carcinoma. British Journal of Cancer 96 1549–1553.

Tian ZQ, Liu Y, Zhang D, Wang Z, Dong SD, Carreras CW, Zhou Y, Rastelli G, Santi DV, Myles DC. Synthesis and biological activities of novel 17-aminogeldanamycin derivatives.Bioorg Med Chem. 2004 Oct 15;12(20):5317-29.

Vidal M, Wells S, Ryan A and Cagan R. ZD6474 suppresses oncogenic RET isoforms in a Drosophila model for type 2 multiple endocrine neoplasia syndromes and papillary thyroid carcinoma. 2005 Cancer Research 65:3538-3541.

Whitesell L, Mimnaugh EG, De Costa B, Myers CE, Neckers LM. Inhibition of heat shock protein HSP90-pp60v-src heteroprotein complex formation by benzoquinone ansamycins: essential role for stress proteins in oncogenic transformation. Proc Natl Acad Sci U S A. 1994 Aug 30;91(18):8324-8

Whitesell L, Shifrin SD, Schwab G, Neckers LM. Benzoquinonoid ansamycins possess selective tumoricidal activity unrelated to src kinase inhibition Cancer Res. 1992 Apr 1;52(7):1721-8

Williams ED. Histogenesis of medullary carcinoma of the thyroid.J Clin Pathol. 1966;19(2):114-8.

Workman P, Burrows F, Neckers L, Rosen N 2007 Drugging the cancer chaperone HSP90: combinatorial therapeutic exploitation of oncogene addiction and tumor stress. Ann N Y Acad Sci 1113:202-216.

Xu W, Mimnaugh EG, Kim JS et al. Hsp90, not Grp94, regulates the intracellular trafficking and stability of nascent ErbB2. Cell Stress Chaperones 2002; 7: 91-96.

Xu W, Yuan X, Xiang Z, Mimnaugh E, Marcu M, Neckers L 2005 Surface charge and hydrophobicity determine ErbB2 binding to the Hsp90 chaperone complex Nat Struct Mol Biol 12:120-126.

Yu W, Rao Q, Wang M, Tian Z, Lin D, Liu X, Wang J. The Hsp90 inhibitor 17-allylamide-17-demethoxygeldanamycin induces apoptosis and differenziation of Kasumi-1 harboring the Asn822Lys KIT mutation and down-regulates KIT protein level. 2006 Leuk Res. May 30(5):575-82

Young JC, Obermann WM, Hartl FUSpecific binding of tetratricopeptide repeat proteins to the C-terminal 12-kDa domain of hsp90.J Biol Chem. 1998 Jul 17;273(29):18007-10.

Zhang M, Windheim M, Roe SM, Peggie M, Cohen P, Prodromou C, Pearl LH. Chaperoned ubiquitylation--crystal structures of the CHIP U box E3 ubiquitin ligase and a CHIP-Ubc13-Uev1a complex.Mol Cell. 2005 Nov 23;20(4):525-38.

Zhao JF, Nakano H, Sharma S. Suppression of RAS and MOS transformation by radicicol. Oncogene. 1995 Jul 6;11(1):161-73

Protein NCOA4 inhibits initiation of eukaryotic DNA replication

Francesca Carlomagno[1*], Teresa Guida[1], Livia Provitera[1], Luigi Alfano[1], Donata Vitagliano[1], Nina A. Dathan[2], Domenico Grieco[1], Vincenzo Costanzo[3], Alfredo Fusco[1], Massimo Santoro[1*]

[1]Istituto di Endocrinologia ed Oncologia Sperimentale del CNR/Dipartimento di Biologia e Patologia Cellulare e Molecolare "L. Califano", Facoltà di Medicina e Chirurgia, Università di Napoli "Federico II", 80131 Naples, Italy; [2]Istituto di Biostrutture e Bioimmagini del CNR 80134 Naples, Italy; [3]London Research Institute, Clare Hall Laboratories, Blanche Lane, South Mimms, EN6 3LD, UK.

Keywords: MCM proteins; thyroid cancer; DNA replication; helicase; nuclear receptor coactivator; chromosomal rearrangement

[*]**Corresponding authors**: E-MAIL persfra@tin.it, FAX +39 081 7463603; E-MAIL masantor@unina.it, FAX: +39-081-7463037.

Running title: NCOA4 in DNA replication.

Abstract

Here we show that NCOA4 protein, coded for by a gene frequently rearranged in thyroid cancer, binds the mini-chromosome maintenance 7 (MCM7) protein required for DNA replication. In *Xenopus laevis* egg extracts, exogenously added recombinant NCOA4 inhibited DNA replication by obstructing MCM2-7 helicase activity, whereas immunodepletion of endogenous XNCOA4 protein augmented DNA synthesis by increasing DNA unwinding. In HeLa cells, NCOA4 bound canonical DNA replication origins. RNAi-mediated depletion of NCOA4 accelerated the onset of DNA replication, whereas adoptive NCOA4 overexpression decreased DNA synthesis. Our findings indicate that NCOA4 is a novel negative regulator of DNA replication.

Introduction

Recurrent chromosomal rearrangements are common in cancer cells (Futreal et al. 2004). Intrachromosomal inversions involving the long arm of chromosome 10 occur frequently in thyroid carcinomas, particularly those induced by radiation (Nikiforova et al. 2000). These events join the DNA sequence encoding the tyrosine kinase (TK) domain of *RET* to the 5'-terminal portion of heterologous genes to form *RET*/PTC oncogenes (Grieco et al. 1990). *RET*/PTC3 is a common chimeric oncogene constituted by exons 1-5 (encoding amino acids 1-238) of the nuclear receptor coactivator 4 (*NCOA4*, also known as RFG/ELE1/ARA70) gene and *RET* exons 12-21 (encoding the TK domain) (Bongarzone et al. 1994; Santoro et al. 1994). The *NCOA4* gene encodes a 70-kDa protein containing a coiled-coil domain (amino acids 17-125) that mediates protein oligomerization (Fig. S1) (Monaco et al. 2001). One functional consequence of the *RET*/PTC3 rearrangement is NCOA4-mediated homodimerization of the RET TK followed by ligand-independent RET activation and gain of transforming activity (Monaco et al. 2001).

The MCM2-7 complex is an evolutionarily conserved hexameric protein complex constituted by six closely related proteins: MCM2 through MCM7 (Bell and Dutta, 2002; Takahashi et al. 2005; Maiorano et al. 2006). MCM2-7 is essential for DNA synthesis. In *Xenopus laevis* egg extracts, inactivation of the MCM2-7 complex immediately arrests DNA replication (Takahashi et al. 2005). MCM2-7 proteins are recruited to the DNA replication origins by two factors, Cdc6 and Cdt1, which, in turn, are bound to the origin recognition complex (ORC) (Bell and Dutta, 2002; Takahashi et al. 2005; Maiorano et al. 2006). MCM2-7, Cdc6, Cdt1 and ORC proteins constitute the pre-Replicative Complex (pre-RC), essential for the DNA replication origins licensing. At the G1/S transition, activation of S-phase kinases, such as CDK2-Cyclin E and CDC7-DBF4, induces phosphorylation of pre-RC components and recruitment of replication factors such as CDC45 and GINS, converting the pre-RC in the pre-Initiation Complex (pre-IC). Upon formation of pre-IC, the replicative DNA helicase

becomes active and unwinds the DNA replication origin forming the replication bubble (Pacek et al. 2006). Thus, generation of single strand DNA allows binding of Primase/DNA polα complex that synthesizes the RNA/DNA primer. This induces the sequential loading of the RFC complex and then of the proliferating cell nuclear antigen (PCNA), the co-factor of primary replicative DNA polymerases such as DNA polδ and DNA polε. Once replicative polymerases are recruited, bidirectional DNA replication starts with a semi-conservative modality (Bell and Dutta, 2002; Takahashi et al. 2005; Maiorano et al. 2006; Pacek et al. 2006). The MCM2-7 complex is thought to be the major DNA helicase (Takahashi et al. 2005; Labib et al. 2000; Pacek and Walter, 2004). Here we show that NCOA4 is a novel negative controller of DNA replication that interacts with MCM2-7 complex and obstructs DNA unwinding.

Results and Discussion

To try to identify functions of the NCOA4 protein that might be disrupted by the thyroid cancer-associated gene rearrangement, we looked for proteins that interacted with NCOA4. To this aim we screened a HeLa cell cDNA library with a bait containing NCOA4 amino acids 2-238 [GAL4-NCOA4(N)] in a yeast two-hybrid system (Fig. S1). NCOA4(N) contains the coiled-coil domain. We isolated 10 different NCOA4-encoding clones, which confirmed that NCOA4 is able to form oligomers (Monaco et al. 2001), and two cDNA clones encoding the COOH-terminal portion (amino acids 576-719) of the mini-chromosome maintenance 7 (MCM7) protein (Fig. S1). To confirm interaction between NCOA4 and MCM7 we performed an *in-vitro* pull-down assay using two NCOA4-derived recombinant proteins constituted by NUS *tag* (NUS) fused to either full length NCOA4 (NUS-NCOA4) or to its NH2-terminal fragment (amino acids 1-238) [NUS-NCOA4(N)] (Fig. 1A). Both NUS-NCOA4 and NUS-NCOA4(N), but not NUS moiety alone or empty beads, pulled-down MCM7 protein from HeLa cells protein extracts (Fig. 1A). Also another subunit of the MCM2-7 complex, the MCM3 protein, was detected in the precipitate suggesting that NCOA4 recombinant proteins were pulling-down, via MCM7, the entire MCM2-7 complex.

To verify NCOA4-MCM7 interaction *in vivo*, we evaluated whether the proteins co-localized and formed a complex in HeLa cells. In sub-cellular fractionation experiments, NCOA4 and MCM7 were detected in both the cytoplasmic and nuclear compartments (Fig. 1B). Like MCM7 (Bell et al. 2002), NCOA4 was present, in part, in the Triton X-100 (0.5%) insoluble fraction, and DNAse treatment was able to solubilize both NCOA4 and MCM7, indicating that NCOA4 was bound to chromatin like the MCM2-7 complex (Fig. 1C). Moreover, NCOA4 co-immunoprecipitated with MCM7, indicating interaction of the two proteins at the endogenous level (Fig. 1D). MCM6 and MCM5 proteins were also present in the complex, enforcing the hypothesis that NCOA4 bound MCM7 in the contex of the entire MCM2-7 complex (Fig. 1D). In HeLa

sub-cellular fractions, NCOA4-MCM7 interaction was confined to the nucleus and occurred preferentially on chromatin (Fig. 1E).

Cell-free systems derived from *Xenopus laevis* (*Xenopus l.*) eggs represent the classical model for studies of cell cycle events (Murray 1991). We used this system to determine the functional consequences of the interaction between NCOA4 and the MCM2-7 complex on DNA replication. The recombinant NUS-NCOA4 protein (full-length human NCOA4 fused to the NUS *tag*) was found to bind to the endogenous *Xenopus l.* MCM7 (Fig. 2A). We incubated *Xenopus l.* egg extracts with demembranated *Xenopus l.* sperm nuclei and different concentrations of NUS-NCOA4. As shown in Fig. 2B, NUS-NCOA4, but neither heat-inactivated NUS-NCOA4 nor the NUS *tag* alone, inhibited DNA replication in a concentration-dependent manner. NUS-NCOA4 did not affect the formation of the nuclear envelope in egg extracts (Fig. S2A); kinetics of DNA replication showed that 150 nM NUS-NCOA4 protein was able to reduce replication to less than 10% throughout the entire reaction (Fig. S2B). Only the full-length NCOA4 protein, but neither the isolated NCOA4 NH2-terminal [NUS-NCOA4(N)] (amino acids 1-238) nor the COOH-terminal [NUS-NCOA4(C)] (amino acids 239-614) fragments, blocked DNA replication (Fig. 2C).

To determine whether the effect exerted by NCOA4 on DNA synthesis was mediated by its interaction with MCM7, we used the COOH-terminal portion of MCM7 [MCM7(C)] to obstruct the interaction between NCOA4 and endogenous MCM7 in the extract. MCM7(C) (amino acids 576-719) corresponded to the protein segment isolated in the two-hybrid screening, and therefore it contained the NCOA4-binding site (Fig. S1 and 2D). MCM7(C) *per se* did not affect DNA replication (Fig. 2D). However, a 3-6 fold molar excess of MCM7(C) blunted the NCOA4-mediated inhibition of DNA replication (Fig. 2E), suggesting that such blockade resulted from the interaction of NCOA4 with MCM7.

To investigate the mechanism underlying the NCOA4-mediated hindrance of DNA replication, we tested whether NUS-NCOA4 altered the loading of replication

factors on DNA by chromatin pull-down experiments. As expected, NUS-NCOA4 protein was bound to chromatin (Fig. 3A). Geminin, which inhibits MCM2-7 binding to DNA (Wohlschlegel et al. 2000), did not reduce NUS-NCOA4 loading (Fig. S3), indicating that the interaction of NUS-NCOA4 with DNA occurred irrespective of binding to the MCM2-7 complex. NUS-NCOA4 did not affect loading of the pre-RC components Cdc6 and MCM7, or pre-IC component CDC45, whereas it greatly reduced the binding of PCNA, which occurs beyond the synthesis of the DNA/RNA primer (Fig. 3A). PCNA loading was restored by competing NUS-NCOA4 with the MCM7(C) peptide (Fig. 3B). These data indicated that NUS-NCOA4 was acting after both licensing and activation of origins had occurred.

One possibility was that NUS-NCOA4 inhibited DNA unwinding, a step secondary to pre-IC formation and preceding primer synthesis, PCNA loading and DNA elongation (Bell et al. 2002; Pacek et al. 2006; Labib et al. 2000; Takayama et al. 2003). To address this possibility, we measured aphidicolin-induced hyperloading of replication protein A (RPA) in the presence of NCOA4. Aphidicolin is a DNA polymerase inhibitor that uncouples DNA unwinding from DNA polymerization, thereby generating long stretches of single-strand DNA that is rapidly covered by the single-strand binding protein RPA. Therefore, aphidicolin-induced hyperloading of RPA is a *bona fide* measurement of replicative DNA helicase activity. NUS-NCOA4 inhibited aphidicolin-induced RPA hyperloading (Fig. 3C), which indicated that it was blocking DNA unwinding. Again, NCOA4 did not affect MCM7 binding to DNA (Fig. 3C). The MCM7(C) peptide, which reduced the NCOA4-induced inhibition of DNA replication (Fig. 2E) and restored PCNA loading (Fig. 3B), also blunted the NCOA4-dependent block of RPA hyperloading, showing that hindrance of unwinding was mediated by NUS-NCOA4 interaction with MCM7 (Fig. 3D). No changes in MCM7 and CDC45 binding to chromatin were detected, indicating that origins licensing and firing were not affected by MCM7(C) obstruction of NUS-NCOA4 action (Fig. 3D). Consistently, association of Primase/DNApol α to chromatin, which is strictly

dependent on origin unwinding (Walter and Newport 2000), was greatly decreased by 150 nM NUS-NCOA4 (Fig. 3E). Interference with DNApol α binding explained reduction of PCNA loading observed in the presence of NUS-NCOA4 (Fig. 2A and B). Finally, NCOA4 did not affect the replication of a circular single-strand DNA template derived from the M13 bacteriophage (Fig. 3F) – a process that occurs independently of replicative DNA helicase (Cox and Leno 1990; Jenkins et al. 1992).

We investigated the function of endogenous *Xenopus l.* NCOA4 protein with respect to DNA replication. Two cDNA species (XNCOA4α and XNCOA4β) homologous to human NCOA4 are present in the GenBank (BC071152 and NM_001095769, respectively). The predicted XNCOA4α and XNCOA4β proteins are 90% identical; moreover, they are 50% identical to human NCOA4 (Fig. S4). XNCOA4α and XNCOA4β cDNAs were cloned and used to generate an affinity-purified antibody. The anti-XNCOA4 was able to immunoprecipitate *in vitro*-transcribed/translated XNCOA4α and XNCOA4β (Fig. S4), as well a protein species from egg extracts with the same molecular weight as *in vitro*-transcribed/translated XNCOA4α and XNCOA4β (Fig 4A). Given the high similarity between XNCOA4α and XNCOA4β, hereafter we will refer to both proteins as "XNCOA4".

Initially, we observed that the endogenous XNCOA4 bound to chromatin during initial phases of DNA replication and formed a complex with MCM7 protein (Fig 4B and C). Subsequently, we evaluated the effects of XNCOA4 depletion with respect to DNA replication monitoring DNA synthesis at different time points (Fig. 4D). Extracts immunodepleted of endogenous XNCOA4 displayed a 2-3 fold increase of DNA replication from the onset (Fig. 4D). In parallel, PCNA chromatin binding was enhanced whereas MCM7 loading remained unchanged (Fig. 4E). Complementation of immunodepleted extracts with exogenous NUS-NCOA4 (30 nM) restored normal DNA replication and PCNA loading (Fig. 4E). Upon XNCOA4 depletion, CDC45 protein binding to chromatin remained unchanged, while RPA loading resulted visibly

increased (Fig. 4F), in accordance with a role for XNCOA4 in controlling DNA unwinding rather than origin firing.

We sought to investigate NCOA4 role in mammalian cells. We first checked whether in HeLa cells the protein was located at canonical DNA replication origins using chromatin immunoprecipitation (ChIP) (Dominiguez–Sola et al. 2007). NCOA4 was present at both c-Myc and Lamin B2 origins. Cdc6 protein was detected at the same origins while neither proteins binding occured on control regions (Fig 5A and B). HeLa cells were transiently transfected with three different NCOA4 small inhibitory duplex RNAs (NCOA4 1i, 2i and 3i) and DNA synthesis was measured by BrdU incorporation. NCOA4 siRNAs, but not the scrambled control, increased the DNA synthesis rate at both 48 and 72 hours. This effect was more pronounced with NCOA4 2i, than with NCOA4 1i and 3i, which is in line with its stronger capacity to knock down NCOA4 protein levels (Fig. 5C and Fig. S5). Moreover, in a G1/S synchronized cell population (double-thymidine block), NCOA4 2i siRNA increased DNA synthesis rate by accelerating entry in S phase (Fig. 5D). Indeed, after 20 minutes from block release, percentage of NCOAi cells in S phase increased from 27% to 44%, while control cells (scrambled RNAi) have not started entering S phase. Consistent with our findings in the *Xenopus l.* system, also in HeLa cells, increased DNA synthesis was paralleled by augmented recruitment of PCNA to chromatin whereas the chromatin-bound fraction of MCM7 remained unchanged (Fig. 5E).

Lastly, we investigated the effects of adoptive NCOA4 overexpression. HeLa cells were engineered to express NCOA4 under the control of a doxycycline-inducible promoter. Induction of NCOA4 protein decreased cell growth and incorporation of BrdU. It also caused cells to accumulate in S phase probably consequent to a reduced rate of DNA synthesis (Fig. S6). In fact, DNA replication origins licensing was not

affected by increased levels of NCOA4 protein, as shown by the unchanged loading of MCM7 on DNA (Fig. S7). Nevertheless, as observed in *Xenopus l.* egg extracts, PCNA binding on chromatin and formation of replication foci was greatly reduced in cells overexpressing NCOA4 (data not shown).

In summary, our study reveals a novel protein network involving NCOA4 and MCM7. By binding to the MCM2-7 complex, NCOA4 inhibits DNA replication and prevents DNA unwinding in *Xenopus l.* egg extracts, thereby acting as a *bona fide* MCM complex regulator. Thus, NCOA4 would function like the 1-400 p110Rb protein fragment, which, by binding to the same MCM7 region where also NCOA4 binds, blocks MCM2-7 helicase activity (Pacek et al. 2004; Sterner et al. 1998). Accordingly, NCOA4 negatively regulated DNA replication in HeLa cells.

NCOA4 functions as a co-activator of several nuclear receptors, namely the androgen and estrogen receptors, peroxisome-proliferator activated receptor γ and the thyroid hormone receptor (Yeh et al. 1996; Heinlein et al. 1999; Moore et al. 2004; Lanzino et al. 2005). Thus, NCOA4 may represent a functional link between steroid hormone receptors and DNA replication control.

MCMs are overexpressed in many types of human cancer (Gonzalez et al. 2005). A gain of the 7q chromosomal region that includes MCM7 has been observed in prostate (Ren et al. 2006) and hypopharyngeal (Cromer et al. 2004) carcinomas. Targeted MCM7 expression to the basal layer of the epidermis in transgenic mice significantly increased the incidence of tumor development after two-stage chemical carcinogenesis (Honeycutt et al. 2006). Thus, MCM proteins are believed to act as important players in the process leading to autonomous growth of neoplastic cells (Gonzalez et al. 2005*)*. Based on our findings, we postulate that chromosomal rearrangements that target the NCOA4 gene in thyroid cancer might release MCM7 mitogenic activity from the negative control exerted by NCOA4. In this context, the NCOA4 rearrangement might represent a novel paradigm of a cancer-associated chromosome rearrangement that directly targets a gene that controls DNA synthesis.

MATERIALS AND METHODS

Yeast Two-Hybrid Screening. The N-terminal portion of the human NCOA4 protein (amino acids 2-238) was fused in frame to the GAL4 DNA binding domain in the pGBKT7 vector (Clontech, Mountain View, CA) to generate the GAL4-NCOA4(N) bait. GAL4-NCOA4(N) was used to screen a MATCHMAKER pre-transformed HeLa cell cDNA library (Clontech). Two-hybrid screening procedure is described in the supplementary information.

Recombinant Proteins. Recombinant proteins cloning is described in the supplementary information. The GST-Geminin protein was kindly donated by J. Gautier (Shechter et al. 2004).

Generation of XNCOA4 antibody. A polyclonal anti-XNCOA4 antibody was generated by immunizing rabbits with the GST-XNCOA4β fusion protein. The serum was affinity-purified by sequential chromatography steps through GST and GST-XNCOA4β columns (AminoLink, Pierce, Rockford, IL) and was used at 1μg/ml for immunoprecipitation and at 0.1 μg/ml for Western blotting. Cloning of XNCOA4α and XNCOA4β cDNAs is described in the supplementary information.

Protein studies. Proteins were extracted according to standard procedures. Details are described in the supplementary information.

Antibodies. Anti-MCM6 (H-300; sc-22781), -MCM3 (N-19; sc-9850), -MCM7 (141.2; sc-9966), -Cdc6 (180.2; sc-9964), -RPA (H-100; sc-28709), -geminin (FL-209; sc-13015) and -lamin (636; sc-7292) were from Santa Cruz Biotechnology (Santa Cruz,

CA). Anti-Tubulin (DM1A; T9026) was from Sigma Chemical Co (St. Louis, MO). Anti-MCM5 (MCA, 1860) was from Serotec (Raleigh, NC). Anti-PCNA (PC10) was from Chemicon International, Inc. (Temecula, CA). Anti-NCOA4 is an affinity-purified rabbit polyclonal antibody raised against the C-terminal protein fragment of human NCOA4 (amino acids 239-614) (Monaco et al, 2001). Anti-CDC45 and anti-RPA for *Xenopus l.* proteins were donated by J. C. Walter (Pacek and Walter, 2004). Anti-DNA polymerase α was donated by S. Waga (Waga et al, 2001). Secondary antibodies coupled to horseradish peroxidase were from Santa Cruz Biotechnology.

DNA replication and chromatin binding assays. Cytostatic factor (CSF)-arrested *Xenopus l.* egg extracts were freshly prepared according to Murray (Murray, 1991). Chromosomal templates for DNA replication were prepared from demembranated *Xenopus l.* sperm nuclei as reported by Murray (Murray, 1991). Nuclei formation was monitored by immunofluorescence after 60 minutes from addition of sperm demembranated nuclei to egg extract. Procedures are described in the supplementary information.

Cell culture methods, immunofluorescence and cytofluorimeter analysis. HeLa cells were grown in Dulbecco's modified Eagle's medium (DMEM) supplemented with 10% fetal calf serum (Invitrogen Groningen, The Netherlands). Anti-NCOA4 siRNAs sequences are reported in the supplementary information. Transfection was performed using 150nM final concentration of siRNA using the oligofectamine reagent (Invitrogen). The human NCOA4 full-length cDNA was cloned in pcDNA/TO/myc-HIS (Invitrogen) and stably transfected in HeLa T-Rex cells containing the Tet repressor under the control of the CMV promoter (Invitrogen). Marker-selected cell clones were isolated and characterized for NCOA4 expression by immunoblot. Two clones (clone 23 and 24) were selected for further studies. Methods for cell

synchronization, DNA synthesis measurement and immunofluorescence are reported in the supplementary information.

Chromatin Immunoprecipitation. Chromatin immunoprecipitation was performed from exponentially growing HeLa cells using preimmune serum, or purified anti-NCOA4 and anti-Cdc6 antibodies. Sequence of PCR primers are reported in the supplementary information.

Acknowledgements

We thank Johannes C. Walter for anti-CDC45 and anti-RPA antibodies and for useful discussion, Shou Waga for anti-DNA polymerase α antibody, Jean Gautier for the GST-Geminin recombinant protein. We thank Giancarlo Vecchio for continuous support, Lorenzo Chiariotti for help on the 2-hybrid screen, Rosa Marina Melillo for useful discussion and Jean A. Gilder for text editing. This study was supported by the Associazione Italiana per la Ricerca sul Cancro (AIRC), the Italian Ministero per l'Istruzione, Università e Ricerca Scientifica (MIUR), the MoMa project, and by the specific targeted project GENRISK-T of the European Commission.

References

Bell, S.P. and Dutta, A. 2002. DNA replication in eukaryotic cells. *Annu Rev Biochem*. **71**: 333-374.

Bongarzone, I., Butti, M.G., Coronelli, S., Borrello, M.G., Santoro, M., Mondellini, P., Pilotti, S., Fusco, A., Della Porta G., and Pierotti, M.A. 1994. Frequent activation of ret protooncogene by fusion with a new activating gene in papillary thyroid carcinomas. *Cancer Res*. **54**: 2979-2985.

Cox, L.S. and Leno, G.H. 1990. Extracts from eggs and oocytes of Xenopus laevis differ in their capacities for nuclear assembly and DNA replication. *J Cell Sci*. **97**: 177-184.

Cromer, A., Carles, A., Millon, R., Ganguli, G., Chalmel, F., Lemaire, F., Young, J., Dembélé, D., Thibault, C., Muller, D., Poch, O., Abecassis, J., and Wasylyk, B. 2004. Identification of genes associated with tumorigenesis and metastatic potential of hypopharyngeal cancer by microarray analysis. *Oncogene* **23**: 2484-2498.

Dominguez-Sola, D., Ying, C.Y., Grandori, C., Ruggiero, L., Chen, B., Li, M., Galloway, D.A., Gu, W., Gautier, J., and Dalla-Favera, R. 2007. Non-transcriptional control of DNA replication by c-Myc. *Nature* **448**: 445-451.

Futreal, P.A., Coin. L., Marshall, M., Down, T., Hubbard, T., Wooster, R., Rahman, N., and Stratton, M.R. 2004. A census of human cancer genes. *Nat. Rev. Cancer* **4**: 177-183.

Gonzalez, M.A., Tachibana, K.E., Laskey, R.A., and Coleman, N. 2005. Control of DNA replication and its potential clinical exploitation. *Nat. Rev. Cancer* **5**: 135-141.

Grieco, M., Santoro, M., Berlingieri, M.T., Melillo, R.M., Donghi, R., Bongarzone, I., Pierotti, M.A., Della Porta, G., Fusco, A., and Vecchio, G. 1990. PTC is a novel rearranged form of the ret proto-oncogene and is frequently detected in vivo in human thyroid papillary carcinomas. *Cell* **60**: 557-563.

Heinlein, C.A., Ting, H.J., Yeh, S., and Chang, C. 1999. Identification of ARA70 as a ligand-enhanced coactivator for the peroxisome proliferator-activated receptor gamma. *J. Biol. Chem.* **274**: 16147-16152.

Honeycutt, K.A., Chen, Z., Koster, M.I., Miers, M., Nuchtern, J., Hicks, J., Roop, D.R., and Shohet, J.M. 2006. Deregulated minichromosomal maintenance protein MCM7 contributes to oncogene driven tumorigenesis. *Oncogene* **25**: 4027-4032.

Jenkins, T.M., Saxena, J.K., Kumar, A., Wilson, S.H., and Ackerman, E.J. 1992. DNA polymerase beta and DNA synthesis in Xenopus oocytes and in a nuclear extract. S*cience* **258**: 475-478.

Labib, K., Tercero, J.A., and Diffley, J.F. 2000. Uninterrupted MCM2-7 function required for DNA replication fork progression. *Science* **288**: 1643-1647.

Lanzino, M., De Amicis, F., McPhaul, M.J., Marsico, S., Panno, M.L., and Andò, S. 2005. Endogenous coactivator ARA70 interacts with estrogen receptor alpha (ERalpha) and modulates the functional ERalpha/androgen receptor interplay in MCF-7 cells. *J. Biol. Chem.* **280**: 20421-20430.

Maiorano, D., Lutzmann, M., and Méchali, M. 2006. MCM proteins and DNA replication. *Curr. Opin. Cell. Biol.* **18:** 130-136.

Monaco, C., Visconti, R., Barone, M.V., Pierantoni, G.M., Berlingieri, M.T., De Lorenzo, C., Mineo, A., Vecchio, G., Fusco, A., and Santoro, M. 2001. The RFG oligomerization domain mediates kinase activation and re-localization of the RET/PTC3 oncoprotein to the plasma membrane. *Oncogene* **20**: 599-608.

Moore, J.M., Galicia, S.J., McReynolds, A.C., Nguyen, N.H., Scanlan, T.S., and Guy, R.K. 2004. Quantitative proteomics of the thyroid hormone receptor-coregulator interactions. *J. Biol. Chem.* **279**: 27584-27590.

Murray, A.W. 1991. Cell cycle extracts. *Methods Cell. Biol.* **36**: 581-605.

Nikiforova, M.N., Stringer, J.R., Blough, R., Medvedovic, M., Fagin, J.A., and Nikiforov, Y.E. 2000. Proximity of chromosomal loci that participate in radiation-induced rearrangements in human cells. *Science* **290**: 138-141.

Pacek, M., and Walter, J.C. 2004. A requirement for MCM7 and Cdc45 in chromosome unwinding during eukaryotic DNA replication. *EMBO J.* **23**: 3667-3676.

Pacek, M., Tutter, A.V., Kubota, Y., Takisawa, H., and Walter, J.C. 2006. Localization of MCM2-7, Cdc45, and GINS to the site of DNA unwinding during eukaryotic DNA replication. *Mol. Cell* **21**: 581-587.

Ren, B., Yu, G., Tseng, G.C., Cieply, K., Gavel, T., Nelson, J., Michalopoulos, G., Yu, Y.P., and Luo, J.H. 2006. MCM7 amplification and overexpression are associated with prostate cancer progression. *Oncogene* **25**: 1090-1098.

Santoro, M., Dathan, N.A., Berlingieri, M.T., Bongarzone, I., Paulin, C., Grieco, M., Pierotti, M.A., Vecchio, G., and Fusco, A. 1994. Molecular characterization of RET/PTC3; a novel rearranged version of the RET proto-oncogene in a human thyroid papillary carcinoma. *Oncogene* **9**: 509-516.

Shechter, D., Ying, C.Y., and Gautier, J. 2004. DNA unwinding is an Mcm complex-dependent and ATP hydrolysis-dependent process. *J. Biol. Chem.* **279**: 45586-45593.

Sterner, J.M., Dew-Knight, S., Musahl, C., Kornbluth, S., and Horowitz, J.M. 1998. Negative regulation of DNA replication by the retinoblastoma protein is mediated by its association with MCM7. *Mol. Cell. Biol.* **18**: 2748-2757.

Takahashi, T.S., Wigley, D.B., and Walter, J.C. 2005. Pumps, paradoxes and ploughshares: mechanism of the MCM2-7 DNA helicase. *Trends Biochem. Sci.* **30**: 437-444.

Takayama, Y., Kamimura, Y., Okawa, M., Muramatsu, S., Sugino, A., and Araki, H. 2003. GINS, a novel multiprotein complex required for chromosomal DNA replication in budding yeast. *Genes Dev.* **17**: 1153-1165.

Waga, S., Masuda, T., Takisawa, H., and Sugino, A. 2001. DNA polymerase epsilon is required for coordinated and efficient chromosomal DNA replication in Xenopus egg extracts. *Proc. Natl. Acad. Sci. U. S. A.* **98**: 4978-4983.

Walter, J. and Newport, J. 2000. Initiation of eukaryotic DNA replication: origin

unwinding and sequential chromatin association of Cdc45, RPA, and DNA polymerase alpha. *Mol Cell* **5**: 617-627.

Wohlschlegel, J.A., Dwyer, B.T., Dhar, S.K., Cvetic, C., Walter, J.C., and Dutta, A. 2000. Inhibition of eukaryotic DNA replication by geminin binding to Cdt1. *Science* **290**: 2309-2312

Yeh, S. and Chang, C. 1996. Cloning and characterization of a specific coactivator, ARA70, for the androgen receptor in human prostate cells. *Proc. Natl. Acad. Sci. U.S.A.* **93**: 5517-5521

Figure Legends

Figure 1. NCOA4 interacts with the MCM2-7 complex.

(*A*) HeLa cell protein extract was subjected to an *in vitro* pull-down assay with the NUS, NUS-NCOA4 or NUS-NCOA4(N) recombinant proteins. Bound proteins were immunoblotted with anti-MCM7 and MCM3 antibodies. (*B*) Total, cytosolic and nuclear proteins, deriving from comparable number of HeLa cells, were immunoblotted with anti-NCOA4 and anti-MCM7 antibodies. Anti-SP1 (nuclear) and anti-SHC (cytosolic) antibodies served to verify the purity of the fractions. (*C*) Cells were lysed with 0.5% Triton and subjected to low-speed centrifugation to obtain "soluble 1" fraction and "pellet 1" fraction, containing chromatin and chromatin-bound proteins. Chromatin-bound proteins were solubilized from pellet 1 upon treatment with DNAse followed by low-speed centrifugation to obtain soluble 2 fraction. For each fraction, protein amounts deriving from comparable number of cells, were immunoblotted with anti-MCM7 and anti-NCOA4 antibodies. (*D, E*) HeLa cell protein total (*D*) or fractionated (*E*) extract was immunoprecipitated with anti-NCOA4 or with preimmune serum. Immunocomplexes were blotted with the indicated antibodies. Lysis buffer alone (-) was immunoprecipitated as a control. The results in panels *A-E* are representative of several independent experiments.

Figure 2. NCOA4 inhibits DNA replication in *Xenopus l.* egg extracts.

(*A*) *Xenopus l.* egg extracts, supplemented or not with the NUS-NCOA4 recombinant protein, were immunoprecipitated with anti-NCOA4 and immunoblotted with anti-NCOA4 or anti-MCM7 antibodies. (*B*) *Upper*: Agarose gel electrophoresis of DNA synthesized in *Xenopus l.* egg extracts using the indicated concentrations of NUS-NCOA4, heat inactivated NUS-NCOA4, or NUS moiety alone. *Lower*: percentage of synthesized DNA in each lane measured by phosphor imaging (average results ± SD of three independent determinations). (*C*) *Upper*: Agarose gel electrophoresis of DNA synthesized in *Xenopus l.* egg extracts using 150 nM of NUS-NCOA4, NUS-

NCOA4(N), or NUS-NCOA4(C). *Lower*: percentage of synthesized DNA in each lane measured by phosphor imaging (average results ± SD of three independent determinations). (*D*) *Upper*: Schematic representation of MCM7 protein and MCM7(C) fragment isolated by the two-hybrid screening. *Lower*: Agarose gel electrophoresis of DNA synthesized in *Xenopus l.* egg extracts in the presence or absence of 300 nM MCM7(C) recombinant protein. (*E*) *Upper*: Agarose gel electrophoresis of DNA synthesized in *Xenopus l.* egg extracts using the indicated concentrations of NUS-NCOA4 alone or with 300 nM MCM7(C). *Lower*: percentage of synthesized DNA in each lane measured by phosphor imaging (average results ± S.D. of three independent determinations).

Figure 3. NCOA4 inhibits DNA unwinding in *Xenopus l.* egg extracts.
(*A*) Loading of replication factors on chromatin measured after 120 min incubation with or without NUS-NCOA4. Time point 0 min, when no protein loading onto chromatin should be detected, was used as control. Proteins were isolated by centrifugation in sucrose gradient, and subjected to Western blotting with the indicated antibodies. (*B*) *Upper and middle*: Loading of PCNA and MCM7 on chromatin after incubation for 120 min with buffer, 100nM NUS-NCOA4 or 100 nM NUS-NCOA4 + 300 nM MCM7(C). Chromatin-bound proteins were isolated by centrifugation on sucrose gradient and analyzed by immunoblot with the indicated antibodies. *Lower*: Agarose gel electrophoresis of DNA synthesized in *Xenopus l.* egg extracts using buffer, 100 nM NUS-NCOA4 or 100 nM NUS-NCOA4 + 300 nM MCM7(C). Bar graphs represent the percentage of synthesized DNA measured by phosphor imaging (average results ± S.D. of three independent determinations). (*C*) *Upper*: loading of RPA and MCM7 on chromatin in the presence of buffer, 150 nM NUS-NCOA4, 150 nM NUS-NCOA4 + aphidicolin (10 μM), and aphidicolin (10 μM) alone. *Lower*: DNA synthesis of each sample was monitored by agarose gel electrophoresis. (*D*) *Upper:* Loading of RPA,

MCM7 and CDC45 on chromatin in the presence of buffer or aphidicolin (10 μM) + buffer, 100 nM NUS-NCOA4 or 100 nM NUS-NCOA4 + 300 nM MCM7(C). *Lower:* DNA synthesis of each sample was monitored by agarose gel electrophoresis. (*E*) Loading of DNA polymerase α (polα) and MCM7 on chromatin in the presence or absence of NUS-NCOA4 (150 nM) after 0, 40, and 80 min from replication onset. (*F*) M13 (*upper*) and sperm nuclei (*lower*) DNA was replicated in the presence of 300 nM NUS-NCOA4 and 10 μM aphidicolin, as indicated. DNA synthesis was monitored by agarose gel electrophoresis. These results are representative of three independent experiments.

Figure 4. Immunodepletion of XNCOA4 from *Xenopus l.* egg extracts increases DNA synthesis.

(*A*) *Xenopus l.* egg extracts were immunoprecipitated with anti-XNCOA4 or preimmune serum and immunoblotted with anti-XNCOA4 antibody. The antibody alone (no extract) served as control. (*B*) Loading of XNCOA4, MCM7 and PCNA on chromatin measured after 0, 30, 60 and 120 min of incubation of eggs extracts. Proteins were isolated by centrifugation in sucrose gradient, and subjected to Western blotting with the indicated antibodies. The bar graphs represent the percentage of synthesized DNA in each lane, measured by Cerenkov counting (average results ± S.D. of three independent determinations). (*C*) Activated *Xenopus l.* egg extracts were supplemented with sperm chromatin. After 20 min of incubation, extracts were immunoprecipitated with anti-XNCOA4 or preimmune serum and immunoblotted with anti-XNCOA4 or anti-MCM7 antibodies. The antibody alone (no extract) served as control. (*D*) *Left*: Western blot of *Xenopus l.* egg extracts that had been mock- (preimmune serum) or NCOA4-immunodepleted (anti-XNCOA4 antibody). Anti-XNCOA4 antibody alone (no extract) was used as control. *Right*: *Xenopus l.* egg extracts that have been mock-depleted or XNCOA4-depleted were harvested at the indicated time points and DNA replication

measured by Cerenkov counting (average results ± S.D. of three independent determinations). (*E*) Agarose gel electrophoresis of DNA synthesized at the indicated time points (*upper*) and loading of replication factors MCM7 and PCNA on chromatin (*middle and lower*) in *Xenopus l.* egg extracts that had been mock-depleted or NCOA4-immunodepleted. Extracts that were NCOA4-immunodepleted and then supplemented with 30 nM of NUS-NCOA4 recombinant protein were used as control. Proteins were isolated by centrifugation in sucrose gradient, and subjected to Western blotting with the indicated antibodies. The bar graphs represent the percentage of synthesized DNA in each lane, measured by phosphor imaging (average results ± S.D. of three independent determinations). (*F)* Loading of MCM7, CDC45 and RPA on chromatin measured after 60 min and 120 min of incubation of eggs extracts that had been mock-depleted or NCOA4-immunodepleted. Extracts that were NCOA4-immunodepleted and then supplemented with 30 nM NUS-NCOA4 were used as control. Proteins were isolated by centrifugation in sucrose gradient, and subjected to Western blotting with the indicated antibodies. The bar graphs represent the percentage of synthesized DNA in each lane, measured by phosphor imaging (average results ± S.D. of three independent determinations).

Figure 5. NCOA4 protein binds to DNA replication origins and influences cell growth and DNA synthesis rate in HeLa cells.
(*A, B*) Chromatin immunoprecipitation of human Lamin B2 (LB2) (*A*) and c-Myc (*B*) DNA replication origins, performed using preimmune serum or anti-NCOA4 and anti-Cdc6 antibodies. *Upper panels*: maps depicting the location of relevant regions of the two loci. PCR fragments at origins and control regions are indicated. *Lower panels*: ethidium bromide staining of PCR products. (*C*) HeLa cells were mock-transfected (-) or transfected with NCOA4 2i or NCOA4 3i siRNAs or scrambled siRNA. After 48 hours, NCOA4 protein levels were measured by immunobloting. Anti-lamin antibody was used for normalization (*left*). DNA synthesis was measured by anti-BrdU

immunofluorescence (*right*). The average results ± SD of three independent experiments made in duplicate are reported. *$P < 0.02$ (two-side paired Student's *t*-test). (*D*) Scrambled or NCOA4 2i transfected cells were released from double-thymidine block at the indicated time points and subjected to flow cytometry. Percentage of cells in G1, S and G2 phases is indicated. (*E*) Cells were lysed with 0.5% Triton and subjected to low-speed centrifugation to obtain "soluble 1" fraction and "pellet 1" fraction, containing chromatin and chromatin-bound proteins. Chromatin-bound proteins were solubilized from pellet 1 upon treatment with DNAse followed by low-speed centrifugation to obtain soluble 2 fraction. For each fraction, protein amounts deriving from comparable number of scrambled RNAi or NCOA4 2i transfected cells were immunoblotted with anti-MCM7 and anti-PCNA antibodies.

Supplementary material

Materials and Methods

Yeast Two-Hybrid Screening. Molecular cloning of the human NCOA4 cDNA (GenBank accession NM_005437) is reported elsewhere (Santoro et al, 1994). The N-terminal portion of the human NCOA4 protein (amino acids 2-238) was fused in frame to the GAL4 DNA binding domain in the pGBKT7 vector (Clontech, Mountain View, CA) carrying the TRP1 selection, to generate the GAL4-NCOA4(N) bait. The plasmid was controlled by DNA sequencing. 10^6 transformants of the MATCHMAKER HeLa cell cDNA library (Clontech) cloned in the pGADT7 vector, carrying the LEU2 selection, were screened with the GAL4-NCOA4(N) bait. Twelve HIS synthase- and ADE synthase-positive cDNA clones were isolated in HTLA (histidine/threonine/leucine/adenine-deprived) medium and confirmed by retro-transformation in the yeast strain AH109; the backbone GAL4 and the empty vector served as negative controls. All the isolated cDNA clones were DNA sequenced and aligned to the GenBank (National Center for Biotechnology Information) by using the Basic Alignment Search Tool (BLAST) software.

Recombinant Proteins. NUS-NCOA4, NUS-NCOA4(N) and NUS-NCOA4(C) were generated by PCR amplification of the entire NCOA4 open reading frame or its 5'-terminal (amino acids 2-238) or 3'-terminal (amino acids 239-614) portions, respectively. Fragments were then fused in-frame to the solubility *tag* NUS in the pET vector (Davis et al. 1999). MCM7(C) was generated by PCR amplification of the C-terminal portion of the human MCM7 cDNA (amino acids 576-719). The PCR product was fused in-frame to NUS *tag* in the pET vector. The plasmids were controlled by DNA sequencing. Recombinant proteins were produced in *Escherichia coli* by using standard protocols.

Cloning of XNCOA4α and XNCOA4β cDNA. We identified two different cDNA species coding for XNCOA4α and XNCOA4β by blasting the GenBank against the human NCOA4 protein sequence. PCR primers were then designed to amplify both XNCOA4α and XNCOA4β cDNAs using Accuprime-Pfx taq polymerase (Invitrogen Groningen, The Netherlands). Primer sequences were as follows:
XNCOA4α Forward: 5'-ATGAATTTGCACCAAGATCATGAATTT-3'
XNCOA4α Reverse: 5'-CATCTGCAAGGGAGACTGGTATAG-3'
XNCOA4β Forward: 5'-ATGAATTTGCACCAAGATCATCAATTCAGC-3'
XNCOA4β Reverse: 5'-CATCTGCAAGGGAGACTGGTATAG-3'
cDNAs were subcloned in PCR2.1 TA cloning vector (Invitrogen), controlled by double strand DNA sequencing and then subjected to *in vitro* transcription/translation using T7 polymerase and rabbit reticulocyte extracts (Promega, Madison, Wisconsin). GST-XNCOA4 recombinant protein was generated by PCR amplification of the 3'-terminal (amino acids 278-625) of XNCOA4β coding region; the PCR products were fused in-frame to the GST moiety in the pGEX2T vector (Amersham Pharmacia Biotech, Little Chalfort, UK). Recombinant proteins were produced in *Escherichia coli* by using standard protocols.

Protein studies. Cells were lysed in a buffer containing 50 mM N-2-hydroxyethylpiperazine-N'-2-ethanesulfonic acid (HEPES; pH 7.5), 1% (vol/vol) Triton X-100, 150 mM NaCl, 5 mM EGTA, 50 mM NaF, 20 mM sodium pyrophosphate, 1 mM sodium vanadate, 2 mM phenylmethylsulphonyl fluoride (PMSF) and 1 μg/ml aprotinin. Lysates were clarified by centrifugation at 10,000 x g for 15 min. Lysates containing comparable amounts of proteins, estimated by a modified Bradford assay (Bio-Rad, Munchen, Germany), were immunoprecipitated with the required antibody or subjected to direct Western blot. Immune complexes were detected with the enhanced chemiluminescence kit (Amersham Pharmacia Biotech). Immunoblotting was carried

out with specific antibodies. For binding assay (pull-down), HeLa cells lysates were incubated with 5 μg of immobilized fusion proteins. Bound proteins were detected by immunoblot analysis.

Cell fractionation and analysis of nuclear fractions. For subcellular fractionation, cells in the mid-exponential phase of growth were collected by scraping from the culture dish after two washings with 20 ml ice-cold 1X phosphate-buffered saline (PBS). Subcellular fractions were prepared using the NE-PER nuclear and cytoplasmic extraction kit (Pierce Biotechnology, Rockford, Il). Triton X-100-extracted nuclei were prepared as follows. Cells cultured in 100-mm dishes were washed three times with ice-cold phosphate-buffered saline and divided in two aliquots. One aliquot was lysed with standard buffer (total). The other aliquot was incubated for 10 min on ice with 200 μl of ice-cold CSK buffer (10 mM PIPES, pH 6.8, 100mM NaCl, 300 mM sucrose, 1mM $MgCl_2$, 1 mM EGTA, 1 mM DTT, 1 mM phenylmethylsufonyl fluoride, 10 μg/ml aprotinin) containing 0.5% Triton X-100 (Pierce Biotechnology). Chromatin-bound proteins (pellet 1) were separated from unbound proteins (soluble 1) by low speed centrifugation (3,000 rpm, 3 min at 4°C). Pellet 1 was divided in two aliquots, one of which was further digested with 1,000 units/ml DNase I (pellet 1 +DNAse) (10 units/μl, RNase-free, Boehringer Mannheim, Germany) in 100 μl of 0.1%Triton X-100 containing CSK supplemented with 1mM ATP at 25° C for 30 min to solubilize chromatin-bound proteins and then subjected to low-speed centrifugation (3,000 rpm, 3 min at 4°C) to generate soluble 2 (supernatant) and pellet 2 fractions. For each fraction, protein amounts deriving from comparable number of cells were analysed by SDS-PAGE and Western blotting.

DNA replication and chromatin binding assays. *Xenopus l.* egg extracts were supplemented with 100 μg/μL cycloheximide and energy mix (7.5 mM creatine

phosphate, 1 mM ATP, 0.1 mM EGTA, pH 7.7, 1 mM $MgCl_2$) and released in interphase with 0.4 mM $CaCl_2$. DNA was synthesized by adding 6.000/μL sperm nuclei (unless differently specified) and 1μCi [α-^{32}P] dATP and incubating the reaction for 120 min at 23°C followed by agarose gel electrophoresis. Gels were exposed for autoradiography and quantified using the PhosphorImager (Typhoon 8600, Amersham Pharmacia Biotech) interfaced with the ImageQuant software. Alternatively, reactions were spotted on GF/C glass microfiber filters, washed with 1% orthophosphoric acid and read at the β-counter using Cerenkov method. Nuclei were visualized by fluorescent microscopy after fixing in paraformaldehyde (4%) and staining with Hoechst 33258 (final concentration 1 μg/ml; Sigma Chemicals Co, St. Louis, MO). For chromatin binding assays, replication reactions were assembled as above. After incubation, each reaction was re-suspended in chromatin isolation buffer (100 mM KCl, 40 mM Hepes pH 7.8, 10 mM $MgCl_2$) supplemented with 0.1% Triton X-100 and overlaid on the same buffer containing 30% sucrose. The chromatin was pelleted at 6,000*g* for 20 min at 4°C. The pellet was re-suspended in 1X Laemmli buffer, run on a 10% SDS-PAGE and analysed by Western blotting with specific antibodies. For immunodepletion, prior to $CaCl_2$ activation, egg extracts were incubated with 5 μg of anti-XNCOA4 antibody or preimmune serum, pre-absorbed on 20 μl of protein G-Sepharose slurry (Roche Diagnostics S.p.A, Monza, Italy), for 45 min rocking at 4°C.

Cell culture methods, immunofluorescence and cytofluorimeter analysis.

Anti-NCOA4 siRNAs were designed with a program available online (http://jura.wi.mit.edu/siRNAext) and synthesized by Proligo (Boulder, CO). SiRNA sense strand sequences were as follows:

NCOA4 1i: 5'-UAUCUCCAUGCCAGAGCAGAA-3'

NCOA4 2i: 5'-AAGAUUCAACUGUCCUGCUCUUU-3'

NCOA4 3i: 5'- GGCCCAGGAAGUAUUACUU-3'

Scrambled: 5'-ACCGUCGAUUUCACCCGGUU-3'

For the double-thymidine block, cells were treated for 12-14 h with complete medium containing 4 mM thymidine, released in 24 μM cytidine for 12 hours and treated again with 4 mM thymidine for additional 12-14 h. Upon thymidine wash-out, cells were harvested at different time points and processed for flow cytometry. For DNA synthesis measurements, cells were seeded on glass coverslips. Bromodeoxyuridine (BrdU; Sigma Chemical Co.) was added to the cell culture medium at a final concentration of 100 μg/ml for 2 h before harvest. Cells were fixed with paraformaldehyde (4%) and permeabilized with Triton X-100 (0.2%) before staining. Coverslips were incubated with anti-BrdU mouse monoclonal antibody and then with a Texas red-conjugated anti-mouse antibody (Boehringer Mannheim, Germany). All coverslips were counterstained in PBS containing Hoechst 33258 (final concentration, 1μg/ml; Sigma Chemical Co.), rinsed in PBS and mounted in Moviol on glass slides. The fluorescent signal was visualized with an epifluorescent microscope (Axiovert 2, Carl Zeiss) interfaced with the image analyzer software KS300 (Carl Zeiss). For cytofluorimetric analysis, cells were harvested and then fixed in cold 70% ethanol in phosphate-buffered saline. Propidium iodide (25 μg/ml) was added and samples were analyzed with a FACScan flow cytometer (Becton Dickinson, San Jose, CA) interfaced with a Hewlett Packard computer (Palo Alto, CA).

Chromatin Immunoprecipitation. Primers for PCR were as follows:

Lamin B2 origin:

Forward 5'-GGCTGGCATGGACTTTCATTTCAG-3'

Reverse 5'-GTGGAGGGATCTTTCTTAGACATC-3'

Control region:

Forward 5'-CTGCCGCAGTCATAGAACCT-3'

Reverse 5'-ATGGTCCCCAGGATACACAA-3'

c-Myc origin:

Forward 5'-TATCTACACTAACATCCCACGCTCTG-3'

Reverse 5'-CATCCTTGTCCTGTGAGTATAAATCATCG-3'

Control region:

Forward 5'-TTCTCAACCTCAGCACTGGTGACA-3'

Reverse 5'-GACTTTGCTGTTTGCTGTCAGGCT-3'

Supplementary material references

Davis GD, Elisee C, Newham DM, Harrison RG (1999) New fusion protein systems designed to give soluble expression in Escherichia coli. *Biotechnol Bioeng* **65**: 382-388.

Santoro, M., Dathan, N.A., Berlingieri, M.T., Bongarzone, I., Paulin, C., Grieco, M., Pierotti, M.A., Vecchio, G., and Fusco, A. 1994. Molecular characterization of RET/PTC3; a novel rearranged version of the RET proto-oncogene in a human thyroid papillary carcinoma. *Oncogene* **9**: 509-516.

Supplementary material figure legends

Figure S1. NCOA4 and MCM7 interact in a yeast two hybrid system.
Upper: Schematic representation of NCOA4 and MCM7 proteins, the NCOA4(N) bait used for the yeast 2-hybrid screen and the MCM7(C) prey isolated in the screening. NCOA4(C) fragment is also indicated. Protein domains able to fold into coiled-coils are indicated. The breakpoint position of NCOA4 in the RET/PTC3 rearrangement is shown. *Lower*: Growth of yeast cells transfected with the indicated plasmids in HTLA (histidine/threonine/leucine/adenine-deprived) selective medium.

Figure S2. NUS-NCOA4 inhibits DNA replication in *Xenopus l*. egg extracts.
(*A*) Nuclei envelope formation in egg estracts supplemented or not with 150 nM NUS-NCOA4. (*B*) *Xenopus l*. egg extracts supplemented or not with 150 nM NUS-NCOA4 were harvested at the indicated time points and DNA replication monitored by spotting the reaction on glass microfiber filters and measured by Cerenkov counting (average results ± S.D. of three independent determinations).

Figure S3. NCOA4 binding to chromatin is independent on the MCM complex.
Upper: Loading of NUS-NCOA4 and MCM7 on chromatin was monitored after incubation for 120 min with or without the recombinant GST-Geminin. Time point 0 min served as loading control. Chromatin-bound proteins were isolated by centrifugation in sucrose gradient and analyzed by immunoblot with the indicated antibodies. *Middle and Lower*: The DNA synthesis of each sample was monitored by agarose gel electrophoresis and the percentage of synthesized DNA in each lane measured by phosphorimaging (average results ± S.D. of three independent determinations).

Figure S4. Cloning of XNCOA4α and XNCOA4β cDNA and generation of anti-XNCOA4 antibody.
(*A*) Alignment between *Xenopus l*. XNCOA4α, XNCOA4β and human hsNCOA4 coding sequences performed with CLUSTALW (www.ebi.ac.uk/clustalw/). Predicted coiled-coil motifs are boxed in grey. (*B*) Products from *in vitro* transcription/translation reactions using XNCOA4α and XNCOA4β cDNA as templates and ^{35}S-Methionine have been subjected to immunoprecipitation with anti-XNCOA4, run on SDS-PAGE, fixed in acetic acid/methanol, dried and exposed to autoradiography. Aliquots of total reactions were loaded as input control.

Figure S5. NCOA4 knock-down increases BrdU incorporation.
(*A*) HeLa cells were mock-transfected (-) or transfected with NCOA4 1i or NCOA4 2i siRNAs or scrambled siRNA. After 72 hours, NCOA4 protein levels were measured by immunobloting. Anti-lamin antibody was used for normalization. (*B*) DNA synthesis was measured by anti-BrdU immunofluorescence. The average results ± SD of three independent experiments made in duplicate are reported. *$P < 0.02$ (two-side paired Student's *t*-test).

Figure S6. Adoptive NCOA4 over-expression reduces cell growth and BrdU incorporation and induces a S-phase arrest.
(*A*) Immunoblot detection of Myc-tagged NCOA4 protein upon doxycycline (Dox) (48 hours) induction in two independent HeLa-NCOA4 clones (clones 23 and 24). (*B*) HeLa-NCOA4 (clones 23 and 24) cell growth with and without Dox; the average results ± SD of three independent experiments performed in triplicate are reported. (*C*) HeLa-NCOA4 clone 24 cells flow cytometry and anti-BrdU immunofluorescence upon Dox treatment (48 hours). The average results ± SD of three independent experiments made in duplicate are reported. *$P < 0.02$ (two-side paired Student's *t*-test). The same results were obtained with HeLa-NCOA4 clone 23 (not shown).

Figure S7. Adoptive NCOA4 over-expression reduces RPA and PCNA loading on chromatin.
HeLa NCOA4-Cl24 cells were treated or not with Dox for 48 hours. Cells were lysed with 0.5% Triton and subjected to low-speed centrifugation to obtain "soluble 1" fraction and "pellet 1" fraction, containing chromatin and chromatin-bound proteins. Chromatin-bound proteins were solubilized from pellet 1 upon treatment with DNAse followed by low-speed centrifugation to obtain soluble 2 fraction. For each fraction, protein amounts deriving from comparable number of cells were immunoblotted with anti-MCM7, anti-RPA and anti-PCNA antibodies.

Fig. 2

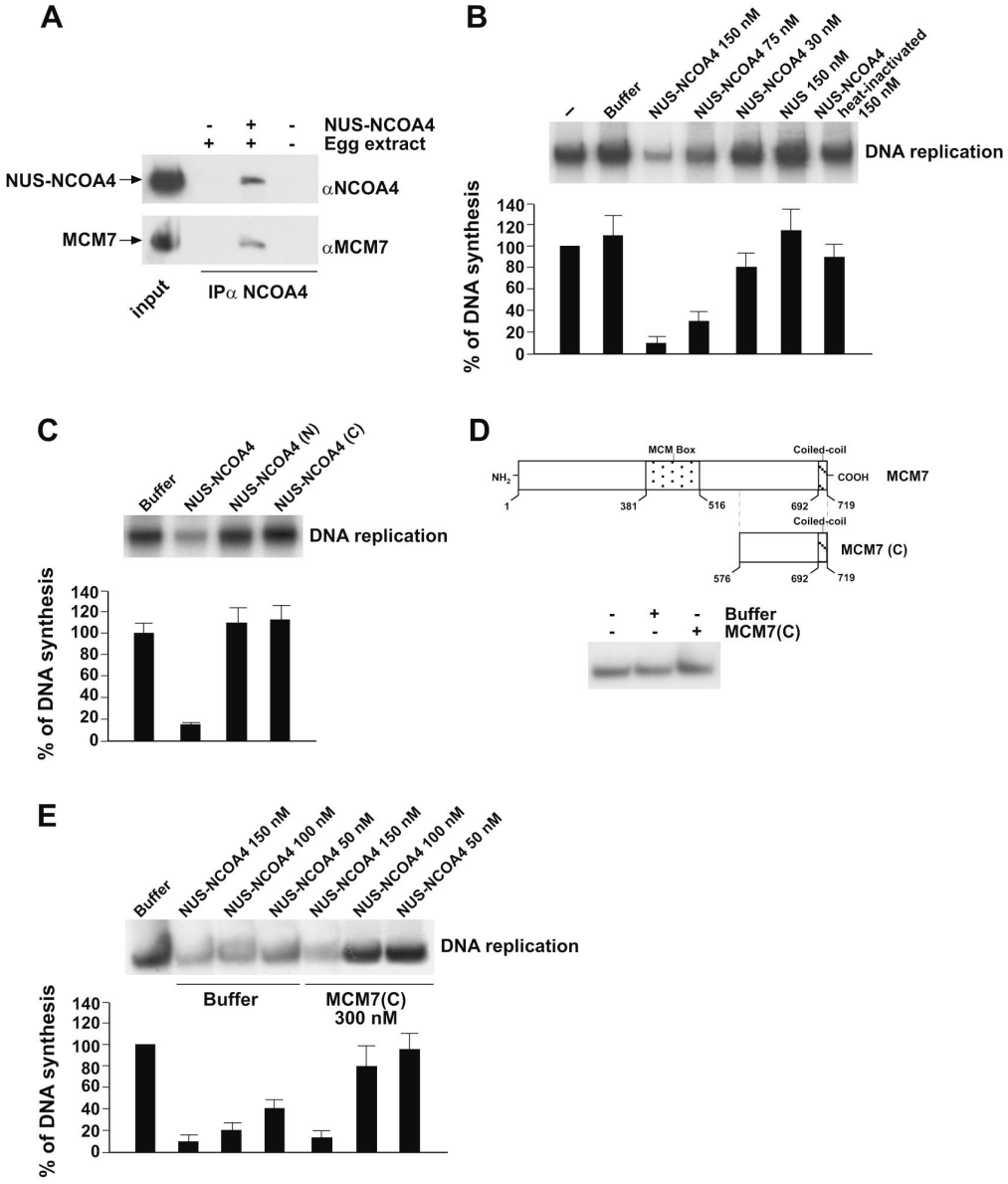
A
- + - NUS-NCOA4
+ + - Egg extract
NUS-NCOA4
αNCOA4
MCM7
αMCM7
input
IPα NCOA4
B
–
Buffer
NUS-NCOA4 150 nM
NUS-NCOA4 75 nM
NUS-NCOA4 30 nM
NUS 150 nM
NUS-NCOA4 heat-inactivated 150 nM
DNA replication
% of DNA synthesis
C
Buffer
NUS-NCOA4
NUS-NCOA4 (N)
NUS-NCOA4 (C)
DNA replication
% of DNA synthesis
D
MCM Box
Coiled-coil
NH2
COOH
MCM7
1
381
516
692
719
Coiled-coil
MCM7 (C)
576
692
719
- + - Buffer
- - + MCM7(C)
E
Buffer
NUS-NCOA4 150 nM
NUS-NCOA4 100 nM
NUS-NCOA4 50 nM
NUS-NCOA4 150 nM
NUS-NCOA4 100 nM
NUS-NCOA4 50 nM
DNA replication
Buffer
MCM7(C) 300 nM
% of DNA synthesis

Fig. 3

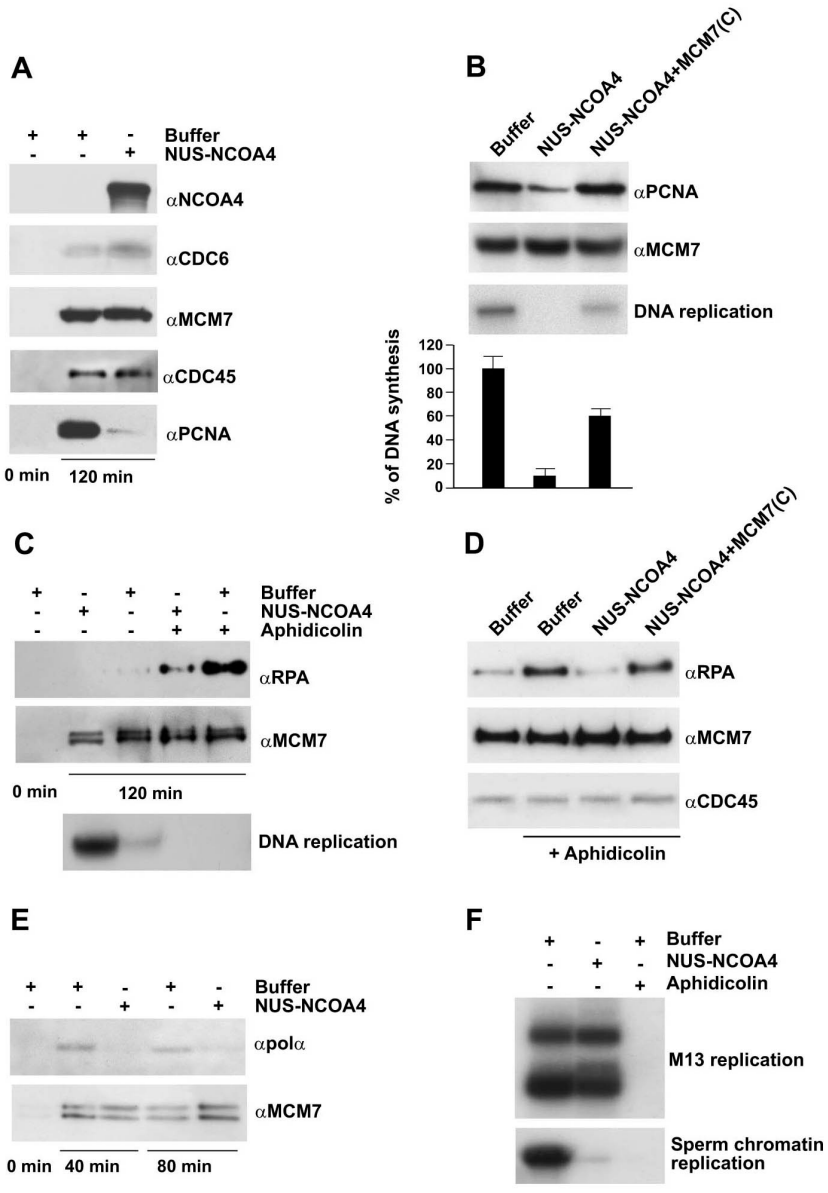
A
Buffer
NUS-NCOA4
αNCOA4
αCDC6
αMCM7
αCDC45
αPCNA
0 min
120 min
B
Buffer
NUS-NCOA4
NUS-NCOA4+MCM7(C)
αPCNA
αMCM7
DNA replication
% of DNA synthesis
120
100
80
60
40
20
0
C
Buffer
NUS-NCOA4
Aphidicolin
αRPA
αMCM7
0 min
120 min
DNA replication
D
Buffer
Buffer
NUS-NCOA4
NUS-NCOA4+MCM7(C)
αRPA
αMCM7
αCDC45
+ Aphidicolin
E
Buffer
NUS-NCOA4
αpolα
αMCM7
0 min
40 min
80 min
F
Buffer
NUS-NCOA4
Aphidicolin
M13 replication
Sperm chromatin replication

Fig. 4

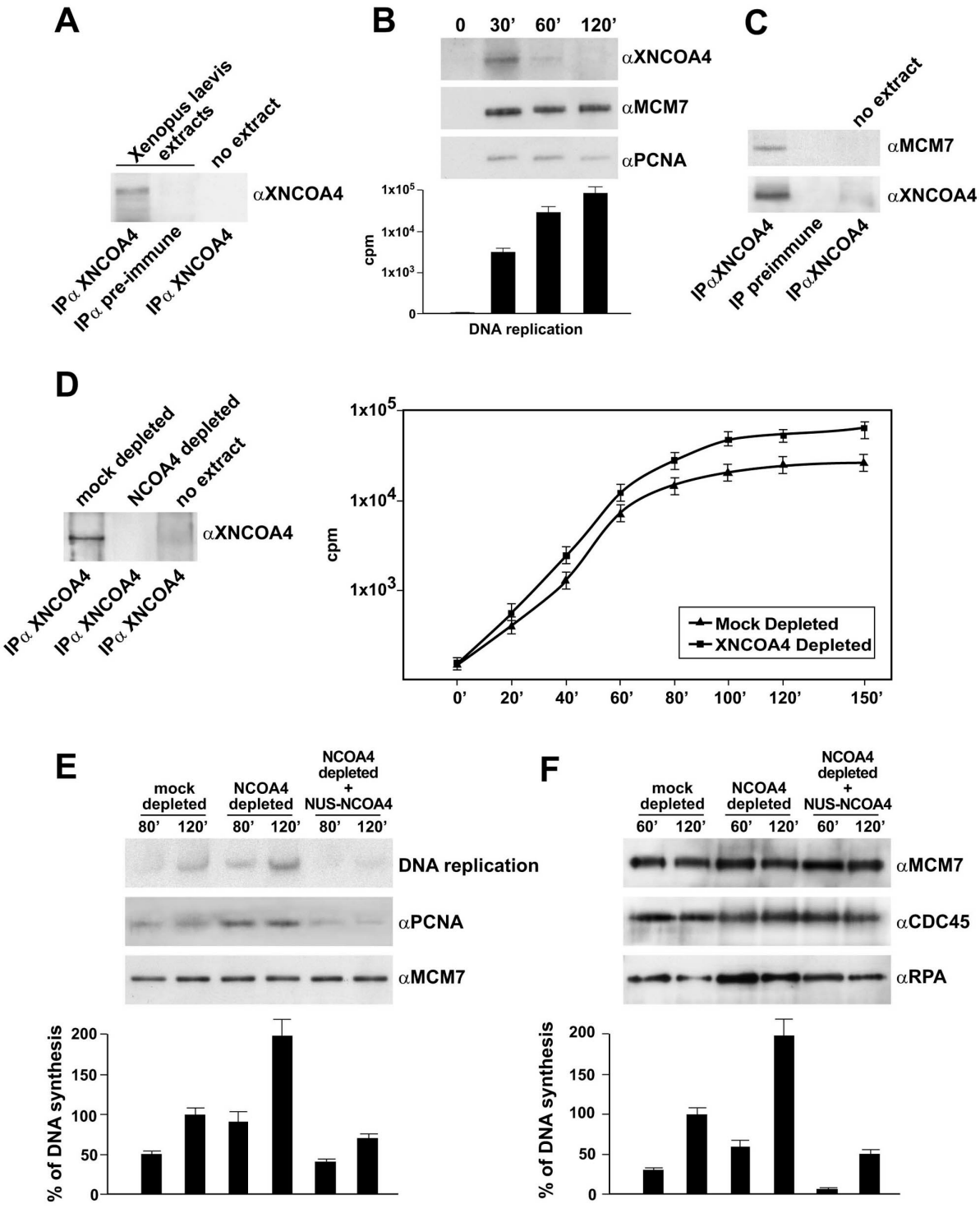
A
Xenopus laevis extracts
no extract
αXNCOA4
IPα XNCOA4
IPα pre-immune
IPα XNCOA4
B
0
30'
60'
120'
αXNCOA4
αMCM7
αPCNA
cpm
1x10^5
1x10^4
1x10^3
0
DNA replication
C
no extract
αMCM7
αXNCOA4
IPαXNCOA4
IP preimmune
IPαXNCOA4
D
mock depleted
NCOA4 depleted
no extract
αXNCOA4
IPα XNCOA4
IPα XNCOA4
IPα XNCOA4
cpm
1x10^5
1x10^4
1x10^3
Mock Depleted
XNCOA4 Depleted
0'
20'
40'
60'
80'
100'
120'
150'
E
mock depleted
NCOA4 depleted
NCOA4 depleted + NUS-NCOA4
80'
120'
80'
120'
80'
120'
DNA replication
αPCNA
αMCM7
% of DNA synthesis
200
150
100
50
0
F
mock depleted
NCOA4 depleted
NCOA4 depleted + NUS-NCOA4
60'
120'
60'
120'
60'
120'
αMCM7
αCDC45
αRPA
% of DNA synthesis
200
150
100
50
0

Fig. 5

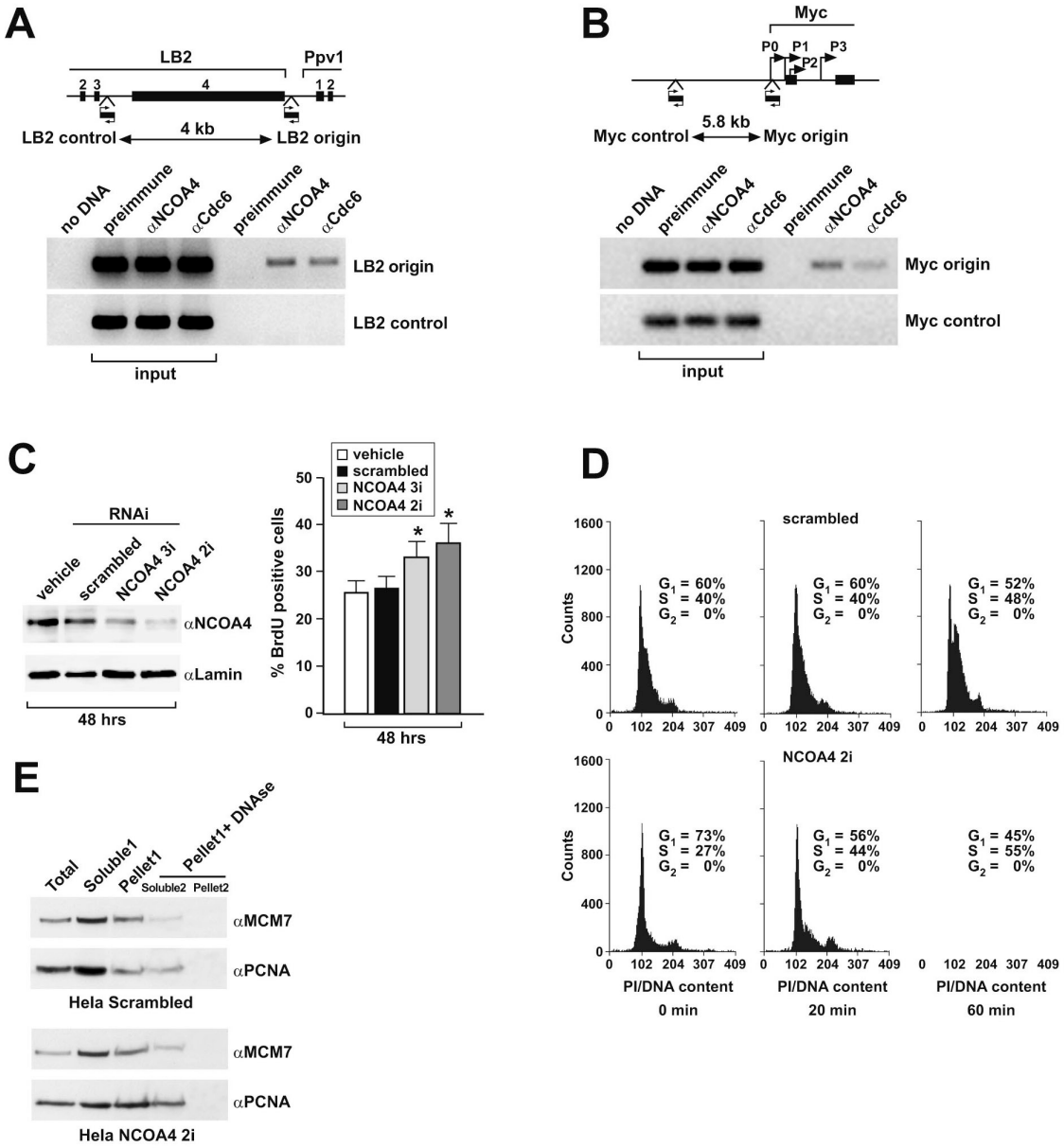
A
LB2
Ppv1
2 3
4
1 2
LB2 control
4 kb
LB2 origin
no DNA
preimmune
αNCOA4
αCdc6
preimmune
αNCOA4
αCdc6
LB2 origin
LB2 control
input
B
Myc
P0
P1
P2
P3
5.8 kb
Myc control
Myc origin
no DNA
preimmune
αNCOA4
αCdc6
preimmune
αNCOA4
αCdc6
Myc origin
Myc control
input
C
RNAi
vehicle
scrambled
NCOA4 3i
NCOA4 2i
αNCOA4
αLamin
48 hrs
vehicle
scrambled
NCOA4 3i
NCOA4 2i
% BrdU positive cells
48 hrs
D
scrambled
Counts
G1 = 60%
S = 40%
G2 = 0%
G1 = 60%
S = 40%
G2 = 0%
G1 = 52%
S = 48%
G2 = 0%
NCOA4 2i
G1 = 73%
S = 27%
G2 = 0%
G1 = 56%
S = 44%
G2 = 0%
G1 = 45%
S = 55%
G2 = 0%
PI/DNA content
0 min
PI/DNA content
20 min
PI/DNA content
60 min
E
Total
Soluble1
Pellet1
Soluble2
Pellet2
Pellet1+ DNAse
αMCM7
αPCNA
Hela Scrambled
αMCM7
αPCNA
Hela NCOA4 2i

Fig. S1

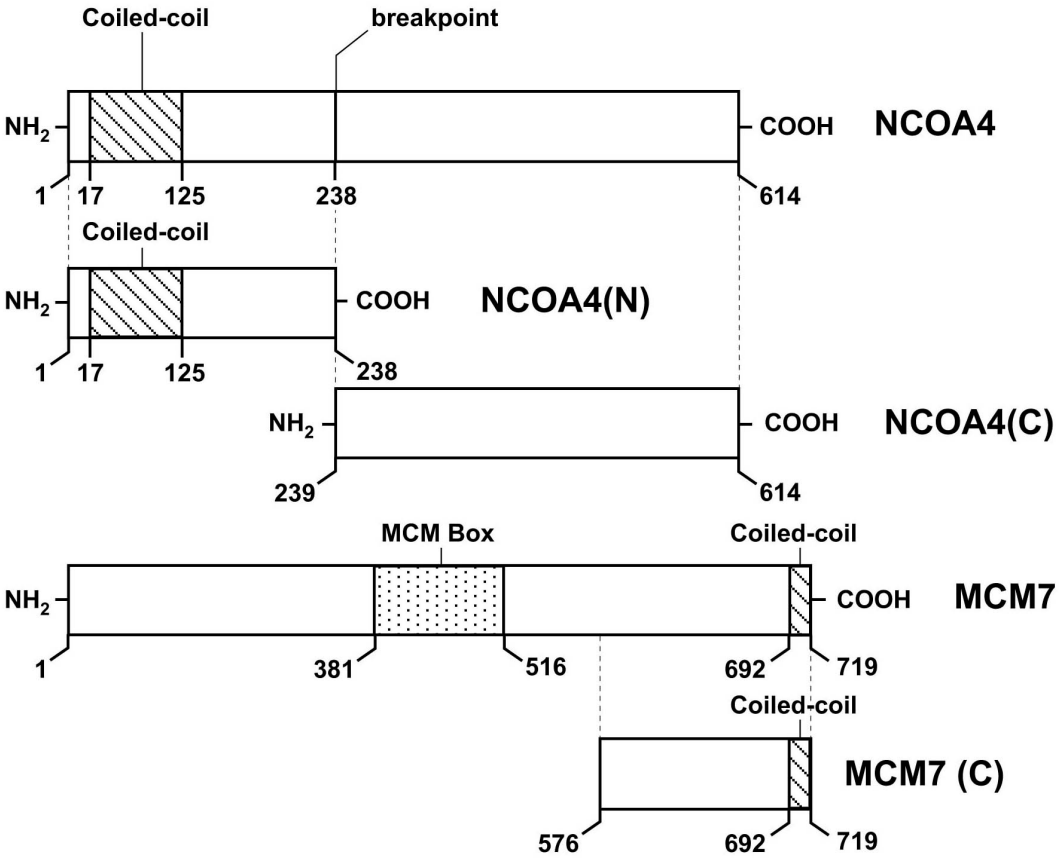

Growth on HTLA

	+ NCOA4(N)	+ empty vector	+ unrelated prey
NCOA4 (10)	++++	-	-
MCM7 (2)	++++	-	-

Fig. S2

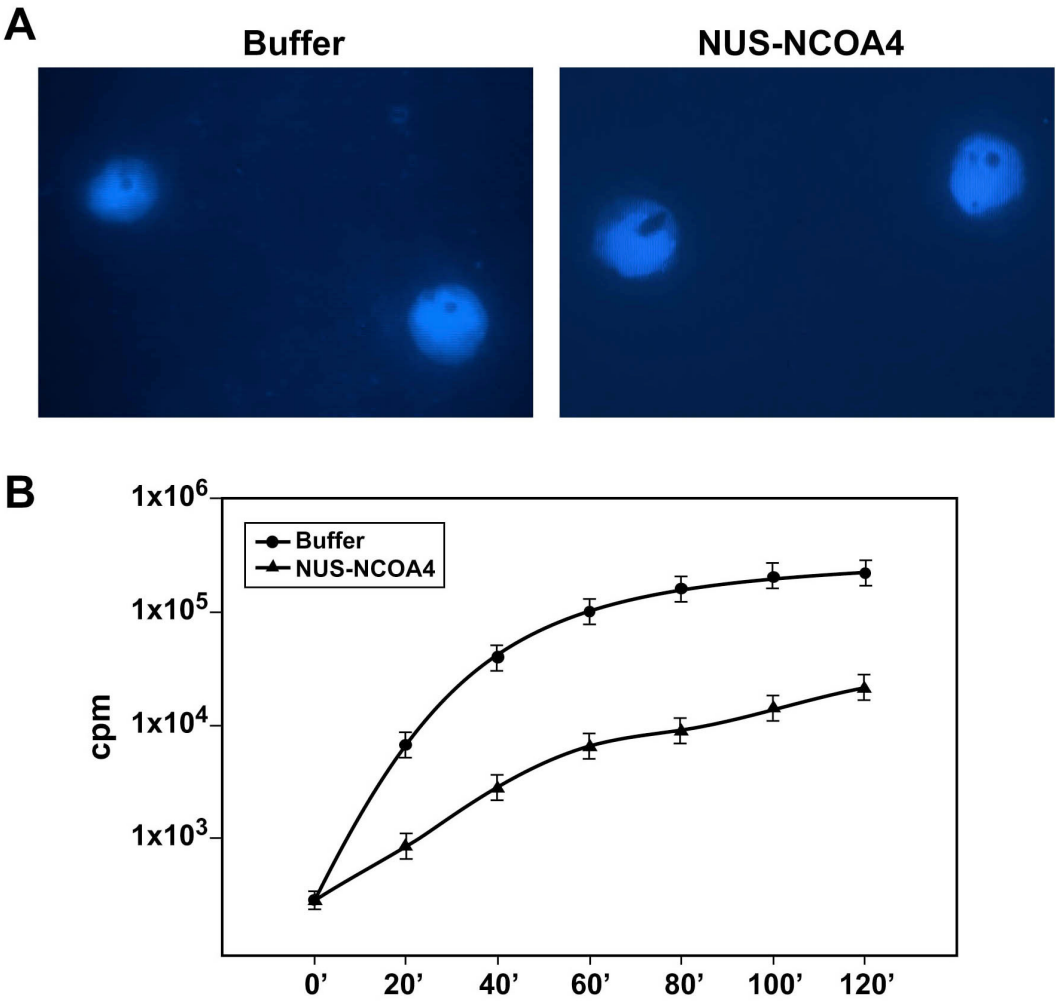
A
Buffer
NUS-NCOA4
B
1x10^6
1x10^5
1x10^4
1x10^3
cpm
Buffer
NUS-NCOA4
0'
20'
40'
60'
80'
100'
120'

Fig. S3

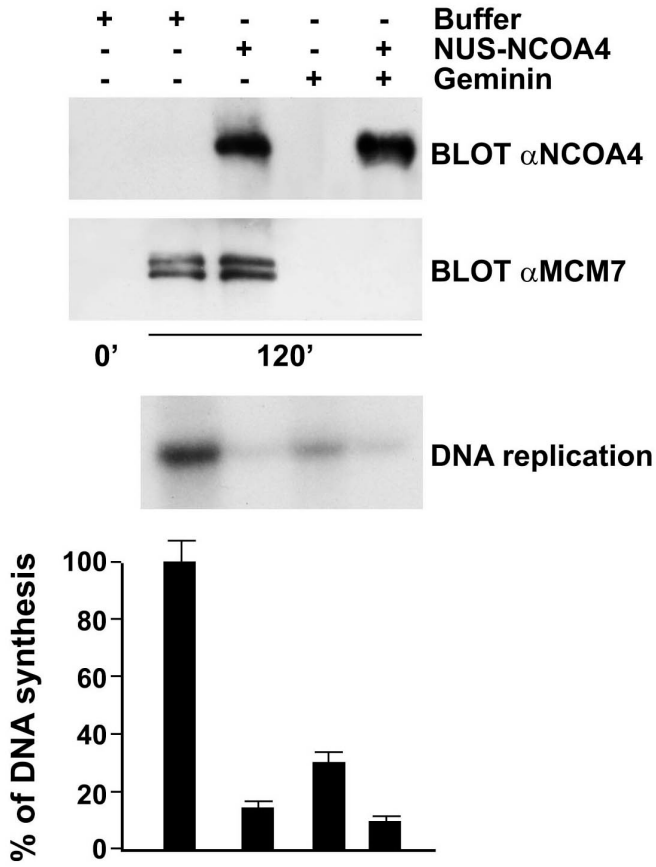
+ + - - - Buffer
- - + - + NUS-NCOA4
- - - + + Geminin
BLOT αNCOA4
BLOT αMCM7
0'
120'
DNA replication
% of DNA synthesis
100
80
60
40
20
0

Fig. S4

A

```
XNCOA4α  MNLHQDHQFSS--QDPLSKCLQAKQELESAISAMLKAEQQVKENGREVKSQVQSCISRHL
XNCOA4β  MNLHQDHEFSS--QDPLSKCLEAKKELESAISAVLKAEQQVKENGREVKSQVQSYISRHL
hsNCOA4  MNTFQDQSGSSSNREPLLRCSDARRDLELAIGGVLRAEQQIKDNLREVKAQIHSCISRHL
         ** .**:. **  ::** :* :*:::** **..:*:****:*:* ****:*::* *****

XNCOA4α  ECLRSREVWLLEQADLVQQLKEEALQQQAQQLYWLLGQFNCLIHQLENPQSNDLVNQISV
XNCOA4β  ECLRSREVWLLEQADLIQQLKEETLQQQSQQLYWLLGQFNCLIHQLETPHSTDLVHQISV
hsNCOA4  ECLRSREVWLYEQVDLIYQLKEETLQQQAQQLYSLLGQFNCLTHQLECTQNKDLANQVSV
         ********** **.**: *****:****:**** ******** **** .:..**.:*:**

XNCOA4α  CLERLGNLALKPEESSTLYFEGDVPFLRQAITKFGSIKTLSSSEEKQVSSLSVPCPFVSQ
XNCOA4β  CLERLGNLALKPEESSTLYFEADVPFLRQAIATFGSIKTLSSSEEKQVLSTAVPCPYVSQ
hsNCOA4  CLERLGSLTLKPEDSTVLLFEADTITLRQTITTFGSLKTIQIPEHLMAHASSA-----NI
         ******.*:****:*:.* **.*.  ***:*:.***:**:. .*.  . : :.     .

XNCOA4α  NPWLLNNCFVPAAEQQPVSGMWNTPLSDWLQQKRPTNISQCYTPHIPSLCTQDWLLKNHV
XNCOA4β  NPWLLNNCFVPAAEQRPLSGMWNTPLSDWLQQKKPTSVSQCYTPYIPSLCTQDWLLKNHV
hsNCOA4  GPFLEKRGCISMPEQKSASGIVAVPFSEWLLGSKPASGYQ--APYIPSTDPQDWLTQKQT
         .*:* :.  :. .**:. **:  .*:*:**  .:*:.  *  :*:***  .**** :::.

XNCOA4α  AEPNGELSKPN--MEQIWGQLGELNNWLLQSQQKKDLECM--ISSSQFSIEKIEDRDVES
XNCOA4β  AEPNEELSKPN--MEEIWGQLGELNNWLLQSQQKENLECK--SSSSQFSIEKLEDKDAES
hsNCOA4  LENSQTSSRACNFFNNVGGNLKGLENWLLKSEKSSYQKCNSHSTTSSFSIEMEKVGDQEL
          * .   *:.   :::: *:*  *:****:*::..  :*    ::*.****  :  * *

XNCOA4α  QDTEDMDLSDWLITPTVT---EDPTDVAEKWRAIFKSFDEDYKISDWLLKVEACGNYCGG
XNCOA4β  QDLEDMDLSDWLISPEVT---EDPTNV-----AVFKAFDEDYKINDWLLKVEACGNCCGR
hsNCOA4  PDQDEMDLSDWLVTPQESHKLRKPENGSRETSEKFKLLFQSYNVNDWLVKTDSCTNCQGN
          * ::*******::*  :   ..* :        ** : :.*::.***:*.::* *  *

XNCOA4α  QTSALEIENLGYLKCLNEQIGGKKNVSS---SNDTWLLQSSQPVFKPQDVCKANEQCSTF
XNCOA4β  QTSALEIENLGKLKCLNDQIGGKNNVSS---SNDIWLLQSSQPVFKPQDVCKANEQCSTF
hsNCOA4  QPKGVEIENLGNLKCLNDHLEAKKPLSTPSMVTEDWLVQNHQDPCKVEEVCRANEPCTSF
         *...:****** *****::: .*: :*:    .: **:*. *   * ::**:*** *::*

XNCOA4α  ADCMCDESCEKEALRKWLWKRDGKDKNGVLQKQGQNLKNHEPEKAKPSISMWLHPCRRDA
XNCOA4β  AECVCDESCEKEALRKWLWKREGKDKNGVLQKQRQNLKNREPEKAEPSISMWLHPCRRDA
hsNCOA4  AECVCDENCEKEALYKWLLKKEGKDKNGMPVEPKP-----EPEKHKDSLNMWLCP-RKEV
         *:*:***.****** *** *::******:  :        **** : *:.*** * *::.

XNCOA4α  KSQSSTQKTEENDPSVKHMMNLLETPLSKWIAKSSLTEEKTSKES--TQSKCSHP--AEM
XNCOA4β  --QSSTQKTQECDPSVKHMMDLVETPLSKWMAKSNLTEEKASKET--TQSKCSPQ--AET
hsNCOA4  IEQTKAPKAMTPSRIADSFQVIKNSPLSEWLIRP-PYKEGSPKEVPGTEDRAGKQKFKSP
           *:.: *:   .  .. :  : ::***:*: :.   :* :.**   *:.:..     .

XNCOA4α  LSQFHLPLNTTSWVLPSKNVDKFEKS---AIEDKWLLRKKA-----------H----DY
XNCOA4β  LSPFHLPLNAANWVLPLKTVDKLEKSEQSAIEDKWLLRKKA-----------H----DY
hsNCOA4  MNTSWCSFNTADWVLPGKKMGNLSQLS--SGEDKWLLRKKAQEVLLNSPLQEEHNFPPDH
         :.    .:*::.**** *.:.::.:    : **********            *    *:

XNCOA4α  YGLPSVCDLFACMKLAADKEKWLYQSPLQM
XNCOA4β  YGLPSVCDLFACMKLAADKEKWLYQSPLQM
hsNCOA4  YGLPAVCDLFACMQLKVDKEKWLYRTPLQM
         ****:********:* .*******::****
```

B

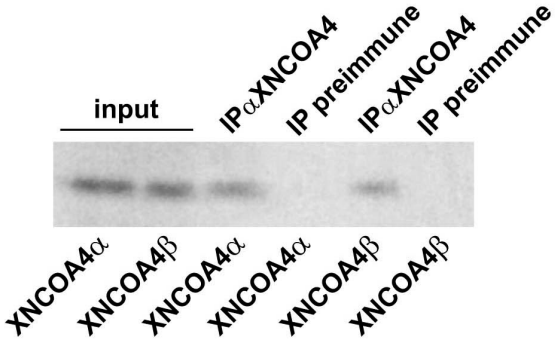

Fig. S5

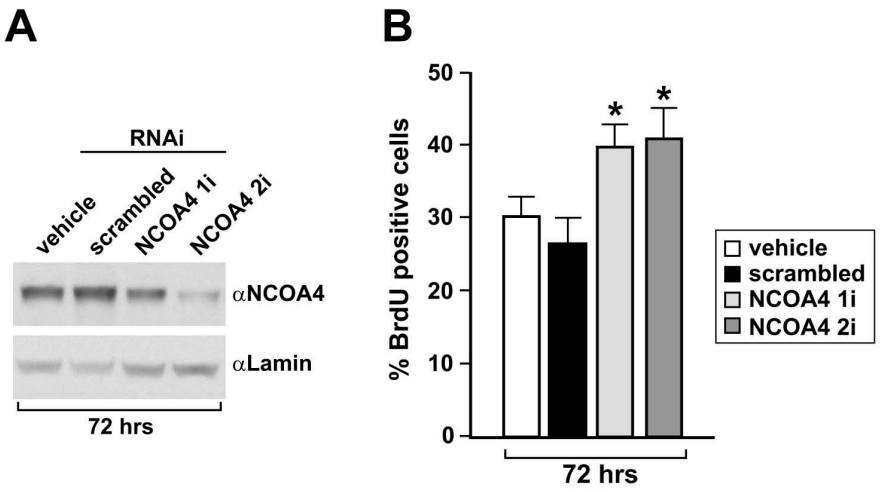
A
RNAi
vehicle
scrambled
NCOA4 1i
NCOA4 2i
αNCOA4
αLamin
72 hrs
B
% BrdU positive cells
50
40
30
20
10
0
*
*
vehicle
scrambled
NCOA4 1i
NCOA4 2i
72 hrs

Fig. S6

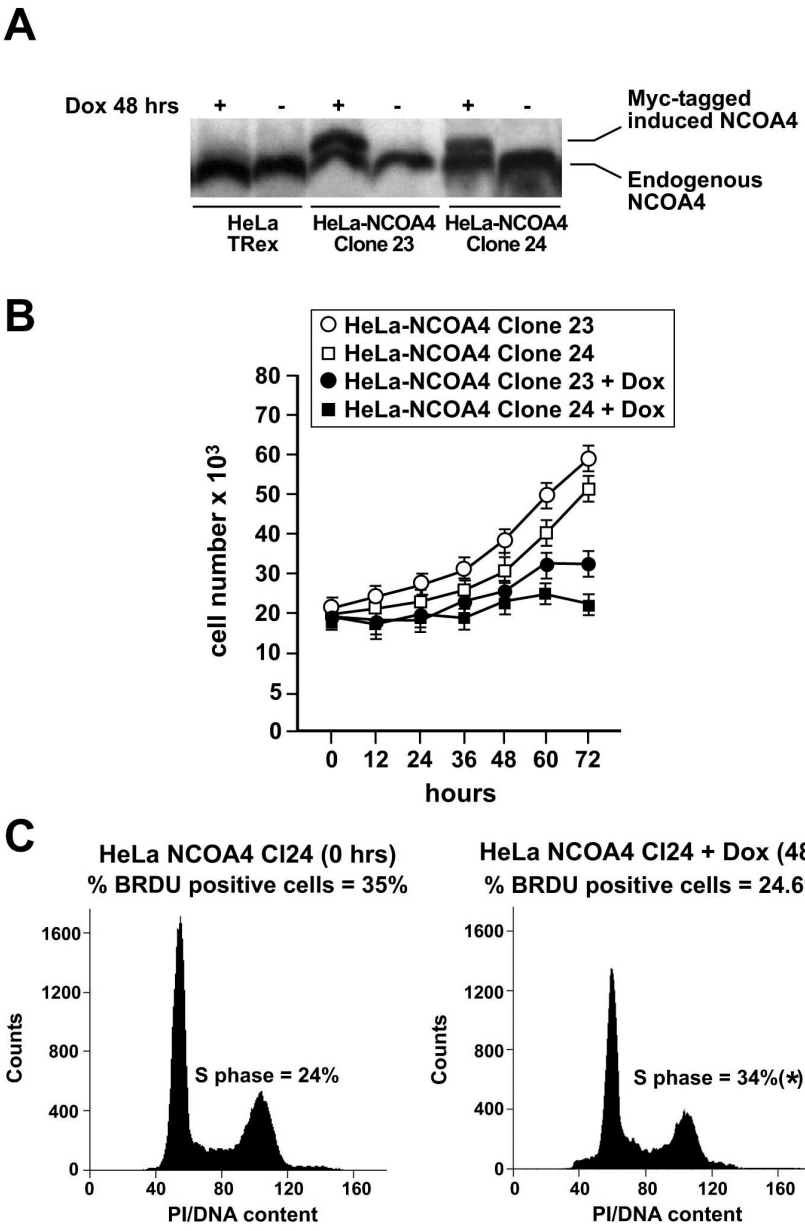
A
Dox 48 hrs + - + - + -
Myc-tagged induced NCOA4
Endogenous NCOA4
HeLa TRex
HeLa-NCOA4 Clone 23
HeLa-NCOA4 Clone 24
B
HeLa-NCOA4 Clone 23
HeLa-NCOA4 Clone 24
HeLa-NCOA4 Clone 23 + Dox
HeLa-NCOA4 Clone 24 + Dox
cell number x 10³
hours
C
HeLa NCOA4 Cl24 (0 hrs)
% BRDU positive cells = 35%
S phase = 24%
HeLa NCOA4 Cl24 + Dox (48 hrs)
% BRDU positive cells = 24.6% (*)
S phase = 34%(*)
Counts
PI/DNA content

Fig. S7

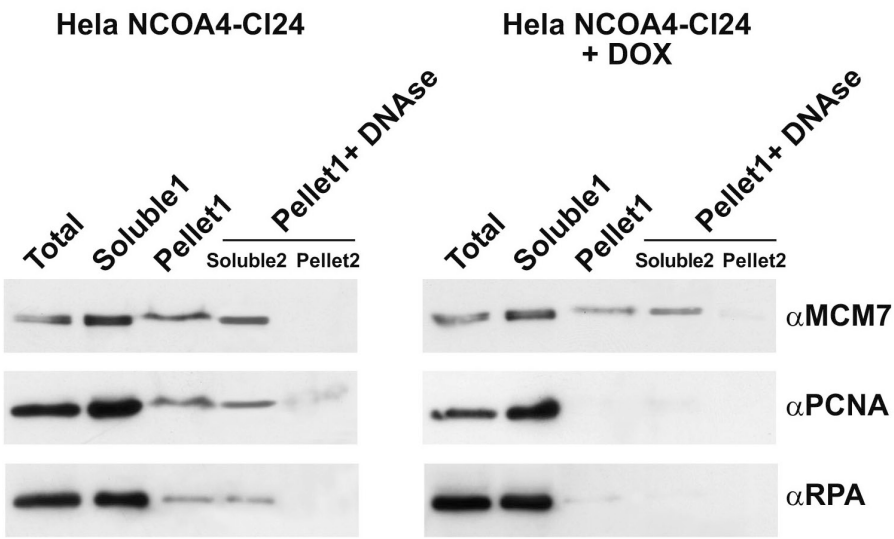
Hela NCOA4-Cl24
Hela NCOA4-Cl24
+ DOX
Total
Soluble1
Pellet1
Pellet1+ DNAse
Soluble2
Pellet2
αMCM7
αPCNA
αRPA

Fig. 1

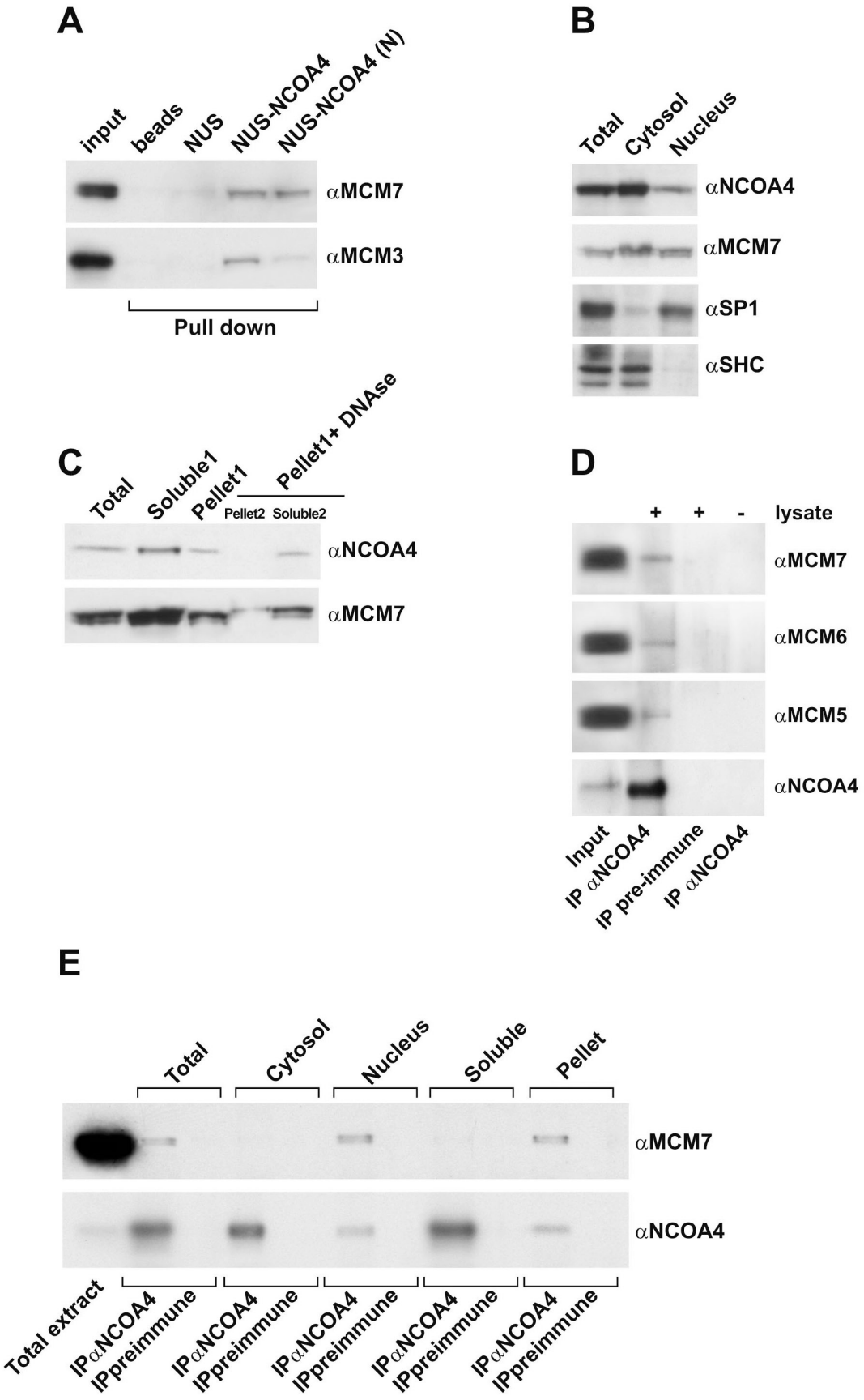
A
input
beads
NUS
NUS-NCOA4
NUS-NCOA4 (N)
αMCM7
αMCM3
Pull down
B
Total
Cytosol
Nucleus
αNCOA4
αMCM7
αSP1
αSHC
C
Total
Soluble1
Pellet1
Pellet1+ DNAse
Pellet2
Soluble2
αNCOA4
αMCM7
D
+
+
-
lysate
αMCM7
αMCM6
αMCM5
αNCOA4
Input
IP αNCOA4
IP pre-immune
IP αNCOA4
E
Total
Cytosol
Nucleus
Soluble
Pellet
αMCM7
αNCOA4
Total extract
IPαNCOA4
IPpreimmune
IPαNCOA4
IPpreimmune
IPαNCOA4
IPpreimmune
IPαNCOA4
IPpreimmune
IPαNCOA4
IPpreimmune